REPUBLIQUE DU CAMEROUN

****

PAIX-TRAVAIL-PATRIE

****

Ecole Nationale Supérieure des Travaux Publics

****

DEPARTEMENT DE GENIE CIVIL
DEPARTMENT OF CIVIL ENGINEERING

****

REPUBLIC OF CAMEROON

****

PEACE-WORK-FATHERLAND

****

UNIVERSITÀ DEGLI STUDI DI PADOVA

****

DEPARTMENT OF CIVIL, ARCHITECTURAL AND ENVIRONMENTAL ENGINEERING

****

DESIGN AND NUMERICAL ANALYSIS OF A GLUED-LAMINATED TIMBER OLYMPIC SWIMMING FACILITY ARC BUILDING

A thesis submitted in partial fulfilment of the requirements for the degree

Of Master of Engineering (MEng) in Civil Engineering

Curriculum: **Structural Engineering**

Presented by:

SEUKAP PANCHA James Landry

Student number: 14TP20757

Supervised by:

Pr. Carmelo MAJORANA

Co-supervised by:

Dr. Eng Guillaume Hervé POH'SIE / Eng. Giuseppe CARDILLO

Academic year: 2019/2020

AKNOWLEGEMENT

My first acknowledgement goes to the **President of the Jury**; Pr. NKENG George ELAMBO, for honouring this presentation with the presence of his eminent authority.

I am also thankful for the presence of the **Examiner**; Pr. Michel MBESSA, adding up to this panel of distinguished jury members.

My next thoughts goes to my **Thesis Supervisor**; Pr. Carmelo MAJORANA and **Co-supervisors**; Dr. Eng Guillaume Hervé POH'SIE and Eng. Giuseppe CARDILLO, for their effort and rationalizing in order to produce a quality thesis.

Further, I acknowledge the **Head of the Civil Engineering Department**; Professor MBESSA Michel for his rigorousness and emphasis on having quality presentable document.

I also wish to thank the **Teaching staff** from **University of Padova** and **NASPW Yaoundé**, whose different contributions enabled me acquire knowledge not only in civil engineering, but also related subjects and other life aspects increasing my whole capacity as a more accomplished human being.

Furthermore I thank the **Administrative Personnel** of the NASPW in general and Professor ESOH ELAME in particular whose efforts enables the cooperation between NASPW and the University of Padova benefitting us future ex-students.

Also, I acknowledge the help received from my **Classmates** whom I have spent time with and whose help enabled further my thesis and to whom I express gratitude all together.

I am very thankful and grateful to my **Family**; (The 'SEUKAP's) and other members non-specifically, whose different contributions, words of encouragements and prayers led me through all challenges and adversities in order to reach this level.

It cannot be left out my gratitude to the craftsmen empowering my practical knowledge on this special topic concerning wood. Here we have Mr. Léandre KUIATE the **General Manager** of **BHYGRAPH Engineering**, whose kindness of enabling me do field work at his company and promptitude in giving me basic lectures in wood technology. Also we have, Mr Emile KUIATE and Mr MESSE, **Personnel members** and finally Mr. Igor NJIA a **Worker** at BHYGRAPH.

My final acknowledgement goes to Mr Alain EMEYENE from the **Material Mechanics and Building Laboratory** at **NASP Yaoundé**, for helping me with some useful data.

DEDICATION

I dedicate this thesis to my parents; Mr SEUKAP Roger and Mrs. SEUKAP PENA Elise Claudine.

ABSTRACT

The thesis work here aimed at designing and numerically assessing the structural capacities of a Glued-laminated timber Olympic swimming pool facility shelter. The standards used to design the building were the Eurocodes; specifically Eurocode 0, Eurocode 1, Eurocode 3, Eurocode 5 and Eurocode 8. Mechanical and geometrical data were collected and used, assumptions were made for less available data, and then the structure was made sure to resists under different physical situations. The type of numerical analysis which was performed was Finite Element Analysis (FEA), specifically simple linear Finite Element Method (FEM) by exploiting linear elastic properties of Glued-Laminated Timber (GLT). It consisted first in the design of the FEM model then the numerical analysis of this model. This performance was assisted using Computer Aided Engineering (CAE) software SAP2000v21 to carry out different simulations, Computer Aided Design (CAD) software Revit 2014 for rendering and finally, Excel 2013 for graphing. The design was done considering a neighbourhood at the suburbs of the city of Yaoundé. Renewable and locally-available building materials such as tropical hardwoods were used, adapting the conception to our geographical context. As result, numerical evidence enabled the proposition of some solutions for safety in Ultimate Limit State (ULS), Service Limit State (SLS), corrosion and fire safety, meanwhile complete safety required further detailed analysis.

Keywords: Glued-Laminated Timber, spatial structure, Finite Element Analysis.

RÉSUMÉ

Ce mémoire de fin d'étude visait à concevoir et évaluer numériquement les capacités structurelles d'un abri piscine olympique en bois lamellé-collé. Les normes utilisées pour concevoir le bâtiment étaient les Eurocodes ; spécifiquement l'Eurocode 0, l'Eurocode 1, l'Eurocode 3, l'Eurocode 5 et l'Eurocode 8. Des données mécaniques et géométriques ont été collectées et utilisées, des hypothèses ont été faites pour des données moins disponibles, puis la structure a été assurée de résister à différentes situations physiques. Le type d'analyse numérique qui a été effectué était la *FEA* (l'analyse par éléments finis), en particulier la MEF (méthode des éléments finis) linéaire simple, en exploitant les propriétés élastiques linéaires du *GLT* (bois lamellé-collé). Il s'agissait d'abord de la conception du modèle de la MEF puis de l'analyse numérique de ce modèle. Ceux-ci ont été effectuées à l'aide de l'IAO (logiciel d'ingénierie assistée par ordinateur) SAP2000v21 pour effectuer différentes simulations, du logiciel de CAO (conception assistée par ordinateur) Revit 2014 pour le rendu et enfin, de Excel 2013 pour la représentation graphique. La conception a été réalisée en considération d'un quartier de banlieue de la ville de Yaoundé. Des matériaux de construction renouvelables et disponibles localement tels que des bois durs tropicaux ont été utilisés, adaptant la conception à notre contexte géographique. En conséquence, les preuves numériques ont permis de proposer des solutions pour garantir une sécurité à l'ELU (l'état limite ultime), l'ELS (l'état limite de service), la corrosion et aux incendies, tandis qu'une sécurité complète nécessitait une analyse plus détaillée.

Mots clés: Bois lamellé-collé, structure spatiale, analyse par éléments finis.

TABLE OF FIGURES

TABLE OF TABLES

TABLE OF ANNOTATIONS

Abbreviations

GLT	Glued Laminated Timber	PVC	Poly-Vinyl Chloride
RFA	Resorcinol Form-Aldehyde	PU/PS	Polyurethane/Polystyrene
ULS/ELU	Ultimate Limit State	CAE	Computer Aided Engineering
SLS/ELS	Serviceability Limit State	m.a.m.s.l	meters above mean sea level
FEA	Finite Element Analysis	HVAC	Heating, Ventilation and Air-Conditioning
FEM	Finite Element Method	EC5	Eurocode5
BEM	Boundary Element Method	FINA	Fédération Internationale de Natation
FVM	Finite Volume Method	pr-EN	pre-European Norm
WFEM	Wavelet Finite Element Method	EMC	Equilibrium Moisture Content
LVL	Laminated Veneer Lumber	RH	Relative Humidity
CLT	Cross Laminated Timber	FE	Finite Element

Symbols

f,c,o,k	characteristic compression resistance parallel to fibres in solid timber	f,c,o,g,k	GLT characteristic compression resistance parallel to fibres
f,t,o,k	characteristic tension resistance parallel to fibres in solid timber	f,t,o,g,k	GLT characteristic tension resistance parallel to fibres
f,m,y,k/f,m,l,k	characteristic flexure resistance in solid timber in solid timber	f,m,g,k	GLT characteristic flexure resistance
f,c,90,k	characteristic compression resistance perpendicular to fibres in solid timber	f,c,90,g,k	GLT characteristic compression resistance perpendicular to fibres
f,t,90,k	characteristic tension resistance perpendicular to fibres in solid timber	f,t,90,g,k	GLT characteristic tension resistance perpendicular to fibres
f,v,k	characteristic shear resistance in solid timber	f,v,g,k	GLT characteristic shear resistance
E,o,mean	average modulus of elasticity parallel to fibres	E,fi,d	design fire modulus of elasticity
E,o,o5	modulus of elasticity at 5% fractile of exclusion	κ	curvature
G,1,k	structural permanent load	γ,g	permanent load, combination safety factor
G,2,k	non-structural permanent load	γ,q	variable load, combination safety factor
Q,1,k	primary variable load (service or wind)	Ψ,i,j	load combination factor for variable load
Q,2,k	secondary variable load (wind)	K,h	stress redistribution factor due to height
Q,3,k	secondary variable load (hand)	K,ls	system effect stress amplification factor
A,d	accidental load	K,m	biaxial stress combination reduction factor
K,mod	service class resistance reduction factor	K,dis	variable inertia stress redistribution factor
γ,m (wood)	partial safety factor	K,v	shear resistance reduction factor due to notch

γ,m (steelplate)	partial safety factor	K,hol	worn-through element stress reduction factor
γ,m (bolt)	partial safety factor	K,n	calculation factor for K,v
γ,m,fi	fire design partial safety factor	K,cr	stability factor
f,m,j,k	flexural stress (multiple-splice finger joint)	K,c,y	compression resistance reduction factor
f,y,k	steel yield stress	K,c,z'	compression resistance reduction factor
l/L	Length	K,y	slenderness factor
h/H	Height	K,def	creep deformation factor
d/X/x/y,1/y,2/y/a/s/b	Distance	a,fi	metal plate thickness adjustment
b	Base	K,fi	characteristic value averaging factor
e	eccentricity	K,mod,fi	temperature and water content reduction factor
R,o	external radius of curvature	K,o	charring depth factor
R,i	internal radius of curvature	V,ref,o	reference wind velocity at sea level
R,n	curvature radius from NA	V,ref	reference wind velocity
CM	centre of mass	C,dir	wind direction coefficient
NA	neutral axis	C,temp	reduction factor due to temporal structures
O.	Origin	C,alt	altitude coefficient
A	Area	q,ref	basic wind pressure
I	moment of inertia	Z,w/Z,i	external/internal building height
M	Mass	Cr(Zw/z,i)	roughness coefficient
V	volume	C,t	topographic coefficient
r/r,i	Radius	Z,min	layer height for constant wind speed
t	Thickness	Z,o	roughness length
f/Z,chord	Sagitta	K,r (curve)	ratio of curvature radius to slat thickness
q/P,dist.	distributed load	t,fi,req	required fire evacuation time/fire thickness of metal plate
ρ,k/ρ,lk	solid wood characteristic density	η	reduction of effects of action due to fire
ρ,g,k	GLT characteristic density	η,30	standardised η for 30min evacuation time
ρ,water	water density	η,0.05	η for 5% fractile of exclusion
g	acceleration due to gravity	t,1	metal plate thickness
β/β,vol	volumetric shrinkage coefficient	t,1,min	minimum metal plate thickness
β,o	charring rate	α, α (FE)	inclination of load to fibres, inclination to global reference system
β (fire)	reduced charring rate	β (buckling)	axial critical buckling load reduction factor
w,ψ	water content	S,fi,d	design value of effect of action under fire
Δε	strain variation	S,d	design value of effect of action
ε	shrinkage strain	P	point load
u	Deflection	d,char	charring depth
Δu	deflection difference	d,o	initial depth
θ	Inclination	d,eff	effective (residual) charring depth
ϕ/D	Diameter	rad.	radial
F, R, l, H	point load	tang.	tangential
F,α	inclined point load	δ	amplification factor

E,d	design value of effect of action	N,cr	critical axial load
R,d	design value of resistance	τ	shear stress
m	Mass	τ,tors	torsional shear stress
F,M	moment induced force (dowel joints: dj)	i/ β,c	radius of gyration/ glulam limit rectitude factor
F,N	axial force per pin (d.j)	λ,y/ λ,z	slenderness ratio
F,V	shear force per pin (d.j)	λ,rel,y/ λ,rel,z	relative slenderness
n,i	number of pins per ring (d.j)	u,1	deflection due to self-weight
F,d	resultant induced joint force (d.j)	u,inst	instantaneous deflection
F,v,d	maximum shear force on wood (d.j)	u,2	time-variable deflection
M/M,u,d	moment	C,pe/C,pi	coefficients of external/internal wind pressure
V/V,u,d	shear	W,e/W,i	external/internal wind pressures
N/N,u,d	axial load	W,tot	total wind pressure
σ,cr	critical stress	i,β(notch)	coefficients for notch calculation

TABLE OF VALUES OF ANNOTATIONS

K,mod	0.8 (predesign), 0.6 (verifications)	K,ls	1.1
γ,m (wood)	1.3	K,m	0.7
γ,m (steelplate/pins)	1.2/1.25	K,n	6.5
γ,m,fi	1	K,r	1 / 0.22
K,fi	1.15	K,c,y	1 (2^{nd} order)
K,o	1	K,c,z'	1
V,ref,o	5m/s	K,def	0.6
C,dir	1	β,o	0.7mm/min
C,temp	1	β (fire)	0.54mm/min
C,alt	1.718	Z,min	8m
C,t	1	Z,o	0.3m
ρ,water	997kg/m3	H	0.6
G	9.8m/s	t,1,min	2mm
d,o	7mm	β,c	0.1
i (notch)	0	η,30	0.45

SUMMARY

GENERAL INTRODUCTION

The design of spatial structures entails consideration of important second order effects in order to obtain solicitation parameters (bending and torsional moments), effects which if not properly taken care of will inevitably lead to rapid failure of parts of the structure or worse still the collapse of the whole structure if main structural members are affected. Another issue is the fact that the building during service will be subjected to chemically aggressive environment emerging from the treatment of the swimming pools. The problematic will be discussed in two phases; one concerning analysis of spatial structures and the other concerning timber structures. In each respective phase will be discussed the necessity of resolving these problems. Spatial structures can be define as structures where loading of few or all its elements is applied out of the centroid principal axes of these elements. Under compressive forces, all straight frame elements will experience second order effects amplifying internal failure mechanisms. A worse situation occurs in curved frame elements, whose un-deformed state is prone to similar effects under eccentric loading, complicating the analysis process. The situation gets worst with the interaction of all elements in a very large 3-D structure. The complex analysis requires the use of numerical software. The type of analysis which will be carried out is simple linear FEA, and the study of elements will be done simplifying them as linear elements (as they are composite solid elements in reality). The most adapted type of structure for the large span design will be a typical three-hinged arched frame model, hence manual FEA has to be carried out consisting mainly in discretization of the curved beam elements into finite linear segments in order to pre-design the roof. Analysis will then be done with SAP2000v21. The next issue considered in design was the aggressive chemical environment to which structural elements will be exposed. Treatment of pools emits chlorine vapour which might encounter overlying structural elements and react with them. Now comparatively between iron/steel, pre-stressed concrete and timber commonly used for large span structure design, timber is the most resistant to corrosion by chlorine gas. Additionally the use of timber offers cost advantage and is eco-friendly. Glued-Laminated Timber (GLT) is the technology type to be used as it offers several advantages over other timber technology types (discussed in literature review). All previous considerations lead to the general objective which was to design a safe Olympic swimming pool facility sheltering structure with GLT. The specific objectives were to ensure a safe structure in ULS, in SLS, under corrosion and under fire. The thesis will proceed through a literature review, bringing out the methodology, and finally giving out results and interpreting them.

CHAPTER 1 : LITERATURE REVIEW

Introduction

The literature review was centred on splitting the two main ideas surrounding this thesis topic. The first is numerical analysis, which is a process by which complex mathematical problems can be resolved. The second is spatial timber reticular structures, a composite term comprising of spatial, timber and reticular structures converging to a common goal. These main ideas will be discussed one after the other. To each ideas will be developed a series of sub-ideas which will be stated and explained after one another. In addition to these, it will be necessary to discuss about Glued-Laminated Timber, which is a composite material which will be used to design the building.

1.1. Numerical analysis

The applicability of this process arises from the fact that as times goes by, engineering limits have met for building more and more complex structures using basic calculation methods and experiments. Important aspects surrounding numerical analysis will be enumerated.

1.1.1. Numerical analysis, its branches and roots

There are several definitions for numerical analyses, from which we sorted some and defined.

According to Merriam-Webster, numerical analysis can be defined as “the study of quantitative approximation to the solutions of mathematical problems including consideration of and bounds to the errors involved” (Webster, 2020).

There is another approach as to define numerical analysis, from a parent perspective as from Numerical methods. These are methods designed for the constructive solution of mathematical problems requiring particular numerical results, usually on a computer. They are also complete and unambiguous set of procedures for the solution of a problem, together with computable error estimates. The study and implementation of such methods is the province of numerical analysis. (OXFORD UNIVERSITY PRESS, 2020)

It is further defined and show its branching from the “Practical Finite Element Analysis” 1st edition where a Numerical method is one of the three methods to solve an engineering problem, unlike Analytical method (classical approach with a 100% accuracy) and Experimental Method (actual measurement requiring time and money for prototypes between three to five of them), the Numerical Method is a mathematical expression where approximate assumptions are made,

it is applicable even without physical prototypes, it is used for real life complicated problems , and finally must be verified by either of the other two methods. There are four classes of Numerical Method which are FEM, BEM, FVM and FDM. (Gokhale et al., 2008)

These definitions comfort the use of numerical analysis to design our spatial structure, over other methods.

1.1.2. Definition of Finite Element Analysis

FEA is a branch of numerical analysis, which is the study and implementation of the FEM, so there is possibility of using both terms interchangeably.

Going further in depth into FEM, there are three primary methods that can be used to derive the finite element equations of a physical system which are; the direct method or direct equilibrium method for structural analysis problems, the variational methods consisting of among the subsets energy methods and the principle of virtual work, and finally the weighted residual methods. (Logan, 2017)

The direct method, is the simplest and gives clear physical insight into the FEM, is recommended during initial stages of learning the FEM concepts. It is however limited in its application to deriving element stiffness matrices for one-dimensional elements involving springs, uniaxial bars, trusses, and beams. (Ibid.)

We have here that there are two general direct approaches traditionally associated with the finite element method as applied to structural mechanics problems. One approach, called the force, or flexibility, method, uses internal forces as the unknowns of the problem. To obtain the governing equations, first the equilibrium equations are used. Then necessary additional equations are found by introducing compatibility equations. The result is a set of algebraic equations for determining the redundant or unknown forces. The second approach, called the displacement, or stiffness, method, assumes the displacements of the nodes as the unknowns of the problem. For instance, compatibility conditions requiring that elements connected at a common node, along a common edge, or on a common surface before loading remain connected at that node, edge, or surface after deformation takes place are initially satisfied. Then the governing equations are expressed in terms of nodal displacements using the equations of equilibrium and an applicable law relating forces to displacements. (Ibid.)

These two direct approaches result in different unknowns (forces or displacements) in the analysis and different matrices associated with their formulations (flexibilities or stiffness).It has been shown that, for computational purposes, the displacement (or stiffness) method is more desirable because its formulation is simpler for most structural analysis problems. Furthermore, a vast majority of general-purpose finite element programs have incorporated the displacement formulation for solving structural problems. (Ibid.)

From defining FEA, we discovered that most of its numerical software incorporate stiffness matrices to extreme order numbers enabling resolution of very complex structures.

1.1.3. Applications of the Finite Element Method

This method has a wide range scope, covering a large spectrum in the construction sector. The finite element method can be used to analyse both structural and non-structural problems. Typical structural areas include; Stress analysis, including truss and frame analysis (such as pedestrian walk bridges, high rise building frames, and windmill towers), and stress concentration problems, typically associated with holes, fillets, or other changes in geometry in a body (such as automotive parts, pressures vessels, medical devices, aircraft, and sports equipment), buckling, such as in columns, frames, and vessels, vibration analysis, such as in vibratory equipment, impact problems, including crash analysis of vehicles, projectile impact, and bodies falling and impacting objects. Non-structural problems include, heat transfer, such as in electronic devices emitting heat as in a personal computer microprocessor chip, engines, and cooling fins in radiators, fluid flow, including seepage through porous media (such as water seeping through earthen dams), cooling ponds, and in air ventilation systems as used in sports arenas, etc., air flow around racing cars, yachting boats, and surfboards, etc., distribution of electric or magnetic potential, such as in antennas and transistors. Finally, some biomechanical engineering problems (which may include stress analysis) typically include analyses of human spine, skull, hip joints, jaw/gum tooth implants, heart, and eye. (Logan, 2017)

Practically, FEM can be used to solve the spatial timber reticular structure consisting of frames and trusses.

1.1.4. Processes of the Finite Element Method

Moving on from applications to a few processes, the FEM is based on conceptual steps which is defined.

The finite element solution for a physical problem consists of several basic conceptual steps. The two first steps that we need to take are to establish the strong form and the weak form of a problem. The strong form consists of mathematical equations physically expressing the conditions that the exact solution of a problem must satisfy at any point inside the system under consideration. The weak form is an alternative, integral version of the mathematical conditions governing a problem. (Koutromanos, 2018)

Also it is discussed one main process of the FEM which is discretization, which imposes a plausible reason for its approximate nature of numerical methods. The domain of the continuous body B is partitioned into non overlapping subdomains, each of them denoted a finite element.

As the shape of the subdomains is generally restricted, the union of all subdomains is only an approximation of the original domain (Schwedler, 2016)

Discretization enables the study of complex geometry structures by simplification into linear elements.

1.1.5. Advances of the Finite Element Method

Research enabled to have an idea about some advances of the FEM. One of the main advances in the finite element method is generalized conforming elements. Firstly, from the view point of theory, the generalized conforming element opens a new way between conforming and non-conforming elements, so that the puzzle of the convergence problem for non-conforming elements can be rationally solved. Meanwhile, various new conforming schemes, including point conforming, line conforming, perimeter conforming, Semi-loof conforming, least square conforming and their combination forms, have been successfully proposed. Secondly, from the viewpoint of applications, the successful application of the generalized conforming element method was first realized for thin plate bending problem, in which a series of high performance thin plate element models were presented. Subsequently, the novel technique was successfully generalized to other fields, and a large number of new models, including membrane elements, membrane elements with drilling DOFs, thin-thick plate elements, laminated composite plate elements, flat-shell elements, curved shell elements, etc., were also successfully constructed. (Long, 2009)

Other advances of FEM are; ‘Sub-region mixed element method’ providing a novel solution strategy for fracture problem by complementarity and coupling of displacement-based element and stress-based element, ‘Analytical trial function method’ which exhibits rewarding cooperation between analytical and discrete methods, and provides effective solution strategy for shear locking, trapezoidal locking and singular stress problems, ‘Quadrilateral area coordinate method’ which indicates that the area coordinate method is generalized from the traditional triangular element field to new fields, ‘Spline element method’ which indicates that the advantages of the spline functions have been adopted by the finite element method. (Ibid.)

The previously mentioned developments in FEM has led to the discovery of effective solution strategies for five challenging problems which are; shear-locking problem in thick plate elements, sensitivity problem to mesh distortion, non-convergence problem of non-conforming elements, accuracy loss problem of stress solutions by displacement-based elements and singular stress problem. (Ibid.)

These advances enabled the study of more specific and localised problems arising in construction.

1.1.6. Software for numerical analysis

There are several software for numerical analysis, with it its own specifications and ranges of applications.

A popular program for numerical analysis is ANSYS, which was also one of the first programs to allow nonlinear analysis. Great impetus for software development was provided by efforts of E. Wilson at UC Berkeley, which spawned two types of programs. The first type evolved from the SAP code, and it ultimately led to a family of software solutions currently distributed by Computers and Structures, Inc., a company based at Berkeley. The main programs of this family, which are used by the civil structural engineering community and emphasize seismic design, are SAP 2000, ETABS and Perform3D (the latter being the product of work by another Berkeley faculty member, G. Powell). The second type stemmed from work by K.-J. Bathe, a student of Wilson's and currently a faculty member at MIT, who created the commercial program ADINA. (Koutromanos, 2018)

Another, two popular commercial programs are ABAQUS, originally created by David Hibbitt and currently marketed by Simulia and LS-DYNA, originally created by John Hallquist at Livermore National Laboratories and currently marketed by Livermore Software and Technology Corporation (LSTC). Both of these programs have a very wide range of capabilities, including nonlinear analysis of solids and structures. They are also very attractive for researchers, by allowing the incorporation of user-defined code and ensuring compatibility with high-performance, parallel computing hardware. (Ibid.)

From these software it was gotten that SAP2000 is one of the most commonly used in civil structural engineering.

We learn from the above that SAP2000 is a good software to perform numerical analysis. This will prompt considerable time and costs in large building projects.

1.2. Spatial timber reticular structures

Timber is a basic and very old construction material. Challenges over decades surrounding construction of large, light and economical cover structures for buildings, for several different uses lead to the implementation of spatial timber reticular structures.

1.2.1. Definition of spatial timber reticular structures

Spatial timber reticular structures are three-dimensional super structures which usually form building skeleton (structural aspect), but due to the physical attractiveness of timber in modern times is also used for its architectural properties.

Spatial structures are defined as “the idealisation of a structure for which the loads are not applied through the centroid principal axes” (Ghali, 2017)

Spatial timber reticular structures have a wide variety of applications such as hangar building (storage, aviation, railway, agricultural etc.), mobile home construction, cottage, bridges, religious edifices, simple housing and even tall buildings in recent years.

1.2.2. Historical background of wood/timber building

The historical background of timber building can be traced back in a chronological order, from the early men era to a more contemporary (19th century) history.

Wood, a previously neglected material was used to build large span structures, towers, homes and sheds. It was used as structural element, cladding, interior finish and furniture. Wood construction encountered problems such as splitting, shrinkage, combustibility, and rot. The success or failure stories depended on its material properties. (Mayo, 2015)

From historical background, bridges are the first examples of man-made large-span timber structures. The need of overcoming obstacles such as rivers or valleys, has always challenged the humans to find suitable structures that could span over considerable distances. (Crocetti, 2016).

Evidence in history, from the Stone Age to Neolithic Egypt to kingdom ages suggests wood as one of the oldest building materials. (Mayo, 2015)

Timber bridges in Mesopotamia (3000 to 2000 B.C.) or in Asia illustrate why this wide spread material was used in the construction of big structures using simple tooling and assembly methods. North American forests, for instance, demonstrate that trees used as cantilever girders can span large widths: sequoias standing 80 m tall or redwoods with a height of 120 m have survived for centuries. The high bending strength of timber compared to its weight is often an advantage. If treated correctly, timber has a long service life, as can be seen in timber bridges and multi-storey framework buildings in Asia or Europe that are over 400 years old. (Gerold, n.d.)

Further evidence for wood construction were hybrid wood-mud brick construction in ancient Egypt, Minoan and Mycenaean wood elements in ancient Greece, Doric architecture still in Greece and finally a primitive hut from Marc Antoine Laugier in the 17th century. (Mayo, 2015)

Norwegians (Vikings) copied northern European timber architecture during their invasions. Log timber construction evolved in alpine Europe, while timber frame oak construction was preferred. All these facts suggests regional, place-based wood architecture. (Ibid)

The advent of steel and reinforced concrete diminished the teaching of wood construction, which was reborn with the discovery of GLT, LVL, CLT, novel connectors and connections such as the Dowel type and new preservation techniques. This lead to the construction of very large span structures such as the Superior dome in Michigan, USA. (Crocetti, 2016)

Historical evidences mentioned demonstrate the durability and reliability of timber as a building material, despite the more recurrent use of other materials in modern times.

1.2.3. Description of wood/timber

In order to build with timber, we must have knowledge about its inherent properties and how to enhance them by engineering.

To begin with, there is this poetic definition of wood as the mother of matter '… she renews herself by giving, gives herself by renewing. Wood is the bride of life in death, of death in life. She is the cool and shade and peace of the forest. She is the spark and ear, ember and dream of hearth. In death her ashes sweeten our bodies and purify our earth. —Carl Andre, 1978', as cited. (Mayo, 2015)

Wood is a complex heterogeneous colloidal system, consisting mainly of; hemicellulose, cellulose and lignin. These constituents have high and varying thermal decomposition limits ranging from 170°C to 400°C. The combustion of wood is affected by its physical structure and properties. (Dúbravská, 2018)

In addition, wood is naturally resistant to chemical action, such as swelling due to liquid absorption, hydrolysis of cellulose by acids and acid salts and finally, delignification and dissolution of hemicellulose by alkalis. (Construction, 2012)

There is the link between wood and timber, as timber is a form of wood. The STEP1 manual defines wood as a solid, organic and natural body. It is a composite material made up of a set of chemical elements, principally cellulose, hemicelluloses, lignin and sap[1]. (SEDIBOIS, 1996)

"There are two main categories of timber; Hardwoods and Softwoods. Hardwood is gotten from angiosperms (flowering plants) while softwood is gotten from gymnosperms (conifers)" (Ibid).

Some different types of timber available in Cameroon in their common naming are; Sapelli, Wengue, Doussié, Bilinga, Bubinga, Ayous, Fraké, Iroko, Pachy, Eyen etc. (Gerard, 2020)

A pictorial description of a typical timber trunk is shown in Figure 1.1. (Expertsmind, 2020)

[1] All references to this book has been paraphrased from French language.

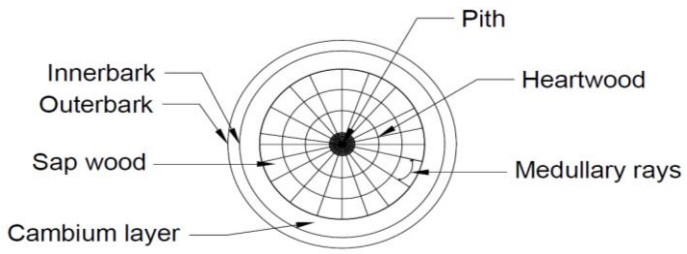

Figure 1.1. Cross-section of a timber trunk

Several boasts credit the use of timber for construction such as; strength (for engineered timber), rapid construction, accuracy, air tightness, adaptability, good ambiance and air quality, natural regulation of moisture, humidity and temperatures. (Mayo, 2015)

Also, in a more technical aspect, timber is attributed excellent specific strength and specific stiffness, hence suitable for large span structures. (Crocetti, 2016)

Generally, wood is a durable material with a very long duration period, exists in different types and is chemically more resistant compared to other building materials.

1.2.4. Historical background of building codes

Since designing a timber building involves the use of timber building codes, we fly over the different codes which lead to modern timber construction.

Building codes in various forms have been around for a very long time. One of them, the Code of Hammurabi, was written in approximately 1775 B.C. near what is now the city of Baghdad. This code included 282 laws, and six of them were related to building construction. In addition to establishing a fee for construction, this code delineated penalties for collapse of a building or faulty construction. One of those, number 229, detailed the penalty this way: “If a builder builds a house for someone, and does not construct it properly, and the house which he built falls in and kills its owner, then that builder will be put to death”. (Avalon Project, 2008)

“Fortunately, today’s codes are less harsh in their penalties and more detailed in their description of required design and construction techniques that prevent harm to both occupants and builders” (Royer, 2015).

Eurocode 5 was began by John Sunley, at the UK forestry product laboratory. He later became the director of TRADA later-on. He sketched out a model of regulations for wooden construction, within the CIB work committee, where he published “rules for calculating wooden structures” in 1983. This was later adopted in Eurocode. (SEDIBOIS, 1996)

A standard code for modern timber construction is the Eurocode 5, widely used in Europe, can be adapted to tropical context.

1.2.5. Methods for testing timber

Generally, there are three groups of methods for testing timber, non-destructive, semi-destructive and destructive methods, used to determine the physical and mechanical properties affecting its structural behaviour.

"Traditionally the bending strength, *fm,k*, and the modulus of elasticity, *E*, are determined by a Four-point bending test according to EN 408, which is a destructive test" (Ravenhorst e.a. 2004), as cited. (MAGNUS, 2008)

There exist alternative testing methods for on site evaluation of timber characteristics. For on site evaluation of timber characteristics non-destructive (ND) and semi-destructive (SD) tests have been developed. The term 'non-destructive' is used when the wood remains intact, the term 'semi-destructive' indicates that holes are made, or stresses are applied, but they do not alter the end-use capabilities of the structure. A classification can also be made between Global Test Methods (GTM) and Local Test Methods (LTM), giving information about either the whole element or a point of the element (Feio, 2005), as cited. (Ibid.)

Visual inspection is a non-destructive testing method, comprising the use of an optical scanner in order to identify knots, grain angle, fissures, reaction wood, fungal and insect decay, and finally mechanical damage, which all affect its strength. (Ibid.)

X-ray visualisation spectroscopy is a complete radioscopy system aimed at the production of radiographs. X-rays give information about decay, structural defects, void types, masonry and embedded carpentry joints, state of knots and preservation of strengthening prosthesis. (Ibid.)

Infrared thermography is another testing method used to detect and asses the conservation of invisible connections by local heating. (Ibid.)

Videoscopy is a semi-destructive testing method consisting of the insertion of a video camera locally, in order to study the state of the structure, material changes and voids. (Ibid.)

The ultrasonic technique is a non-destructive technique used to predict dynamic modulus of elasticity (MOE) by the transmission of low frequency waves and wood inspection using high ultrasonic frequencies. (Ibid.)

Finally, we have static MOE/bending test. This involves application of different forces and measuring displacements, or measuring loads for fixed deflections. It is considered semi-destructive, as it induces stress. (Ibid.)

Examples of physical and mechanical properties gotten with these tests are; void ratio, grain angle, density, compressive strength, strain, bending strength etc.

1.2.6. Structural aspects concerning reticular structures

The literature review of spatial timber reticular structures could not be done living out structural aspects for design, which are important and would influence the design.

Talking about framed structures**,** all structures are three-dimensional. However, for analysis purposes, we model many types of structures as one-, two-, or three-dimensional skeletons composed of bars. Thus, an idealized *framed* structure can be one-dimensional (a beam), two-dimensional (a plane frame or truss), or three-dimensional (a space frame or truss, or a grid). The skeleton usually represents the *centroid axes* of the members (Ghali, 2017)

The indeterminacy of a structure may either be external, internal, or both. A structure is said to be externally indeterminate if the number of reaction components exceeds the number of equations of equilibrium. Thus, a space structure is in general externally statically indeterminate when the number of reaction components is more than six. (Ibid.)

"Some structures are built so that the stress resultant at a certain section is known to be zero. This provides an additional equation of static equilibrium and allows the determination of an additional reaction component" (Ibid.).

Talking about spans, large spans structures should ideally be designed so that they work primarily in tension and/or compression. In fact, minimizing bending moments leads in general to an optimum utilization of the structure, regardless what material is chosen. This often results in slender and elegant shapes. (Crocetti, 2016)

As spans become longer, a number of problems arises. For example, as compression members get longer, buckling begins to be an issue. (Ibid.)

Lateral braces provide lateral support to members, hence increasing buckling strength. Compression forces on members to be braced are determined assuming a single wave sinusoidal mode deformation of these members, with a maximum allowable deflection at span/500. (Porteous, 2007)

"The bracing ratio is defined by dividing the number of the braces at the wall with the number of the resisting cells" (Psalti, 2017).

Lamination is different aspect for design. The principle of separating and re-joining timber has produced a large variety of linear and two-dimensional building elements with defined

characteristics, so that adapted solutions are also found for very special requirements. By this approach the limited dimensions of a tree have been overcome. (Gerold, n.d.)

According to RAMAGE *et al*. (2017), the use of timber in larger structures on fire engineering design to ensure that the building can retain its structural integrity for sufficient time either for building occupants to be evacuated, or for the fire to be extinguished and in construction using large cross-section timber features, this may be done by assuming rate at which the timber chars (BS EN 1995-1-2:2008. Eurocode 5), as cited. (Dúbravská, 2018)

The type of foundation structure which can be used for the design is simple concrete slab foundations. The post foundation junction is made up of metal connectors between wood and masonry, in order to avoid direct contact which is a cause of humidity problems. An ideal distance between wood and masonry is a minimum of 10cm. (The Ministry of Economy P. a., 2015)

The structural aspects considered gives us a basis for designing the different constituting structural members.

1.2.7. Advances in timber construction

Apart from structural aspects, modern technological advances also influence timber construction.

For secondary Structures, new developments In the past the main load bearing timber structures like beams, bows or frames were mainly covered with trapezoidal sheet metal as single or insulated double layer or as sandwich elements with PU or PS as a core. Also non-insulated corrugated fibre cement panels were used. In the recent past, more and more timber elements were used as secondary structure. The prefabricated (box) elements or panels are nowadays an industrial product with a very high rate of prefabrication including insulation, indoor panelling and exterior roofing. This type of secondary structure speeds up the building process, reduces the carbon footprint of the structure, increases the quality of the structure by industrial production and thanks to increased steel prices is nowadays the more economical solution in many cases. (Winter, 2012)

Robustness is a design item, which is unfortunately not observed in many cases. After the disastrous roof collapse of the Bad Reichenhall ice-rink arena roof, many investigations were done in Germany and the neighboring countries. Some of the results are presented also. But a special look should be taken at robustness. One of the main principles of robust design is that if there is a damage of one of the primary members, the secondary structure should not be able to transfer the additional loads to the neighboring girders because this will immediately cause an overload of these beams and a progressive collapse is the result. (Ibid.)

"To enable a single collapse of a main girder the purlins will be single span beams, but to avoid down-falling of a destroyed purlin, a continuous supporting system of the purlins may be required" (Ibid.).

A few construction projects are; first of all a Sequential Roof which is a 2308m2 timber roof structure consisting of 48'624 geometrically unique, softwood elements, robotically fabricated and assembled layer-wise into 168 truss-like beams with a simple face-to-face nailed connection technique. Initiated as a research study and realized as a full-scale construction project, the project gave an opportunity to combine academic and applied approach, to validate and verify research concepts in a real-life scenario. (Apolinarska, 2018).

Robot-Assisted Assembly of Complex Timber Structures was a research project investigating spatial timber structures based on T-shaped joints and new connection techniques suitable for sequential robot-based fabrication and assembly. The project focussed on single- and double layer reciprocal frame structures, butt-jointed using fast-curing adhesives. (Ibid.)

Both projects involved a collaboration with structural engineers, timber engineers and robotic fabrication experts form academia and industry. This setting allowed a comprehensive view on the subject, tight integration and cross-validation of the findings between disciplines. Both being settled in the same context of robotically assembled timber bar structures, the two projects are mutually complementary in terms of geometric complexity, connection technique, scale, scope and stage. This provided an opportunity to cover different facets of the problem within the same context. (Ibid.)

What can be retained above is the employment of robust construction systems. Robustness also contributes to the durability and safety of a timber building.

The most remarkable aspect of spatial timber reticular structures among the many others is its definition, which segregates curved frame structures as spatial reticular structures. This foreshadows already, the type of structure which is most adapted for the design.

1.3. Glued-Laminated Timber as a building material

GLT is a novel technology for the exploitation of timber. It is necessary to present it as a peculiar building material, with its method of obtaining, its usage, advantages and disadvantages.

1.3.1. Obtainment of Glued-Laminated Timber

The main engineering process, to obtain GLT is the process of lamination. GLT possesses several advantages over solid timber. Figure 1.2 depicts a non-homogenous GLT cross section (SWEDISHWOOD, 2020).

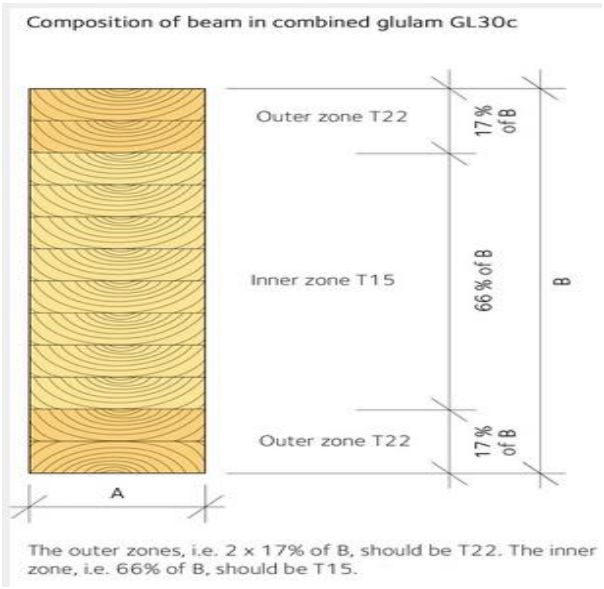

Figure 1.2. Cross section of a combined glulam beam

Laminated timber (GLT) is a structural wood product made from strips of wood Glued together. It is made up of at least four strips or sheets of sawn goods, maximum 45 mm thick, with the grain direction running along the length of the laminated timber product. The Finnish Glulam Association recommends that the strength class for glued laminated timber is GL 30c in accordance with Standard SFS-EN 14080. (https://www.woodproducts.fi/content/glued-laminated-timber, 2020).

There are two forms of laminated timber; vertical GLT and horizontal GLT. The former has glued line planes perpendicular to the shorter length of cross section, while the later with its own plane perpendicular to the longer length of cross section. (Porteous, 2007)

It can also be learned that glulam is adapted for the future. “The laminated woods and panel materials available today permit almost any three dimensional curvature of beam-shaped and two dimensional timber elements. In terms of aesthetics and high spans, two-dimensional structures are the future structural elements!” (Gerold, n.d.)

In order to further appreciation on the process of lamination it shall be necessary to identify on site the industrial manufacture of GLT.

1.3.2. Usage of Glued-Laminated Timber

Several techniques can be used in order to preserve GLT alike wood, but the premise of preservation is knowing about the state of dryness of conserved timber.

There are four main dryness states for wood as function of its water content; green (30%), commercially dried (between saturation and 23%), commercially dried (18% to 22%), and finally air-dried (depending on the local climatic zone). The dryness state affects the processing and storage of timber. (The Ministry of Economy P. a., 2015)

Off-site fabrication is a technical element enabling the industrial manufacture of more accurate and durable timber structural elements. (Smith, 2015)

Durability of wood is enhanced by a cutting pattern technique known as the 'through and through' method, including a series of quarter and plain sawing. The cutting pattern affects the shrinkage, warping and abrasion resistance of sawn lumber. Good cutting patterns control cracking, hence reduces the possibility of attack by fungi and insects. (Larsen, 2016)

Concerning treatment of wood, many impregnating substances have been used to enhance the natural resistance of wood to chemical degradation. One of the more economical treatments involves pressure impregnation with a viscous coke-oven coal tar to retard liquid penetration. Acid resistance of wood is increased by impregnation with a phenolic resin solutions, followed by appropriate drying and curing. Treatment with fufuryl alcohol increased resistance to alkaline solutions. Another procedure involved massive impregnation with a monomeric resin, such as methyl methacrylate, followed by polymerization. (Construction, 2012)

Preservation of historic timber structures with chemical preservatives (insecticides and fungicides) should be kept to a minimum and done only where necessary. (Larsen, 2016)

Another aspect for preservation is the external coating. Even if other materials can be used, such as thin briquettes to stick on a panel, plywood panels or HDF (High Density Fiber board) water-repellent possibly grooved, PVC or aluminum sheets, we will recommend here wooden cladding , taking into account the availability of the raw material for their local production. (The Ministry of Economy P. a., 2015)

Several historical evidence show the increase of durability of timber structures due to preservation. For example, there is an 1800 year old Buddhist temple in India. Emphasis here lays on the fact that microstructure variation due to ageing is negligible. (Larsen, 2016)

Good processing and the use of chemicals contribute in preservation of timber. These techniques depend on the water content of wood.

1.3.3. Advantages of Glued-Laminated Timber construction

As advantages of GLT compared to solid timber, we have the possibility of having very long spans, different shape and variable inertia sections, more economical (pertaining the use of

different strength class of wood stripes), has less deformation due to humidity, and finally high engineering precision by using software. (SEDIBOIS, 1996)

The use of structural glued joints are stiffer and more corrosive resistant, uses less timber and look better than mechanically fastened connections. (TRADA, 2007)

Complex shapes could be designed and the use of laminates increases strength by distributing defects throughout the section. It is possible to incorporate pre-cambers into the sections. (Porteous, 2007)

Other advantages of GLT include; cost effectiveness, lower transportation costs, higher load bearing capacity than concrete per pound, wide spans, has trusses with fewer joints, possibility of using 3-D bracings and finally can be used in hybrid structures. (Gerold, n.d.)

The mentioned advantages of GLT prompts the use of this technology for large span structures.

1.3.4. Disadvantages of Glued-Laminated Timber construction

As for construction with every other material, timber construction also comes short in a few aspects.

The characteristics of the materials used in construction and their implementation must comply, given their existence with the norms enacted by the competent national authority in charge of norms, technical usage instructions jointly approved by professionals and in any case with the rules of construction. (Ephraim, 2008)

Some more important fact is that many structural engineers forget about this problem as they are used to work with isotropic materials. A possible measure is to improve the training of structural engineers about problems directly connected to timber, such as consequences of strength anisotropy and shrinkage properties, and how to cope with that in design. For more advanced timber structures, special checking of the potential risk for perpendicular to grain failure should be included in design control procedures. Since moisture induced stresses often contribute to this type of problem it is natural to do this checking in connection with control plans for moisture effects. (Frühwald, 2007)

High level of training and local norms are required to solve problems arising with timber construction.

GLT as a building material is obtained from the process of lamination. Different techniques employed in its usage fosters its preservation. There are several advantages for the use of GLT as well as a few drawbacks.

Conclusion

Knowledge from numerical analysis, spatial timber reticular structures and Glued-Laminated Timber as a building material enabled to begin the design as there is a basis for the design of the building. It is already know the type of structure (a large span arched structure), the technology to be used (GLT), the software to be used for design (SAP2000v21) and the central design code (Eurocode 5). Further knowledge for the design will be unravelled though the methodology.

CHAPTER 2 : METHODOLOGY

Introduction

In applying spatial timber construction in order to enhance swimming sporting activities sporting activities in Cameroon, and also to remain within a limited scope of study (numerical analysis), we adopted a Design method for this thesis. A Multi-method approach was used to support this strategy. This Multi-method consisted in; Theoretical research (through a generalised literature review), Scientific applied research (for specific studies about GLT, and the Eurocodes 0, 1, 3, 5 and 8), and Explanatory research (by evaluation of structural parameters with the aid of numerical software and proposition of solutions). By using both quantitative and qualitative data collection techniques, we aimed at designing a safe Olympic swimming pool facility shelter structure with GLT. This was done by meeting specific safety requirements in ULS, SLS, corrosion and fire safety, and also by making assumptions where necessary. The four axes of this chapter are the design elements, material properties, preliminary design and numerical analysis.

2.1. Design elements

One very important part of our design method was to define the different necessary design elements.

This subchapter constituted in presenting the structural typology, which is the basis of the layout of the structural model design. It also included the architectural parametrization of the building, which in itself is the foundation for every building design. This will enable relate the building design to its functions (an Olympic swimming facility building). After that, there was the need to collect data through interview for the design process. This was summarised by Table 2.1.

Table 2.1. Summary on interview

N°	Interviewee	Position of responsibility	Data collected	Extra data collection tools
1	Pr. Carmelo MAJORANA, Dr. Eng Guillaume Hervé POH'SIE and Eng. Giuseppe CARDILLO.	Supervisor and co-supervisors.	General design principles, theoretical and practical references, and finally important tips to perform numerical analysis.	

2	Pr. Michel MBESSA	Head of Department	Implementation of thesis document	
3	Mr. Léandre KUIATE	G.M. BYGRAPH ENGINEERING (B.E.)	Basic timber design principles	
4	Mr. Alain EMENYENE	Material Mechanics lab.	Some timber mechanical properties	
5	Mr. MESSE	Worker (B.E.)	Timber design techniques, CIRAD booklets, timber specie documents, GLT building examples	photography
6	Mr. Igor NJIA	Worker (B.E.)	Timber product manufacturing machines presentation	photography

The last part of the design elements was to display the geographical context of the design, which will directly impact the obtainable results.

Having these done the next step consisted in the description of material properties of Glued –Laminated timber.

2.2. Material properties

Building with timber (especially GLT), is an engineering field which requires detail knowledge about the material.

These basically are the volumetric properties and the mechanical properties. Other properties of significant importance are the chemical and thermal properties, but have already been taken care of inside timber building codes. Some of the necessary properties where readily available from detail property research, and their sources were stated where ever used. Other properties required a series of calculations in order to obtain them.

The material properties served mainly as input parameters for numerical analysis using software SAP2000v21.

2.3. Preliminary design

Preliminary design ensures the design of an optimal structure, in an optimal amount of time saving financial saving financial and management costs.

This part includes the preliminary design of secondary structural elements (joists and girts), the primary structural elements (curved beams and columns), the connecting elements and devices, bracing elements, and finally the harbouring foundation structure. These where done

while considering implementation restrictions, joint constraints and restraints, and the laminating structural elements (slats and multiple-splice finger joints).

A preliminary building model was designed following researched guidelines, and two other models designed following a similar procedure (without displaying once more the lengthy process). All these was done considering the same external actions on each of them.

2.4. Numerical analysis

The analysis of the building was done specifically to meet with predefined objectives. So in order to reduce document bulk and remain within scope of study, emphasis was laid mainly on frame elements, bracing systems, main connections (ridge, abutment and internal curve element vertical splice) and foundation design.

Other unmet specificities were partly or fully assumed, approximated or voluntarily left out as 'out-of-scope' elements of analysis. This regards secondary element connector design which was assumed as being well designed and adapted to the structure (pertinence of this assumption holds for industrial connector types for primary or secondary elements which don't necessitate design). Since the main work is the numerical analysis of the structure proper it was done detail in the different limit states.

Numerical analysis entailed the modelling of the building in the software SAP2000v21, the description of the basis of limit state calculations, the description of actions (forces) acting on the building, a comparative analysis to discern a best fit structural model design, and finally the making of safety verifications in the different limit states (Ultimate Limit State, Service Limit State, corrosion and fire). For each of the different steps of analysis we identify each different necessary element in the structure to analyse and display results where necessary and make comparison between different design states or reinforcement models based on the main criteria being displacement. Due to the heavily densified number of elements, the selected necessary elements were those with maximum solicitation parameters. It will then be immediately at each step proposed alternatives where requirements will not be met. This was done with help of a series of equations, figures and tables and their descriptions presented here.

2.4.1. Limit state calculations

The load combinations we will use in the design, value and their uses were described as shown in Table 2.2.

Table 2.2. Load combination table

Load combination situation name	Value	Uses
Persistent/Transient	$\gamma,gG1,k+\gamma,gG2,k+\gamma,qQ1,k+\gamma,q\psi_{,02}Q2,k+\gamma,q\psi_{,03}Q3,k$	For ULS verification
Combination/Rare	$G1,k+G2,k+ Q1,k+\psi_{,02}Q2,k+\psi_{,03}Q3,k$	For SLS of structural elements
Quasi-permanent	$G1,k+G2,k+ \psi_{,21}Q1,k+\psi_{,22}Q2,k+\psi_{,23}Q3,k$	For SLS joint verification
Accidental	$G1,k+G2,k+ A,d+\psi_{,11}Q1,k+\psi_{,22}Q2,k+\psi_{,23}Q3,k$	For fire design

The values of $\psi_{,0i}$, $\psi_{,1i}$ and $\psi_{,2i}$ (i=1,2) was gotten for wind and operating loads.

The design value of a mechanical property was calculated using Eq. 2.1.

$$X,d = K,mod(^{X,k}/_{\gamma,m}) \quad \textbf{(Eq. 2.1)}$$

K,mod used here is for the permanent of load duration class for ULS, SLS, corrosion and fire analysis (conservative approach), case of the self-weight for the different service classes (Class 1 and 2). For seismic analysis we will use instantaneous load duration class for same service class.

The design value of a geometric property is given by Eq. 2.2.

$$a,d = a,k + \Delta d \quad \textbf{(Eq. 2.2)}$$

The work to be done in limit state calculation is the clear definition of the load combinations and load combination factors which was used in each design phase as shows Table 2.3.

Table 2.3. Load combinations with applied safety coefficients

Load combination situation	Value
Persistent/Transient	$1.35G1,k+1.35G2,k+1.5Q1,k+1.5\psi_{,02}Q2,k+1.5\psi_{,03}Q3,k$
Combination/Rare	$G1,k+G2,k+ Q1,k+\psi_{,02}Q2,k+\psi_{,03}Q3,k$
Quasi-permanent	$G1,k+G2,k+ \psi_{,21}Q1,k+\psi_{,22}Q2,k+\psi_{,23}Q3,k$
Accidental	$G1,k+G2,k+ A,d+\psi_{,11}Q1,k+\psi_{,22}Q2,k+\psi_{,23}Q3,k$

The partial safety coefficients are given in Table 2.4.

Table 2.4. Partial safety coefficient for variable actions

	$\psi,0$	$\psi,1$	$\psi,2$
Q,k service	0.7	0.7	0.6
Q,k wind/hand	0.6	0.5	0.0

2.4.2. Wind action on the structure

For wind action, we first calculate v,ref (reference velocity for 50years life) from Eq. 2.3, where v,ref,0 is gotten from the national reference wind map. In our case a web article was used (Mas'ud, 2020) and C,alt from British Standard (BSI, 2002)

$$v,ref = C,dir * C,temp * C,alt * v,ref,o \quad \textbf{(Eq. 2.3)}$$

The next calculation is that of reference wind pressure q,ref in Eq. 2.4.

$$q,ref = 0.5 * \rho,air * v,ref^2 \quad \textbf{(Eq. 2.4)}$$

The formulas for C,r(Z,w) and C,e(Z,w), Z,w being function of building geometry were calculated with Eq. 2.5, Eq. 2.6 and Eq. 2.7.

$$C,r(Z,w) = K,r * ln(^{max(Z,w;Z,min)}/_{Z,o}) \quad \textbf{(Eq. 2.5)}$$

$$C,e(Z,w) = (C,r(Z,w)^2 * C,t^2) + (7C,r(Z,w) * K,r * C,t) \quad \textbf{(Eq. 2.6)}$$

$$Z,w = f \quad \textbf{(Eq. 2.7)}$$

The values of K,r, Z,min and Z,o is gotten for a category III site considered in suburban zone of the city of Yaoundé (considering availability of space).

Depending on the wind direction, the coefficient of external pressure (C,pe) on walls is gotten from Figure 2.1, considering a maximum value capped at +0.6 (L/h ,l/h>=4,), and A>10m², with value of e,w in Eq. 2.8.

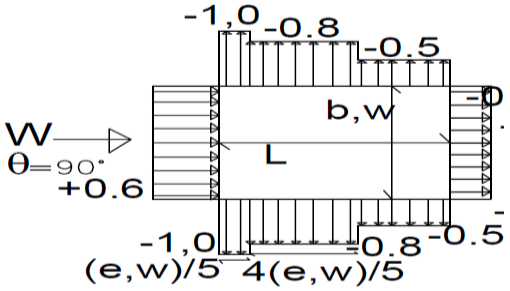

Figure 2.1. Coefficient of external pressure on walls

$$e,w = min(b,w; 2h) \quad \textbf{(Eq. 2.8)}$$

On the other side, the coefficient of external pressure for the curved roof is gotten from Figure 2.2, for wind parallel to gable walls (A=+0.22, B=-0.82, C=-0.4).

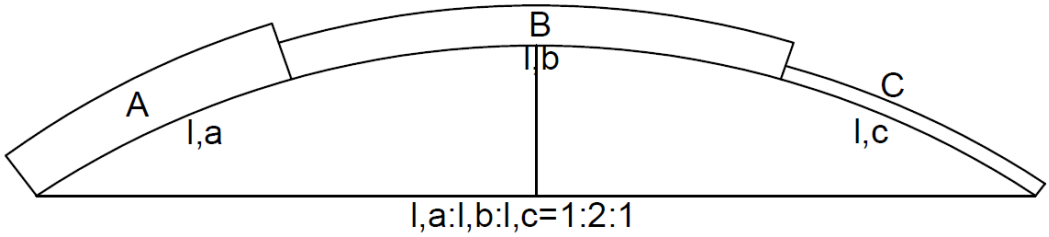

Figure 2.2. Diagram for C,pe of curved roof

The value of C,pi is affected by the presence of openings and the permeability of walls, so for every buildings with normally closed doors and windows, generalised values is taken for calculations.

We then now calculate wind pressures W,i and W,e, with Eq. 2.9 and Eq. 2.10.

$$W,e = q,ref * C,e(Z,w) * C,pe \quad \textbf{(Eq. 2.9)}$$

$$W,i = q,ref * C,e(Z,i) * C,pi \quad \textbf{(Eq. 2.10)}$$

Where C,e(Z,i) is calculated using same formula as for C,e(Z,w), but replacing Z,w by Z,i. Zi depends on the openings mean height on each wall as follows with window (left), doors (centre and right) on Figure 2.3.

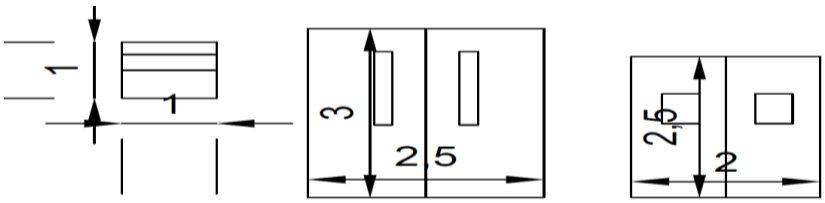

Figure 2.3. Openings geometry (in meters)

Finally the total wind pressure is calculated for all faces of the building as the net difference of the two wind pressures above (Eq. 2.11).

$$W,tot = W,e - W,i \quad \textbf{(Eq. 2.11)}$$

2.4.3. Effect of actions

The effects of actions (M, V, N, σ) are gotten from numerical analysis using SAP2000. We show in tables the results of numerical analysis from which we carry out verification and report them. Formulas for shear stress and torsional moment was given later-on, while bending moment is calculated by hand, using the formula of maximum moment for simply-supported elements (Eq. 2.12).

$$M = {ql^2}/{8} \quad \textbf{(Eq. 2.12)}$$

The flexural stresses are gotten from Euler-Bernoulli theory in Eq. 2.13, considering the centroid axis at mid height of elements;

$$\sigma = {N}/{A} \pm {M,z * y}/{I,z} \pm {M,y * z}/{I,y} \quad \textbf{(Eq. 2.13)}$$

For curved beam particularly, the necessary solicitation parameters were obtained from SAP2000, For three-hinged arch (assumedly the structure with fictitious restraining horizontal force at roller abutment equal to that of pinned abutment as arch is instantaneously fixed) we can calculate reaction and solicitation parameters with Eq. 2.14 to Eq. 2.21.

$$V,i = -H * sin\alpha + V,b * cos\alpha \quad \textbf{(Eq. 2.14)}$$

$$R,l = q * l/2 \quad \textbf{(Eq. 2.15)}$$

$$H = {q * l^2}\Big/{8 * f} \quad \textbf{(Eq. 2.16)}$$

$$N = {q * l^2}\Big/{8 * f} * cos\alpha + {q * l}/{4} * sin\alpha \quad \textbf{(Eq. 2.17)}$$

$$M,\left(\frac{1}{4} * l\right) = 0 \quad \textbf{(Eq. 2.18)}$$

$$V,(x = o) = V,spring = {q * l^2}\Big/{8 * f} * sin(\alpha,spr) + {q * l}/{2} * cos(\alpha,spr) \quad \textbf{(Eq. 2.19)}$$

$$\alpha,spr = {180}/{\pi} * arctan({2 * f}/{l}) \quad \textbf{(Eq. 2.20)}$$

$$V,\left(\frac{l}{2}\right) = 0 \quad \textbf{(Eq. 2.21)}$$

For second order effect M is calculated manually using Eq. 2.22.

$$M'' = \frac{M,o}{1 - {H}/{H,cr}} \quad \textbf{(Eq. 2.22)}$$

The effects of actions on curved beams are shown in Figure 2.4.

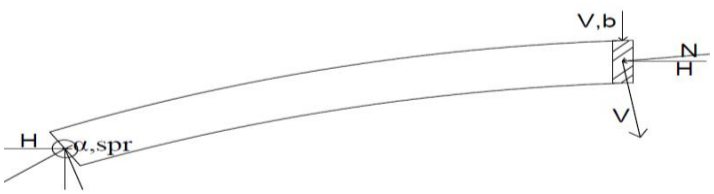

Figure 2.4. Effects of action on curved element

Since the fictitious restraining horizontal load at roller abutment is unknown and requires further calculation, the use of FEA software already integrates this force and also second order effects on the structure when running analysis. This one why we directly get solicitation parameters from SAP2000.

The method for calculating σ (flexural stress) in curved beams is quite different from straight beams. We have for symmetric-regular sections (conferring figure II), the Eq. 2.23 to Eq. 2.25.

$$\sigma = \frac{M}{A*e} * \frac{y}{R,n-y} \quad \textbf{(Eq. 2.23)}$$

$$R,n = {}^{h}\Big/_{\ln({}^{R,o}\Big/_{R,i})} \quad \textbf{(Eq. 2.24)}$$

$$y = R,o - R,n \quad \textbf{(Eq. 2.25)}$$

The theory of bending in curved elements is shown (for negative moments we change direction of M and fibre is intrados) in Figure 2.5.

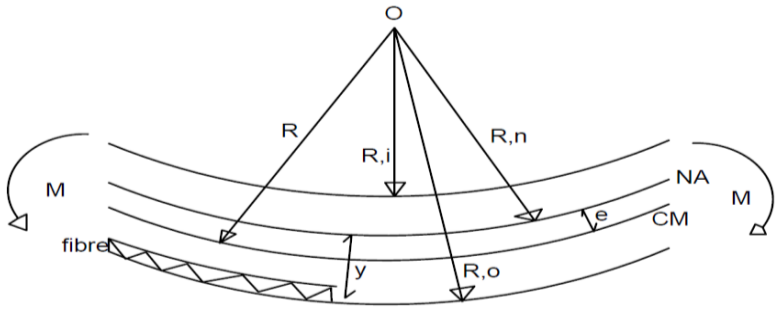

Figure 2.5. Curve flexural stress theory for positive moments

Also, still for curved beam theory we have to take note that corrosion alters section so the calculation must be revised in corrosion combination.

The dynamic effect of actions are so small that a dynamic calculation is not necessary (STEP1).

2.4.4. Volumetric properties of wood

The effect of shrinkage is non-negligible in wood structures and affect all other properties of GLT but for creep. The variation of the base or height of section can be calculated using Eq. 2.26, applicable for water contents from 5%-20%.

$$h,2 = h,1\left[1 + {}^{\beta}\Big/_{100} * (|w,2 - w,1|)\right] \quad \textbf{(Eq. 2.26)}$$

Also as important, is the effect of differed water content between top and bottom of beam elements. The differential shrinkage or enlargement between the internal and external fibres (with respect to the beams with different water contents due to environment) produces an initial bow or counter-bow given by Eq. 2.27 and Eq. 2.28.

$$u = {\kappa l^2}/{8} \quad \textbf{(Eq. 2.27)}$$

$$\kappa = {-\Delta\varepsilon}/{h} \quad \textbf{(Eq. 2.28)}$$

2.4.5. Mechanical properties of wood

The analysis in SAP2000 is based on linear properties of Glued-laminated timber. Any modification factor on mechanical properties is input in SAP2000 during material definition. The mechanical properties of GLT are gotten from TROPIX 5.0 with unauthorized public disclosure (CIRAD, 2003), from prEN 1194 and EN 338 both cited in EC5. The choice of resistance class depends on the combination of economic and safety reasons for optimal design.

2.4.6. Traction

This consists in verifying that the geometries assigned for preliminary design are in favour of safety in both ULS (and also SLS). The design values for the resistances (f,t,0,d, f,t,90,d, f,t,90,d,vol, f,t,α,d,) of elements are respectively given by Eq. 2.29 to Eq. 2.32.

$$\mathrm{f,t,0,d} = {\mathrm{K,mod} * \mathrm{f,t,0,k}}/{\gamma,\mathrm{wood}} \quad \textbf{(Eq. 2.29)}$$

$$f,t,90,d = {K,h * K,mod * f,t,90,k}/{\gamma,wood} \quad \textbf{(Eq. 2.30)}$$

$$f,t,90,d,vol = K,dis * \left[\left({V,0}/{V}\right)^{0.2}\right] * f,t,90,d \quad \textbf{(Eq. 2.31)}$$

$$f,t,\alpha,d = K,mod * \left[\frac{f,t,0,k * f,t,90,k}{(f,t,0,k * sin^2\alpha) + (f,t,90,k * cos^2\alpha)}\right] / \gamma, wood \quad \textbf{(Eq. 2.32)}$$

The maximum values of the acting stresses (σ,t,90,d, σ,t,0,d), are gotten from SAP2000 as previously mentioned with building under ULS/SLS loading. The oblique stress (σ,t,α,d) is gotten as the resultant of the tangential and axial stresses.

The general verification to be carried is if the design value of the acting stresses are less than or equal to the resistant stresses. For traction orthogonal to fibres, we check whether the design value of acting stresses are less than or equal to volumetric resistant stresses.

2.4.7. Compression

This consists in verifying that the geometries assigned for preliminary design are in favour of safety in both ULS (and also SLS). The design value for the resistances (f,c,0,d, f,c,90,d f,c,90,d,vol, f,c,α,d) of elements is given by Eq. 2.33 to Eq. 2.36.

$$\mathrm{f,c,0,d} = {}^{\mathrm{K,mod} * \mathrm{f,c,0,k}}/_{\gamma,\mathrm{wood}} \quad \textbf{(Eq. 2.33)}$$

$$f,c,90,d = {}^{K,h * K,mod * f,c,90,k}/_{\gamma,wood} \quad \textbf{(Eq. 2.34)}$$

$$f,c,90,d,vol = K,c,90 * f,c,90,d \quad \textbf{(Eq. 2.35)}$$

$$f,c,\alpha,d = K,mod * \left[\frac{f,c,0,k * f,c,90,k}{(f,c,0,k * sin^2\alpha) + (f,c,90,k * cos^2\alpha)}\right] / \gamma, wood \quad \textbf{(Eq. 2.36)}$$

The maximum values of the acting stresses (σ,c,90,d, σ,c,0,d), are gotten from SAP2000 as previously mentioned with building under ULS/SLS loading. The oblique stress (σ,c,α,d) is gotten as the resultant of the tangential and axial stresses.

The general verification to be carried is if the design value of the acting stresses are less than or equal to the resistant stresses. For localised compression we check whether the design value of acting stresses are less than or equal to volumetric resistant stresses.

2.4.8. Combined shear and perpendicular traction

For combined shear and perpendicular traction of curved beams we need to verify (for K,dis=1.4) in Eq. 2.37 to Eq. 2.39.

$$\tau,\mathrm{d}/_{\mathrm{f,v,d}} + ({}^{\sigma,\mathrm{t},90,\mathrm{d}}/_{\mathrm{K,dis} * \mathrm{K,vol} * \mathrm{f,t,90,d}}) \leq 1 \quad \textbf{(Eq. 2.37)}$$

$$K,vol = \left({}^{0.01}/_{V}\right)^{0.2} \ (< 1\ for\ SLS) \quad \textbf{(Eq. 2.38)}$$

$$\sigma,t,90,d = {}^{h * \sigma,m}/_{4 * r} \ (r \geq 5m) \quad \textbf{(Eq. 2.39)}$$

The value of K,r=r,in/t is gotten from Table 2.5.

Table 2.5. Table of values of K,r

r,in/t	K,r
Greater or equals 240	1
Less than 240	0.76+0.001(r,in/t)

2.4.9. Flexion in beams

For curved beam flexion, we need to consider the axial critical load N,cr, (with l,eff=1.25s) given by Eq. 2.40.

$$N, cr\ (\frac{l}{4}) = \frac{\pi^2 * E * I}{1.17 * s^2} \quad \textbf{(Eq. 2.40)}$$

The resistance of in flexion is calculated from equation 2.41.

$$f, m, d = {}^{K, mod * f, m, k}/_{\gamma, m} \quad \textbf{(Eq. 2.41)}$$

In the case of uniaxial flexure we check that the acting flexure in any direction is less than the resistant flexure. In the case of biaxial flexure, the stresses should validate the following checks in Eq. 2.42 and Eq. 2.43.

$$\mathrm{K, m} * \left({}^{\sigma, \mathrm{m, y, d}}/_{\mathrm{f, m, y, d}}\right) + ({}^{\sigma, \mathrm{m, z, d}}/_{\mathrm{f, m, z, d}}) \leq 1 \quad \textbf{(Eq. 2.42)}$$

$$\left({}^{\sigma, m, y, d}/_{f, m, y, d}\right) + K, m * ({}^{\sigma, m, z, d}/_{f, m, z, d}) \leq 1 \quad \textbf{(Eq. 2.43)}$$

For curved beams checks to be carried out consider N,cr,(l/4). It is gotten from first other analysis using linear elasticity theory, also considering finite elements of the curve and second order analysis due to differential strain from software. If the axial load acting does not exceed we verify Eq. 2.44 and Eq. 2.45.

$$\left({}^{\sigma, \mathrm{m, y, d}}/_{\mathrm{K, cr} * \mathrm{K, r} * \mathrm{f, m, y, d}}\right)^2 + ({}^{\sigma, \mathrm{c, o, d}}/_{\mathrm{K, c, z'} * \mathrm{f, c, o, d}}) \leq 1 \quad \textbf{(Eq. 2.44)}$$

$$\left({}^{\sigma, \mathrm{c, o, d}}/_{\mathrm{K, c, z'} * \mathrm{f, c, 0, d}}\right) + 0.7({}^{\sigma, \mathrm{m, y, d}}/_{\mathrm{K, r} * \mathrm{f, m, y, d}}) \leq 1 \quad \textbf{(Eq. 2.45)}$$

2.4.10. Stability of beam elements

The factor of stability K,cr depends on relative slenderness λ,rel,m (Eq. 2.46 to Eq. 2.48).

$$\lambda, rel, m = \sqrt{({}^{f, m, k}/_{\sigma, m, crit})} \quad \textbf{(Eq. 2.46)}$$

$$\sigma, m, crit = {}^{0.75 * E, 0.05 * b^2}/_{h * l, eff} \quad \textbf{(Eq. 2.47)}$$

$$\sigma, \mathrm{m, crit} > \sigma, \mathrm{c, max} \quad \textbf{(Eq. 2.48)}$$

The value of K,cr as function of relative slenderness is obtained from Table 2.6.

Table 2.6. Values of K,cr with respect to relative slenderness

λ, rel, m	K,cr
Less than or equal to 0.75	1
Between 0.75 and 1,4 inclusive	1.56-(0.75* λ, rel, m)
Above 1.4	1/(λ, rel, m^2)

The check to be carried out here is Eq. 2.49.

$$\sigma, m, z, d \leq K, cr * K, inst * f, m, z, d \quad \textbf{(Eq. 2.49)}$$

For curved beam, if N,cr,(l/4) is exceed, (K,c,y =1 for 2nd order analysis) we verify Eq. 2.50.

$$\left({}^{\sigma, m, y, d}/_{K, r * f, m, y, d}\right) + ({}^{\sigma, c, o, d}/_{K, c, y * f, c, 0, d}) \leq 1 \quad \textbf{(Eq. 2.50)}$$

2.4.11. Shear and torsion

For appropriate section of elements (all rectangular), the acting shear stress is gotten from SAP2000 (Eq. 2.51) and is verified using Eq. 2.54.

$$\tau, v = {}^{3 * V, max}/_{2 * A} \quad \textbf{(Eq. 2.51)}$$

Torsion is calculated using the formula for rectangular sections in Eq. 2.52.

$$\tau, tor = {}^{M, tor}/_{\alpha * h * b^2} \quad \textbf{(Eq. 2.52)}$$

The checks to be carried out are Eq. 2.53 and Eq. 2.54.

$$\tau, tor \leq f, v, d \quad \textbf{(Eq. 2.53)}$$

$$\tau, v \leq f, v, d \quad \textbf{(Eq. 2.54)}$$

2.4.12. Combined shear and torsion.

In the case of combined shear and torsion (where f,tor,d is taken as f,v,d for conservativeness) we check with Eq. 2.55.

$${}^{\tau, tor, d}/_{f, tor, d} + ({}^{\tau, v, d}/_{f, v, d})^2 \leq 1 \quad \textbf{(Eq. 2.55)}$$

2.4.13. Influence of semi-rigid node rotation on structural elements

The main beams have already been analysed as simply supported with no reduction of constraints in favour of safety. The joists form the non-rigid plane which is partly restrained rotation by imposing lateral bracings, so no effect of rotation is calculated here. The factor β is then multiplied by σ, c, o, d and calculation from equations II-55 to II-61 are repeated for verification. In SAP2000 the effects of action are gotten for static loading.

2.4.14. System effects

There exist an amplification factor for resistance (K,l,s) for small-sloped roof. This factor applies only for members which carry continuous loads. This factor has to be included in its flexure verification.

2.4.15. Lateral bracing design and analysis

The load in the lateral bracings carries exceeding moment (instability moment of joists and girts) as axial load. We are going to use thin glulam sections for cross bracing for the structure, so we need to design sections that the system resists maximum load. The maximum axial load could be calculated using Eq. 2.56.

$$N,d = (1 - K,cr) * {}^{M,d}/_{h} \quad \textbf{(Eq. 2.56)}$$

Since the structure is very large we could get it directly from running analysis of pre-designed and adjusted structure in SAP2000. Area of bracings is calculated directly from SAP2000 running analysis values together with tensile and compressive design resistance

2.4.16. Buckling-based design and analysis of columns

The calculations in any principal transversal direction (local y, z axes of elements) are given, and Eq. 2.57 to Eq. 2.60 was recalculated replacing y by z.

$$i = \sqrt{({}^{I,hom}/_{A,hom})} \quad \textbf{(Eq. 2.57)}$$

$$\lambda,y = {}^{L,eff}/_{i,y} \quad \textbf{(Eq. 2.58)}$$

$$\sigma,crit,y = \pi^2 * {}^{E,0.05}/_{\lambda,y^2} \quad \textbf{(Eq. 2.59)}$$

$$\lambda,rel,y = \sqrt{({}^{f,c,0,k}/_{\sigma,crit,y})} \quad \textbf{(Eq. 2.60)}$$

For λ,rel,y and λ,rel,z less than or equal to 0.5, we verify respectively Eq. 2.61 and Eq. 2.62. Stresses and deflections from SAP2000 (static analysis) and hand calculation are to be used used for theses verifications.

$$({}^{\sigma,c,o,d}/_{f,c,o,d})^2 + {}^{\sigma,m,y,d}/_{f,m,y,d} + {}^{K,m * \sigma,m,z,d}/_{f,m,z,d} \leq 1 \quad \textbf{(Eq. 2.61)}$$

$$({}^{\sigma,c,o,d}/_{f,c,o,d})^2 + {}^{K,m * \sigma,m,y,d}/_{f,m,y,d} + {}^{\sigma,m,z,d}/_{f,m,z,d} \leq 1 \quad \textbf{(Eq. 2.62)}$$

For λ,rel,y and λ,rel,z greater than 0.5, we verify respectively Eq. 2.63 and Eq. 2.64.

$$\sigma,c,o,d/_{K,c,z*f,c,o,d} + {}^{K,m*\sigma,m,y,d}/_{f,m,y,d} + {}^{\sigma,m,z,d}/_{f,m,z,d} \leq 1 \quad \textbf{(Eq. 2.63)}$$

$$\sigma,c,o,d/_{K,c,y*f,c,o,d} + {}^{\sigma,m,y,d}/_{f,m,y,d} + {}^{K,m*\sigma,m,z,d}/_{f,m,z,d} \leq 1 \quad \textbf{(Eq. 2.64)}$$

The value of K,c,y or K,c,z is given by Eq. 2.65 and Eq. 2.66, replacing y by z.

$$K,c,y = \frac{1}{K,y+\sqrt{(K,y^2-\lambda,rel,y^2)}} \quad \textbf{(Eq. 2.65)}$$

$$K,y = 0.5*[1+\beta,c*(\lambda,rel,y-0.5)+\lambda,rel,y^2] \quad \textbf{(Eq. 2.66)}$$

The deflection of columns is calculated and checked for using Eq. 2.67.

$$u,max < {}^{h}/_{500} \quad \textbf{(Eq. 2.67)}$$

2.4.17. Notched beam under shear

Figure 2.6 gives a representation of a notched beam under tangential whear.

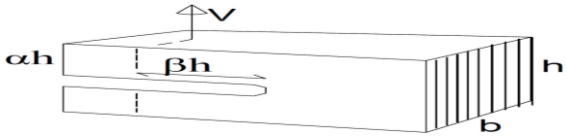

Figure 2.6. Notched beam end with orthogonal traction

The notch appears at abutments and ridge node. It reduces shear acting on the beam and is materialised by a shear reduction factor K,v in Eq. 2.68.

$$K,v = \frac{K,n*(1+{}^{1.1*i^{1.5}}/_{\sqrt{h}})}{\sqrt{h}*(\sqrt{(\alpha}-\alpha^2)+0.8*\beta*\sqrt{({}^{1}/_{\alpha}-\alpha^2)})} \quad \textbf{(Eq. 2.68)}$$

The design shear stress and verification condition are respectively given by Eq. 2.69 and Eq. 2.70.

$$\tau,d = {}^{3*V,d}/_{2*b*\alpha*h} \quad \textbf{(Eq. 2.69)}$$

$$\tau,d \leq K,v*f,v,d \quad \textbf{(Eq. 2.70)}$$

2.4.18. Worn through beam

Similarly to notched beams, effect of holes in structural elements was analysed. There exist a coefficient of shear reduction due to the presence of holes in elements (K,hol). According to Carling Johanesson, K,hol is function of D/h (Table 2.7).

Table 2.7. Carling Johanesson relationship between D/H and K,hol

D/h	K,hol
Less than or equal to 0.1	1-555(D/h)^3
Greater than 0.1	1.62/(1.8+D/h)^2

If b>90mm, K,hol is multiplied by a factor (90/b)^0.2. To avoid cracks around the worn zone we use ply wood Glued around the hole(s) and nailed. The check to be carried out is either Eq. 2.71 or Eq. 2.72.

$$\tau, d \leq K, hol * f, v, d \quad \textbf{(Eq. 2.71)}$$

$$\tau, d \leq \left({}^{90}/_{b}\right)^{0.2} * K, hol * f, v, d \quad \textbf{(Eq. 2.72)}$$

2.4.19. Dowel joints under flexure

The eccentricity of joint elements from its centre of rotation generates additional moment at the joints which should be able to resist. A dowel ring connection is presented in Figure 2.7.

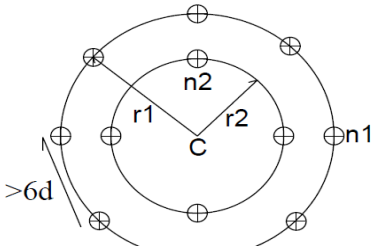

Figure 2.7. Circular connection type

Dowel calculations includes Eq. 2.73 to Eq. 2.77.

$$F, M = \frac{r, i}{\sum_{i=1}^{n}(n, i * r, i^2)} * M, u, d \quad \textbf{(Eq. 2.73)}$$

$$F, V = {}^{V, u, d}/_{\sum n, i} \quad \textbf{(Eq. 2.74)}$$

$$F, N = {}^{N, u, d}/_{\sum n, i} \quad \textbf{(Eq. 2.75)}$$

$$F, d = \sqrt{(F, M + F, V)^2 + F, N^2} \quad \textbf{(Eq. 2.76)}$$

$$F, V, d = \left(\frac{M, u, d}{\pi} * \frac{\sum n, i * r, i}{\sum_{i=1}^{n}(n, i * r, i^2)}\right) - \frac{V, u, d}{2} \quad \textbf{(Eq. 2.77)}$$

The check is given by Eq. 2.78.

$$F,d \ < F,v,d \qquad \textbf{(Eq. 2.78)}$$

2.4.20. Resistance of GLT finger joints

The effect of finger joints is analysed using necessary modification factors (Given the geometric data from figure II.8), using Eq. 2.79.

$$f,m,j,k,r = 1.3 * f,m,g,k \qquad \textbf{(Eq. 2.79)}$$

For the formula above we check Eq. 2.80.

$$f,m,j,k,r \geqslant f,m,j,k \qquad \textbf{(Eq. 2.80)}$$

The geometry of a multiple-splice finger joint (Figure 2.8) is shown in top view (max. 50mm thick slats).

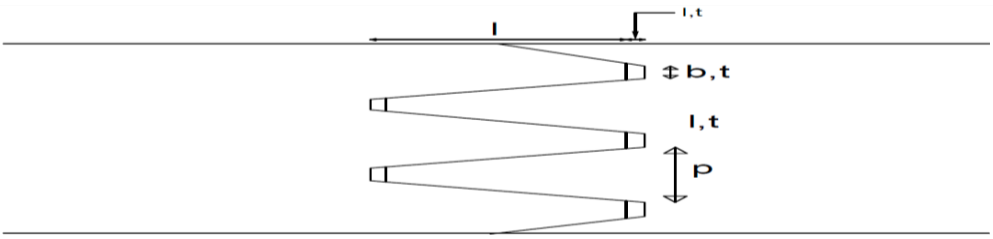

Figure 2.8. Multiple splice finger joint

The total surface of a finger joint must exceed 10 times that of the cross section of individual slats.

2.4.21. Deflection check

The deflection of beam elements is given by SAP2000 (static deflection) and could be calculated by hand. From Figure 2.9, a deflection value is given (u,max).

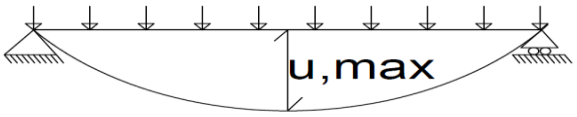

Figure 2.9. Simple-supported element maximum deflection

Under uniformly distributed load p, all elements are analysed as simply-supported beams as referred in condition above, except for curved beams. The max. deflection is given by Eq. 2.81.

$$\text{u, max} = (^{5}/_{384}) * (^{\text{p} * \text{l}^4}/_{\text{EJ}}) \qquad \textbf{(Eq. 2.81)}$$

For point load P applied at mid-section we have max. deflection given by Eq. 2.82.

$$u, max = (1/48) * (P * l^3/EJ) \quad \textbf{(Eq. 2.82)}$$

The verification to be carried out is given by Eq. 2.83.

$$l,0/500 \leq u \leq l,0/300 \quad \textbf{(Eq. 2.83)}$$

For curved beam flexure we have a maximum amplified deflection (δ,tot) given (Eq. 2.84).

$$\delta, tot = \delta, o / 1 - H/H, cr \quad \textbf{(Eq. 2.84)}$$

2.4.22. Creep

Under SLS rare combination, creep is the difference between final and instantaneous deflection. Our interest is the effect of creep in the long-term (maximum creep deflection, u,2 which acts on simply supported beam elements). It can be calculated with Eq. 2.85 to Eq. 2.87.

$$u, 2 = K, def * u, inst \quad \textbf{(Eq. 2.85)}$$

$$u, 2 \leq l/300 \quad \textbf{(Eq. 2.86)}$$

$$u, inst = u, 1 - u, 0 \quad \textbf{(Eq. 2.87)}$$

2.4.23. Corrosion safety verification

The main agent of corrosion which also affect structural properties of timber is chlorine gas. For calculation, the effective area considered is given in Eq. 2.88 from which necessary calculations was done. It includes a reduction up to 20mm inside structural elements.

$$\mathrm{A, eff, cor} = (\mathrm{h, max} - 40) * (\mathrm{b} - 40) \quad \textbf{(Eq. 2.88)}$$

2.4.24. Fire safety verification

The combination used in the design is the accidental combination from Table 2.2. We are going to design members assuming 4-side exposure which is the worst exposure case. Any thermo-mechanical properties of strength and stiffness are calculated from a general formulation. The different resistance classes for fire design are R15, R30 and R60.

The design value of a fire parameter is given by Eq. 2.89.

$$X, fi, d = K, mod, fi * K, fi * X, k/\gamma, M, fi \quad \textbf{(Eq. 2.89)}$$

The young modulus of fire design is calculated from Eq. 2.90.

$$E,fi,d = K,mod,fi * {}^{E,mean}/_{\gamma,m,fi} \quad \textbf{(Eq. 2.90)}$$

For fire design the effects of actions are affected by fire implementing a reduction factor (Eq. 2.91).

$$S,f,d = \eta * S,d \quad \textbf{(Eq. 2.91)}$$

The most economic methods of evaluating fire resistance of elements is through the method of effective sections and the method of reduced resistances and stiffness. For unprotected faces have formulas for d,eff (Eq. 2.92 and Eq. 2.93), which should be greater than 60% for bracings.

$$d,eff = d,char + K,0 * d,0 \quad \textbf{(Eq. 2.92)}$$

$$d,char = \beta,0 * t,fi,req \quad \textbf{(Eq. 2.93)}$$

The value of t,fi,req yields the value of K,0 in Table 2.8.

Table 2.8. K,0 as function of time

t,fi,req	<20min	≥20min
K,0	t,fi,req/20	1.0

The considered area through the method of effective sections for four-sided exposure is given by Eq. 2.94.

$$A,eff = (h,max - 2 * d,eff) * (b - 2 * d,eff) \quad \textbf{(Eq. 2.94)}$$

The areas obtained from preliminary design were all used to redesign the building under fire resistance.

Due to the use of R>15 fire class, and similar connections, there is an adjustment of joint hole spacing due to fire resistance for a1,a2,a3 and a4 as shown in Table 2.9.

Table 2.9. Table for spacing increment

	a,1 and a,2	a,3 and a,4	
		<β,0*(t,fi,req+15)	≥β,0*(t,fi,req+15)
a,fi (mm)	β*(t,fi,req-15)	β*(t,fi,req-15)	0

Fire resistance constraints on thickness of laterally jointed GLT members. The parameters for calculating this influence are Eq. 2.95 to Eq. 2.98.

$$t,1 \geq {}^{t,fi,req}\Big/_{(1.25-\eta,n)} \quad \textbf{(Eq. 2.95)}$$

$$\mathrm{t,1} \geq 1.6 * \mathrm{t,fi,req} \quad \textbf{(Eq. 2.96)}$$

$$\mathrm{t,1} \geq \mathrm{t,1,min} + \mathrm{a,fi} \quad \textbf{(Eq. 2.97)}$$

$$\eta = \eta,30 * ({}^{30}\Big/_{\mathrm{t,fi,req}})^2 \quad \textbf{(Eq. 2.98)}$$

For internal metal plates, for resistance class R30, a minimum thickness of 2mm and minimum width of plate of 200mm is necessary. For external plates, if $\eta \leq 0.45$ a minimum of 6mm thickness is required.

The limits of the numerical analysis were the insufficient data available concerning tropical timber mechanical properties, the limited scope of study (numerical analysis and spatial timber reticular structures) which gave no room for detail verification and detail solution proposition, and finally the problem of convergence (finding the correct geometry of structural elements with least structural parameters and least deformations), so as to find optimal reticular structure design.

Conclusion

Concerning results depending on the CAE software, results were gotten from step-by-step calculation and numerical assessment of the structure. When the results converged (when numerical results verified all necessary checks or when variation of geometric property didn't ameliorate results or even worsened them), the geometry designed was adopted. In addition, at some points illustration of interpretations was necessary. This was done by presenting generalised figures and much literary explanations for secondary members which were very numerous to be represented individually. For main structural elements it was illustrated more detailed figures and further literary explanations. Head now to the presentation of these results and interpretations.

CHAPTER 3 : RESULTS AND INTERPRETATIONS

Introduction

The design an numerical analysis of a GLT Olympic swimming facility arc building entails succinct description of structural analysis, which was used for step-wise verification of numerical models and was based mainly unless otherwise stated, on the STEP1 manual as translated; WOODEN STRUCTURES AT LIMIT STATES Introduction to Eurocode 5 STEP 1 Materials and basis for calculation (SEDIBOIS, 1996) and GLULAM BAND BOOK (GLULAM HANDBOOK FRANCE, 2020). Data for software analysis was input from personal theoretical knowledge, further enhanced by documentary research. The type of numerical analysis which was performed was FEA and more specifically simple linear FEM (By exploiting only linear elastic properties of GLT). Simulations was carried out using CAE software SAP2000v21, designing done with Revit 2014 and other numerical applications with Excel 2013. The results and interpretations were centred on the different study areas mentioned in the methodology.

3.1. Design elements

These are the bases on which the structural model will rely on, and lead to the obtainment of a numerical design model in SAP2000v21. This gave specific knowledge on what was to be designed, increasing its reliability.

3.1.1. Presentation of the structural typology

There are five structural typologies; solid, frame, shell, membrane and composite structures. We are concerned here with a “frame structure”. The term “spatial timber reticular structure” refers to a net-like connection of frame elements made up of timber in 3D space. A frame is described according to Chegg Study as an engineering structure of different shapes (curved or straight) containing a multi-force member (has equals or more than three acting forces). It is a combination of beams, columns and slabs which resists moments due to external loading and are of two types; rigid and non-rigid (Chegg, 2020) Also, there are two classes of frames; rigid and braced, which are further subdivided into pinned and fixed end frame for the former, whilst portal and gabled frame for the later (Hamakareem, 2020). The building is a globally free to expand across building structure with allowance for a certain degree of displacements (at abutment on one side of building. It is a combination of roller pinned-end non-rigid frames (one planar constraint free on one abutment side) and two gable frames at edges. There has to be

provided roller support for all contacts to the ground in direction perpendicular to curved frame in order to have a more optimal frame element design.

Since the structure is made of three hinged curved frames with one roller abutment (hypostatic in their respective planes), the roof is therefore **not fixed** in direction parallel to curved frame planes. Roller supports in perpendicular direction at base of any elements in contact with ground makes the building **not fixed** in that direction despite any bracing due to its largeness. Other conditions influencing roof fixity are; the stiffness of the curved beams constituting each frame which affects buckling of beams and the rigidity of the ridge joint which have as effect impeachment of relative rotation between the two roof sides, apart from thermal and humidity-related variation. The rift joint is analytically a pin joint but practically a rotationally fixed one (a condition lying between the two given the type of connection, because using pinned connectors makes it rotation-free). With all these considerations the global structure is considered non-rigid.

In order to have appreciation of the applicability of GLT on real structures, we observed real-life construction projects. Bhygraph Engineering is a principal stakeholder at different construction sites we visited. It is a limited liability company headed by Mr. Léandre KUIATE. This company was kind to open us doors. A total of three different construction projects where visited (Annex 15). They were all roof structures, one with curved geometry and others with linear truss geometry. Appreciation was in terms of materials used, construction technology employed for each roof type and section geometry (for the Saint Vincent Palotti Parish, were we had access to the roof structure and data from Bygraph personnel).

3.1.2. Architectural parametrization

The utility, functionality, geometry and material constraint of the building forecasts its design. The building is a shelter for swimming pool so it was opted to design a hangar for an Olympic-size pool assuming a relatively flat terrain. Figure 3.1 illustrates the pool hall plan.

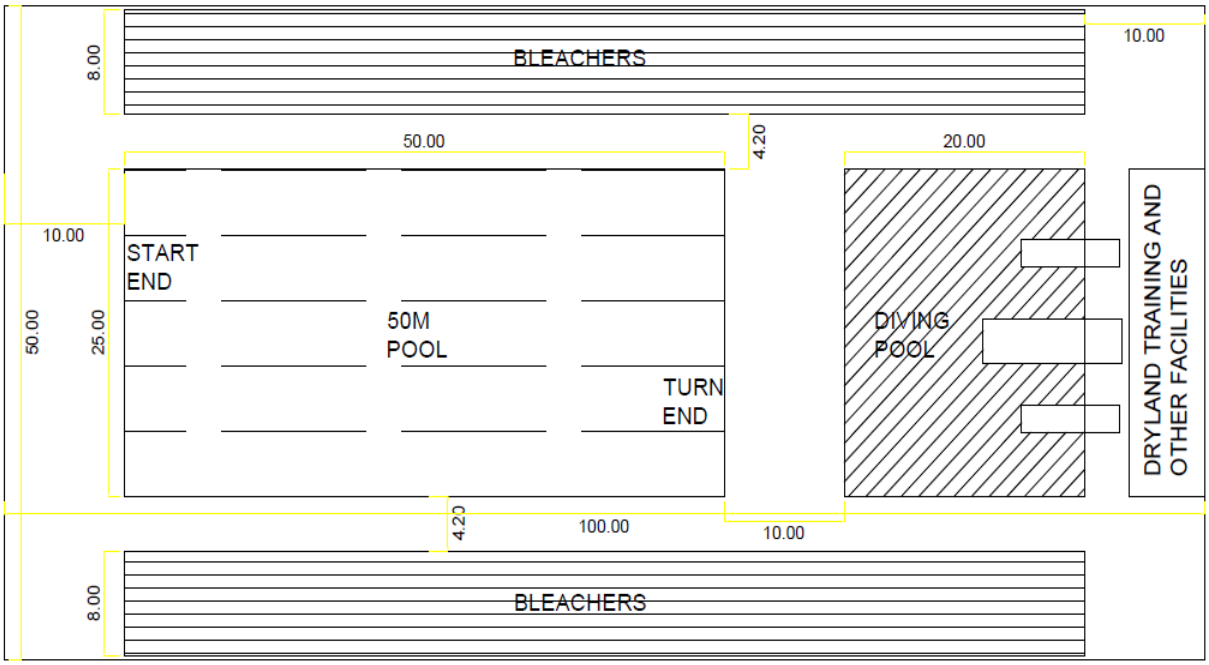

Figure 3.1. Plan view of Pool Hall

Dimensions for the building plan were obtained from Sports England and FINA recommendations. The former necessitated 7m from start end to close border, a 4m wide space from pool edges to bleacher wall and at least 5m wide space after the turn end (SPORTS ENGLAND, 2011). The latter recommended the lengths and widths of both pools, the 10m separation between them, a 4.5m break off diving pool edge for largest (10m) diving platform, and a 8.66m long dryland training hall (FINA, 2017). Geometric constraints in the transverse plan such as a 30° maximum comfortable view from spectator with eye-to-floor average distance of 1.32m, led to the adoption of pool sideways of 4.2m close to the 4m previously mentioned and a bleacher of 8m wide to leave a margin of 0.8m for curved beam height limitation. The beam span greater than 30m implies use of finger joints (GLULAM HANDBOOK FRANCE, 2020). The 10m width was used on both ends of the field greater than expected respective 7m and 4.5m to correspond the curved beam floor-projected length. The plan gives a 50mX100m rectangle for the hall, and a total 100mx100m building floor plan.

The transvers superstructure view show a symmetric building about central vertical axis (Figure 3.2).

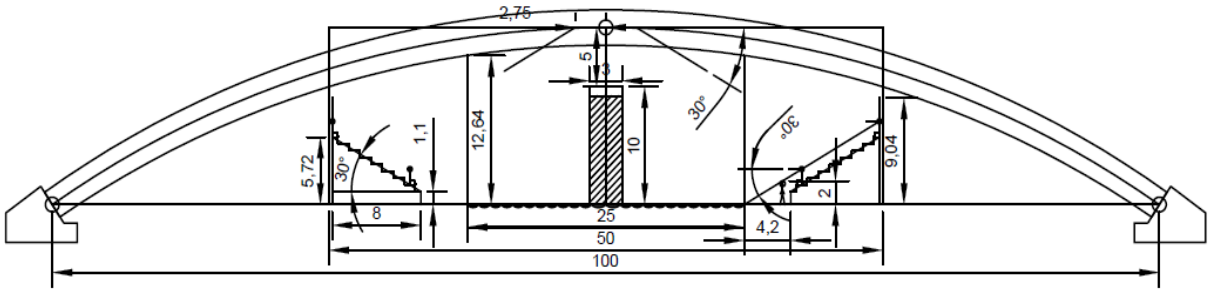

Figure 3.2. Building transverse section showing swimming hall in a box.

It is proceeded with elevation recommendations by FINA. A 5m height above 10m diving platform at centre of plan is required (located here because it is the tallest internal space available). At 2.75m offset from centre on both left and right at 15m high, a maximum slope of 30° with the horizontal is necessary for any obstruction of space from the roof. A 12.64m (varies a little due to deflection) free height was gotten at the pool side which is greater in any case than 7m required Room for dryland training is at least 5.7m from floor level we choose any position outside hall (FINA, *op.cit.*). The height at ridge is 15m from beam central axis. For straight elements according to the AIRM (AIRM, 2020), a "flat roof" describes a roof with slope less than 1.5° and even less than higher up to 5° (Eurocode Applied, 2020). From Bauder, a minimum slope of 1/40 is required to avoid ponding (Bauder, 2020). The roof of the structure is parabolic so is not subjected to ponding. The choice of this geometric type minimises deflection due to lengthy constraint of main beam (100m). Using the 8m wide bleacher and its 30° slope, we got a 9.04m high minimum useful height (including a 2m margin) which is less than hall side wall height 9.84m.

According to DOUBLET and having the following entries; bleachers dimension 80mX8mX7.94m, sports hall stand, fixed grandstand and shell with backrest type of seat yields an average of 3036 seats for both stands (DOUBLET, 2020). For 3m high exit doors (for maximum vertical objects such as folded trampoline); eight 2.5m and two 2m wide (can accommodate two wheelchairs side past), opening to fire safe outdoors, an exit capacity of 2866 people was gotten using a hall volume (approximated to the 15mx50m box) which is the maximum occupancy since it is smaller than the current occupancy of 3036 people (Merton council, 2020). The number of seats adjusted due to openings (reduced number) will compensate the disparity between the previous numbers of people.

For a hall volume of about 2476000ft3 (70100m3), in the HVAC system, for the air change rate/hour of an auditorium (12/hr), the CFM per person for 2866 people is about 173 (Falke, 2016). This value by far outnumbers the 15 CFM per person, recommended ventilation for good

indoor air quality (Bhatia, 2020). The excess volume will compensate for material volumes occupying internal space.

As concerns windows, 2% floor area is required for cross ventilation of deep plan buildings (Bhatia, 2020). The building swimming hall floor area is 5000m², implying 100m² window openings (i.e. 100 1mx1m window size). The building then has four 3-m tall doors and 50 windows on each side (facing north and south in prevailing wind direction) and only a 2.5m tall door on each gable end walls without windows. The windows on the roof was placed at a height from the ground projecting to the uppermost portion of the hall side wall as it not only serves natural ventilation for human comfort but also evacuation of accumulating evaporated chloride concentration beneath structural elements directly exposed to.

Architectural considerations enabled us to proceed to the next step which is structural model design.

3.1.3. General overview of interview-collected data for design

Some data was obtained by interview through a personnel member of Bhygraph Engineering by name Mr. MESSE. It was obtained the thickness of stripes depend on wood essence (‘Movingui’ for straight elements with good adhesiveness to gluing and ‘Ayous’ for curved elements for its greater flexibility) and the power of pressure machine. It was also gotten that Cameroon is mainly populated by hardwoods, also gotten a reference website for wood construction (www.bois.com), under legal notice of usage CIRAD booklets on tropical wood species containing most physical and mechanical properties of tropical woods. In addition, locations of other realized structures were obtained, the fact that metallic angles were prefabricated on-site gotten and finally, some geometric data for preliminary element design and joint design was given. We were also presented some machines for GLT manufacture in Annex 16. Identification was done with the assistance of Mr. Igor NJIA, a worker at Bygraph Engineering. Confer Annex 1 containing a picture of a form machine (www.glued-laminated-timber.com, 2020).

3.1.4. Geographical context

The geographical context is important, as it directly influences wind forces on the building. The required site for the project was based on a pre-existing similar structure’s site characteristics. The Saint Vincent Palloti Parish is found in the neighbourhood of Nlongkak in Yaoundé, the political capital of Cameroon. Also, the city has as coordinates (3.70899°, 11.36133°) N-S, (4.02899°, 11.68133°) E-W, with an average elevation of 718m.a.m.s.l. The altitude onsite is about 760m.a.m.s.l (topographic-map.com, 2020). The average temperature

ranges from 19.2°c-31°c, the average humidity from 79%-86% (Weather-Atlas, 2020), and the maximum monthly wind speed 19km/hr and annual prevailing wind from the North (Freemeteo, 2020). All these conditions were used for the design.

All the important design elements for design have been considered such as the structural typology, architectural parameters, interview-data overview and the geographical context. The next step is to define building material properties.

3.2. Material properties

The most important GLT properties for building design are its physical (volumetric) properties (solid and laminated densities, volumetric coefficients and strain) and its mechanical properties (strengths, Young and shear moduli, Poisson coefficients), have direct influence on building solicitations and motility.

3.2.1. Volumetric properties of wood

Volumetric properties are one of the most important aspects to be considered when designing with wood, as it greatly affects design due to the nature of wood itself (variable density and water content) as function of environmental conditions (humidity and temperature). Each factors affecting wood volumetric properties was considered in here. When choosing values of constants at 12% water content from their ranges found in CIRAD or other documents, we chose mean values for dependent constants (β,v depending on volume of element, target moisture content depending on stocking conditions), lower bound values for independent constants like ρ and upper bound values for other independent constants (ε,tan and ε,rad.).

In SAP2000, the effect of shrinkage or enlargement is calculated by hand. The characteristic density (ρ,g,k) of Glued laminated timber depends upon its resistance classes and is given in EC5 for a temperature of 20° and a relative humidity of 65% implying on site climatic conditions for execution and service must be approximate to this temperature and relative humidity. This is done so by ensuring proper ventilation and protection of the structure. As cited from prEN 1194 (September 1993) the resistance class of GLT calculated with ρ,k and from EN 338 we calculate the resistance classes of the component solid timer stripes and their ρ,k. Fire resistance entails the use of ρ,g,k minium of 350kg/m3 for hardwood. ρ,l,k,min (Movingui)=667.99kg/m3 (implying ρ,g,k=634.59kg/m3) ; ρ,l,k,min (Ayous)= 329kg/m3 (implying ρ,g,k=312.56 kg/m3 assumed relatively close to the target) and any other material to be used was specified later. The density used for calculation is a minimum density since it is subject to greater volumetric and differential strains.

Given the average monthly high and low temperatures of Yaoundé respectively 31°c and 19.2°c and average monthly relative humidity between 79% and 86% (Weather-Atlas, 2020), humidity-moisture relationship is applicable since the obtained equilibrium moisture contents vary within the range previously mentioned. We got these moisture contents from average sorption isotherms for wood, which were gotten from EMC table. There is a fair scientific relationship of all woods, between moisture, relative humidity and temperature. Using approximately equal temperatures of 21.1°c and 32.2°c, we had moistures of 15.68%, 18.42%, 15.1% and 17.8% by approximation assumption by linear extrapolation every 5% RH change (Glass, 2014). The target commercial moisture content is 18% (SIS, 2017), as the most adverse advisable moisture content for storage prior execution. This target commercial content gave us the desired analytical dimensions needed based on commercial pre-dimensions. From here we still use equation II-27 to get analytical shrink dimensions, as the water content varies in the long term with the difference between set RH for the material (65%) and any RH within climatic range. Target moisture can be checked using an electrical resistance moisture ratio master.

Using the target moisture content we get Eq. 3.1 and Eq. 3.2 (volumetric relations for 'Movingui').

$$h,2 = h,1\left[1 + {}^{36}/_{100} * (\left|18\% - 12\%\right|)\right] = 1.0216 * h,1 \quad \textbf{(Eq. 3.1)}$$

$$b,2 = b,1\left[1 + {}^{36}/_{100} * (\left|18\% - 12\%\right|)\right] = 1.0216 * b,1 \quad \textbf{(Eq. 3.2)}$$

The coefficient of volumetric shrinkage β,vol is 0.54%. It is considered in STEP1 as a generalised transversal coefficient, average of radial and tangential coefficients (since longitudinal is approximately zero and tangential is approximately double the radial coefficient). The value is mitigated due to the randomness of sawn sapwood and heartwood Glued together.

The value obtained for transversal coefficient $\beta,transversal$ was;

$$\beta, transversal = {}^{2}/_{3} * \beta, vol = 0.36\%$$

The obtained analytical dimensions are presented in Table 3.1.

Table 3.1. Analytical dimensions at 12% moisture content

	Commercial dimension (m)		Analytical dimension (m)	
	h,2	b,2	h,1	b,1
Curved beam elt	2.084[a]	0.24	2.04	0.24
Joists	0.33	0.08	0.32	0.08

Gable-column	0.19	0.7	0.18	0.06
Girts	0.33	0.08	0.32	0.08
'a' represents adjusted commercial dimension for analytical greater than 2m				

We want to apply moisture content maximum variation (Δψ) for environmental service conditions as intrinsic deformation loads. The maximum moisture content of 18.42%, is lower than saturation of 23% for 'Movingui', value which must never be exceeded. The Δψ from EMC table occurs at 21.1°c, of value 2.74%.

We used this Δψ to obtain shrinkage dimensions still using moisture-depth derived relationships in Eq. 3.3 and Eq. 3.4.

$$h,1 = h\left[1 + {}^{36}/_{100} * (|2.74\%|)\right] = 1.009864 * h \quad \textbf{(Eq. 3.3)}$$

$$b,1 = b\left[1 + {}^{36}/_{100} * (|2.74\%|)\right] = 1.009864 * b \quad \textbf{(Eq. 3.4)}$$

Also, we have the moisture content related differential variation effect (Δε) of shrinkage on large dimension elements of the structure such as curved beams was analysed in terms of initial counter-bow of elements. The maximum longitudinal shrinkage strain ε is the difference between maximum volumetric strain ($\varepsilon_{,vol}$) and transversal total strain ($\varepsilon_{,tang+}\ \varepsilon_{,rad}$). Total strains are 4.2% and 6.8%, respectively for radial and tangential strains *(CIRAD, TROPIX 5.0 - Fiche n° 153, 2003)*. A table summarises the displacement loads according to curvature formulae.

The volumetric shrinkage $\varepsilon_{,vol}$ is given by Eq. 3.5.

$$\varepsilon, vol = \varepsilon, tang + \ \varepsilon, rad + \varepsilon, long = \frac{V - V,1}{V,1} * 100\% \quad \textbf{(Eq. 3.5)}$$

For the latter predesigned curved beam and columns, the respective longitudinal shrinkages;

$$\varepsilon, long = \frac{0.2537}{25.88} * 100\% - (6.8\% + \ 4.2\%) = -10.02\%$$

$$\varepsilon, long = \frac{4\text{x}10^{-3} * \text{l}}{0.392 * l} * 100\% - (6.8\% + \ 4.2\%) = -9.98\%$$

The tangential direction for curves and columns will not be subjected to differential strains as they remain at similar temperatures. Service conditions entails maintaining internal temperature and RH at respectively (20°c and 65%) for service class 1. This means no internal ε,long, implying volumetric shrinkage is solely due to external environment. That explains why we considered volumetric shrinkage as function of only radial and tangential total strains from

the onset of volumetric analysis. It also explains why we are able to calculate $\Delta\varepsilon$ simply as $\varepsilon_{,long.}$ Table 3.2 shows differential, shrinkage, curvatures and counter bows for different elements.

Table 3.2. Counter bow in radial/tangential direction due to volume changes

	$\varepsilon_{,long,ext}$ (%)=$\Delta\varepsilon$	κ (%)	u (m)
Curved beam	-10.02	4.912	(-)[a]
Gable-column	-9.98	5.092	6.365x10^(-3)xl²
'a' require further analysis			

3.2.2. Mechanical properties of wood

There exist two main categories of GLT. We have first, "Combined" glulam which has at least four laminates and is denoted with the letter c (GL c). Other, we have "Homogeneous" glulam which has fewer than four laminates and is denoted with the letter h (GL h). Here all the laminates have the same strength. There is also another sub-category of combined GLT named "split" combined glulam (GL cs) with 'cs' = combined split. Glulam split timber beams (For widths dimension of less than 90 mm) are usually made from glulam beams in strength class GL30, but after re-sawing with a band saw, the remaining parts lose less than 2MPa in bending strength and are therefore classified as GL28cs. Glulam split timber beams are manufactured with a height to width ratio of less than or equal to 8:1. (SWEDISHWOOD, 2020)

When we get the different element solicitations, the linear variation of stress across the cross section enables the possibility of using material of lower grades in inner laminate zones of elements subject to less flexural stress given their maximum resistances. To simplify calculation we use homogenous GLT for design. Solid wood and corresponding GLT classes for use are non-standardised classes of tropical hardwood species whose properties are calculated from prEN1194, EN 338 and other experimental relationships.

According to TROPIX 5.0, 'Movingui' has f,m,k=116MPa (standard deviation of 13), E,0,mean=14740MPa (four point bending test with standard deviation of 3053). This gives f,t,0,l,k= 61.8MPa using minimum f,m,k also, giving f,m,g,k= 63MPa with possible name GL63h (CIRAD, TROPIX 5.0 - Fiche n° 153, 2003). According to TROPIX 7, 'Ayous has' f,m,k=52MPa (standard deviation of 9), E,0,mean=7260MPa (four point bending test with standard deviation of 1574). This gives f,t,0,l,k= 25.8MPa using minimum f,m,k also, giving f,m,g,k= 27MPa with possible name GL27h (CIRAD, 2012). We later calculate other GLT strength parameters according to prEN 1194, EN 384:2004 and predetermined moduli and ratios of US hard wood species specifically Oak wood with similar flexural properties to

'Ayous' and 'Movingui' as is contained in Wood Handbook (Service, 2010) and other documents (Sangree, 2009), (Brenco, 2020), (Aicher, 2018). So from E,0,mean we calculate other E ,G and ν values.

Basically, analysing the structure refers to assuring that the design resistance to any solicitations is superior to the solicitation itself. According to the solicitations and their directions we will apply modification factors accordingly and peculiar analysis equations were dealt in following subchapters. The resistance characteristic values of GLT are; f,m,g,k, f,t,0,g,k, f,t,90,g,k, f,c,0,g,k, f,c,90,g,k, f,v,g,k, E,o,mean,g and E,0.05,g. From these we get the design values by dividing by $\gamma_{,M}$ and multiplying by K,mod (for strength).

Annex 13 shows solid timber characteristic properties, their sources, their formulae and the used values in the design (some values were still to be modified during verifications and was specified promptly). Annex 14 shows Glulam timber characteristic properties, their sources, their formulae and the used values in the design (Still as before, some values are still to be modified during verifications and was specified promptly).

Unlike volumetric properties, when choosing values of constants at 12% water content from their ranges found in CIRAD or other documents, we chose mean values for dependent constants (E,0.05), lower bound values for independent constants like characteristic resistances (unless not meeting structural requirements, otherwise using average or upper-bound values).

3.3. Preliminary design

Preliminary design was based on adapting architectural requirements and the chosen structural system. This was based on a wide variety of formulas and parameters stated in situ. This step ranged from superstructure elements right down to a deduced foundation system.

3.3.1. Evaluation of joint constraints and restraints

As already mentioned in the presentation, the building comprises roller and pinned-end frames and gable frames. For both manual calculation and numerical analysis using software, the following was considered for element analysis; pinned node attachment of gable frame on main beam and ground, pinned nodes for all girt, joist or brace attachment to columns and main beams, ridge joints are pinned. For joint design, straight element joints are to be considered fixed in their vertical and horizontal plans (recessed ends). Bracing joints are analysed as pinned, as braces which carries only axial load (but actually its joints must resist self-weight moment so should be individually assessed numerically as fixed ends under their self-weight). All base of elements in contact with ground are unrestrained perpendicularly to curved frame.

3.3.2. Joists pre-design

We now have to pre-design joists using maximum wind load. According to Twiza (Bois, 2020) and Vogeslam (SAS, 2020), the maximum joist length from their abacuses is 12m. In the design process, three design models of respective lengths 5m, 8m and 10m which will all be predesigned similarly to the chosen 5m model for analysis (the others being used for some comparative analysis). The main reason for choosing the 5m span for numerical analysis is having joist length as factor of total building length of 100m for uniformity of loading. Also for other reasons (to minimise joist deflection and for symmetry of building), the 5m joist was chosen for the design. Comparative structural and economic analysis will be provided. Maximum allowable stress was used in order to have the number of joists. As regards the sections we already have pre-dimension formulas which enables us to get h=0.29m and d=0.029m (GLULAM HANDBOOK FRANCE, 2020), but we use a commercial dimension d=0.08m (The Ministry of Economy, 2015) to account for corrosion. The thickness is same as the 0.08m which were given on site but the height h=0.33m (also accounting for corrosion) is further away from onsite values due to the difference in elements; the onsite being main beam while the value for joist. 'h' and 'd' are the height and thickness of the simple supported element.

The maximum joist centre distance (X) for one way slab support of joists is 2.5m (using the ratio of 2 between long side and short side). Flexure depends on anisotropic behaviour of GLT, so for pre-dimensioning we need to use material design properties more specifically for orthotropic GLT. The value of f,m,l,k for Movingui =103MPa as lowest value (CIRAD, 2003). Using formulas for conversion from table of prEN 1194, γ=1.3 and K,mod=0.8 (service class 1 and 2 for average term service load for a less conservative pre-design with respect to the service dominant load), we have f,m,g,d =38.77MPa for homogenous beams.

The maximum linear resistant load q, max has value 18014.0928N/m using a derived formula (Eq. 3.6).

$$q, max = \left({}^{4}/_{3}\right) * \left({}^{f, m, g, d * d * h^{2}}/_{l^{2}}\right) \quad \textbf{(Eq. 3.6)}$$

The X is gotten considering joist section geometry from the derived Eq. 3.7 (where q,max is the surface vertical load on joists of value +807.1641N/m²). Due to the curved geometry of main beam, X is considered as a finite element of curved geometry (chord distance) and the assigned radial load is approximated to a surface load from which we get q,t = 292.3N/m (for roof total pressure of 58.46N/m².

$$X = {}^{q,max}/_{q,t} \quad \textbf{(Eq. 3.7)}$$

X has as value 2.76m (greater than the maximum joist span of 2.5m for curved frame span 5m), so for a calculated curved frame length of 105.72m, we get 43 chord spans of about 2.5m length each. This implies around 44 joists (Number may vary in FEA hence changing section).

3.3.3. Curved frame span implementation restrictions

Now we verify frame spans considering implementation restrictions. A 5m wide span between curved beams is sufficient for any small-size large operating vehicle and installation elements so there is no restraint in this consideration to the design we used. During assembly and erection, no forces should be applied to a component that could cause the permissible stresses to be exceeded in that or any other component. Prefabricated arches are assembled element by element (using high power truck with mounted cranes) and also frame by frame on already laid abutment foundations and requires temporal bracing (by cables) to each other for joist and bracing installation in other to have continuously stable structure during execution. Secondary work like ground work could be done later by smaller vehicles after the structure frames are all erected and stiffened.

3.3.4. Pre-design of gable wall frames and sections

There is a need to pre-design gable wall frame and sections, considering openings. Considering the left support of the curved beam, we assign an orthonormal (x,y) reference plane. There exist an equation (Eq. 3.8) relating x and y displacements in this system (GLULAM HANDBOOK FRANCE, 2020)

$$y = 4\,{}^{f}/_{l}\,(x - {}^{x^2}/_{l}) \quad \textbf{(Eq. 3.8)}$$

Given we follow joist positioning for gable wall columns, the first column (y,1) at 1.25m away from apex (under finite length approximation with the 43 X we found prior), and the next column (y,2) still approximatively at 2.5m from the first, we find y values for their respectively deduced x values as y,1=14.99m and y,2= 14.91m which a very close so we can say column y,1 carries load effectively over 2.5m width.

Analysing gable column as simply supported, we derive an equation (Eq. 3.9) for minimum buckling area for critical loading of one column under maximum axial stress of 53MPa. We obtain the derived formula assuming a square section of size s.

$$s^2 = \frac{12 * l^2 * \sigma,crit,d}{\pi^2 * E,0.05d} \quad \textbf{(Eq. 3.9)}$$

We obtain $s^2=1.52m^2$. We have 42 columns with tallest columns carry each 22.81KN (axial load from the curtain wall load of $62.1kg/m^2$ and total surface of $37.475m^2$ per column). The actual critical buckling stress acting on each gable column is obtained by dividing the axial load by s^2 giving $\sigma=15kN/m^2$. We still use the buckling formula above using σ as the new critical load to obtain a minimum surface of 4.304x10^(-4) m^2, hence a minimum base of 0.007m and minimum height of 0.07m which is adjusted (given corrosion and minimal commercial width) respective values of b,c = 0.06m and h,c =0.11m still adjusted later-on for analysis model. This section is assigned to every other column for simplicity and since the load carried by column reduces as we go towards abutment, we follow the roof joist location to position the columns.

Using same formula as in Eq. 3.1 and Eq. 3.2, we need to find X for gable beams. We use curtain wall vertical load and similar section to roof joists. We obtain X=5.441m greater than maximum vertical spacing for one way spanning which is 2.5m, so we use this value as vertical span (permits a 2.5m high door). After verifying for loading in vertical direction (curtain wall load), we got a same section 0.33mx0.08m as joists, which also verified for horizontal loading (wind and hand load). We notice that their length reduces as we move outwards the curved frame. When analysing with SAP2000 we will check using stud wall loads since there is random positioning between curtain and stud-wall pieces.

3.3.5. Bracing placement

For the bracing placement, the system considers both principal wind directions to and fro. The longitudinal and transverse roof bracing look alike beam trusses. Both longitudinal and transversal bracing trusses spacing must be symmetric about respective vertical planes cutting building into two equal halves. For pre-dimensioning, whilst transversal bracing trusses are 20m apart for external spanning and 30m apart for internal spanning, the longitudinal consist of a two ridge trusses and two curved frame base stabilisation braces towards abutments. Span to depth ratio also was applied for the section to have a 0.27mx.08m section. Window openings was positioned depending on bracing dispositions (avoiding braces). The transverse bracing was placed at second 5m span from gable end. A horizontal distance of 5.28m is necessary from the abutment to have an opening height of 3m on roof portions at side, which implies a finite element length chord of about 6.07m meaning at least two curved spans of length about 2.64m from base joist must be left out before the first longitudinal truss. For roof bracing we are recommended a bracing angle between 45° and 60° from Glulam Handbook Vol.2, so about 46.59° from the design. We have 20 cross braces in transverse beam and 20 of them in longitudinal truss beams. Forecast for gable bracings must consider the fact that they must not interfere directly with roof as gable contributes minimally to the lateral stiffness of the building

against rolling edge movements. Since bracings cannot have section height greater than those of joist or girts, we first use their dimensions as pre-dimensions for braces which was adjusted to final bracing sections depend on axial solicitations of braces, easily obtainable after pre-running analysis in SAP2000.

3.3.6. Curved frame pre-design

For the main beams (curved frame), it is first presented the representation of the structural model for main beams in Figure 3.3.

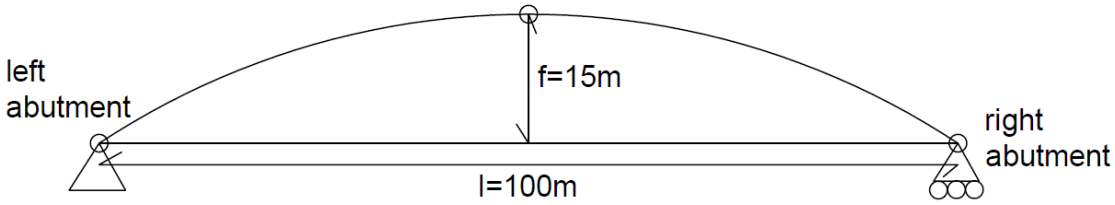

Figure 3.3. Structural model representation.

The curved GLT section was designed with same material 'Movingui' as other elements, which was recommended from interview. Still from interview, the preliminary design section from interview 80mmx600mm could be used to appreciate pre-dimensioning sections but expectation of large variation due to disproportionate global structure size.

From Glulam handbook, a recommended value for f/l is between 0.14 and 0.15 inclusive (ours is 0.15). A counter bow is provided for beam design equal to maximum deflection of each beam of the frame (at l/4). The curved beam has a constant height of h between l/50-l/30 so we start with a value of h=2.04m (considering corrosion). Using height to depth ratio of 10, we start with a base b=0.25m.

3.3.7. Pre-design of slats and multiple-splice finger joints

Every GLT structural elements is composed of slats and multiple-splice finger joints. There exist two principal laminating types; vertically and horizontally laminated GLT. The most adapted type for the structure (curved frame arc) is the horizontally laminated type as it is easily flexible. The spans between finger joints depend on commercial dimensions of sawn lumber available. The minimum number of slats is four. The sections can be gotten from a national annex (The Ministry of Economy, 2015). Since we intend to have curved members we use slats thickness of 0.02m, as an industrial dimension enabling higher pre-curving flexibility (additional geometric contribution to material flexibility). For straight members we use a minimum number of 4 slats as a generality.

All straight frame elements are to be pre-fabricated and are easily transportable, given their very short lengths by far inferior to 30m. They are to be engineered as continuous slats of 20mm Glued together with Resorcinol Formaldehyde. For curved elements which are very long, the slats are glued together with staggered multiple-splice finger joints along its length (staggering about 5m). Curved beam as the calling entails required pre-curved slats respecting curvature for each beam segment. Each curved beams are made up of two segments, between which we have one vertical splice connection whose segment lengths will depend on the moment diagram obtained from ULS analysis. The number of slats for each element could also be calculated only after carrying out ULS verifications. The staggered distribution of the multiple- splice finger joints is shown in Figure 3.4.

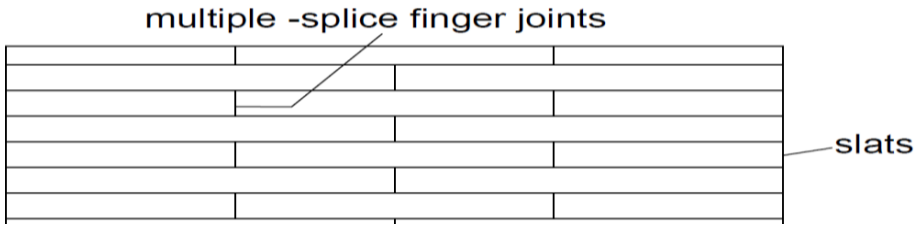

Figure 3.4. Disposition of multi-splice finger joints

3.3.8. Pre-design of structural joints

This consists in making forecasts for adapted industrial connectors, in-between structural elements in order to remain within our subject range. The identified type of joints we are going to use are; metallic connectors such as joist boxes (used for joist-main beam and girt-gable column connection to provide discontinuity and reduce torsional solicitation of main elements compared to continuous system), metal brackets (used for gable wall braces anchorage, column-curved beam and column-base joints were it participates in resistance, for joining curved beam base to each pin bearing), metallic angles (joining of secondary non-structural elements via secondary elements to primary elements) and finally dowel ring connectors at the ridge and intra-curved frame splice. The connecting elements are pins/bolts and nails. The only joint types which was design are the ones connecting curved frame elements composing the main structural element while assuming others well designed industrially.

Since inverted ‘V’ bracings are used, the kink of the inverted ‘V’, transmits shear on joists or girts. Using specialised multiple truss hangers (ASC, 2020) is adapted connector type.

We also have vertical splice joints linking curved beam elements located away from maximum flexure on curved frame elements. This joint type is reinforced with pins (forming dowel connectors).

Special forecast entails tightening of bolts from six to 8 weeks after commissioning of the structure when timber reaches equilibrium moisture content. This implies connected joints must be accessible and also large structural member check year after completion is also recommended.

After getting effects of actions from software, we chose suitable industrial connector systems for the ridge and abutments, and check whether they resist the effects of actions. The different type of connector systems to be used are; Rocker pin bearings and roller bearings for bridges since the large span structural system is parented to bridges. They carry massive loading and are able to rotate and move for the roller bearings (Constructor, 2020). A thick T- stainless plate (metal bracket) can be inserted at abutment region of curved beams by splicing and pinned while the plate itself is bolted and/welded to the platform of the bearings. For the ridge connection between curved beams and ridge beams, a simple highly-resistant pinned connector is necessary and is attached by thick T-stainless metal plates as internal splicing between two beam edges and is pinned.

3.3.9. Pre-design of foundation structure

Preliminary design of the foundations consist first in the identification of the type of foundation structures to be used with respect to building template. The dimensions recommended by FINA are 2m (min.) and 5m (max.) water depth below pool surface respectively for the 50m pool and the diving pool (FINA, 2017). Considering an average 16cm thick pool layer, it is safe and possible to have tie beams at 2.5m and 5.5m below ground level in order to resist huge lateral loads from the curved frames. This also implies the stretching of the foundation a little deep below ground level (CEN, 2005).

It is noted from preliminary design the pre-design similarity between joists and girts, the dependency of columns to joists position, the possibility of industrial connector usage and the indisposition of the common tie-beam between curved frame abutments.

3.4. Numerical analysis

The onset of numerical analysis arises at the determination of volumetric properties, as a pre-requisite for the determination of additive intrinsic structural overweighs and initial bows. The due process from modelling the building in software to the carrying out of safety verifications is necessary.

3.4.1. Modelling the structure with SAP2000v21

The structure is composed mainly of linear frame elements which were easily modelled in SAP2000 but had to be mounted on already modelled curved frame elements (curved beams)

which was an enormous task. Since modelling with parabolic curve leads to complications as for assigning equal finite element curve segments (for FEA), we started-off modelling with circular curve having an external constant radius of curvature. This was possible because at large scale (the curved frame), circular geometry is good approximation of parabolic behaviour and gives more accurate FE discretization for joist placement. Still we had few joist locations diverging with the circular curved frame elements (due to order of approximation during discretization). We just proceeded in adjusting the deviated joist locations on the curve. This gave us an abutment inclination of 32.4° (instead of the theoretical 16.7°), and a chord segment of 5.24m subtending each FE arc segment containing each joist. Other details pertaining the reshaping process was discussed later during analysis as the model further depends on running analysis in SAP under ULS. Necessary data for parametrization of the software was given in the DESIGN REPORT in the ANNEXES.

3.4.2. Basis of limit state calculations

For the load combinations we first need to numerically analyse the effect of vertical and horizontal loading on a curved hypostatic GLT frame. We do so using SAP2000, where we set orthotropic GLT material properties with pre-dimensioned element sections, applying necessary restraints (pinned abutment nodes and free ridge node with roller support at other abutment) to the nodes similar to the structure we will analyse later. We check the worst load effect on either structural element or joints to be designed.

The loading configuration on the building was done considering the hypostatic curved frame plane and the gable frame plane. The curved frame is considered analytically as three-hinged unfixed structure.

The loading is done considering curved frame under the different symmetric loads, which has greater influence area and apply its design on other frame while also considering adjustments for the external curved frames where external moments act.

Load conditions are analysed separately for roof and gable walls separately so as to find the most unfavourable loading considering building symmetries and neglecting accidental load (fire) to be verified later. The combinations are done in ULS and SLS. Second order effects can calculated using formulas and aided by SAP2000. Horizontal loads are wind loads and hand loads in same direction for gable wall loading, while it depends on loading conditions in curved frame direction.

Curved beam geometry of roof imposes the decomposition of roof loading into horizontal component which is non negligible, provided the roof braces resist the loading when well

designed (GLULAM HANDBOOK FRANCE, 2020). This problem is resolved directly in sap by orienting joists radial axes to be orthogonal with curve axis.

3.4.3. Actions on the structure

Design will correspond to a building of the third class (design life of 50years). The utilization is of class 1 for a category C (gathering of people) for the building and class 2 of inaccessible category H of roof (inaccessibility except for maintenance).

Due to the small roof slope (pre-dimension maximum of 16.7 less than 20°), it is projected a vertical variable short term distributed service loading of 0.75 kN/m². Given each frame's curved beam is simply supported, loading has to be continuous over the node, so 0.75kN/m² is a vertical load on a horizontal surface which has to be projected on the surface of roof (subtended by chord). For roof slope greater than 20°, we still consider this same load since it will always be less than 40° from numerical model (précising special security precautions for maintenance work such as high adherence shoes and boundary warning markings).

Concerning the self-weight of non-structural elements, we have; curtain walls which are used at some areas of gable walls to maximise lightening, and improve the aesthetic of the building. The self-weight of curtain walls and wood panels (stud wall) is about 61.2kg/m² of curtain surface (Hessong, 2020) and considered acting on girts. On other portions of wall we have stud walls weighing 72.12kg/m² of wall surface (NAFFA, 2020) still acting on girts. In addition to these, there are the self-weight of roofing elements; Glazing patent glass blocks weighing 25.9kg/m² and laminated board weighing 12.2kg/m² (BSI, 1999), from which we use the heavier one.

A horizontally short term distributed load acts on each wall surface due to human hands of value 1.5 kN/m, and at an average of 1m from ground (on wall) and at the top of roof parapet (metal guardrail for safety only on edge curved beam as from height above 3m) 1.1m high (ISO, 2020).

There are additional loads due to shrinkage loads and creep which was analysed later.

The effect of uplift wind in the absence of service loads can be concluded less than that in the presence of service for both ULS and SLS, so we always carry out design in the presence of service loads since self-weights of the structure are by far greater than maximum uplift wind which only impedes self-weights (for example considering the predesigned joist only and its influence area we obtain a surface self-weight of about 6 times wind uplift and about 3 times wind uplift on roofing sheet members alone).

Analysis of external actions involves calculation of wind loads and getting the service loads acting through the service period of the building. This was done neglecting self-weight of structural elements. A summary of variable loads acting is shown in Table 3.3.

Table 3.3. Variable loading summary

Structure	Variable load type	ULS/SLS load
Roof	Service (primary load)	0.75kN/m²
	Wind (secondary load)	(-)
Gable wall	Hand (-)	1.5kN/m
	Wind (-)	(-)
Parapet	Hand (primary load)	1.5kN/m
	Wind (non-existent)	No load wind on parapet
'(-)' represents to be determined values or load type		

For wind loads Q2,k assignment in SAP2000, for the roof we directly apply the radially distributed load into predefined rotated local coordinates, joists always tangential to curve beams at any point. We assigned service load Q1,k as projected vertical load on beam elements round the curve as maximum slope is not exceeded. Self-weight of non-structural elements (G2,k) and hand loads (Q3,k) are respectively vertical and horizontal loads in the global coordinate system. The influence area of a finite increment length of chord for application of surface loads corresponds to joist spacing of each 5.244m. Parapet load was applied on the structure as distributed nodal forces (also Q3,k) and resulting moments at external joist-curve intersections where necessary. For Gable wall we have Q2,k and Q3,kin global horizontal direction while G2,k is vertical in global coordinate system. Hand loads on parapet or on roof always act outwards the building.

The wind calculations yielded the following values;

$v,ref = 1.718 * 1 * 1 * 1.5 = 8.59m/s$

$q,ref = 0.5 * 1.25 * 8.59^2 = 46.118N/m^2$

$z,w = f = 15m$

$C,r\ (z,w) = 0.22 * \ln(\max(15,8)/0.3) = 0.86$

$C,e\ (z,w) = (0.86^2 * 1^2) + (7 * 0.86 * 0.22 * 1) = 2.064$

$e,w\ (\theta = 90°; \theta = 0°) = [\min(100,15 * 2)] = 30.00m$

$z, i\ (\theta = 90°; \theta = 0°) = (2.5m; 1.17m)$

$C, r\ (z, i; \theta = 90°; \theta = 0°) = 0.22 * \ln(\max(2.5\ or\ 1.17{,}8)/0.3) = 0.72$

$C, e\ (z, i) = (0.72^2 * 1^2) + (7 * 0.72 * 0.22 * 1) = 1.6272$

The derived formulae for wind pressure calculation are given in Eq. 3.10 and Eq. 3.11.

$W, e = 46.118 * 2.064 * C, pe = 95.188 * C, pe$ **(Eq. 3.10)**

$W, i = 46.118 * 1.6272 * C, pi = 75.043 * C, pi$ **(Eq. 3.11)**

Total wind loads on roof is given in Table 3.4.

Table 3.4. Table of total wind loads

θ(°)	90 (for gable wall)		0 (for Roof)		
C,pe	+0.6	-0.3	+0.22	-0.82	-0.4
W,tot. (leverage, C,pi=+0.8;N/m²)	-2.92	-88.59	-39.09	-138.09	-98.11
W,tot. (suction, C,pi=-0.5;N/m²)	+94.63	+34.67	+58.46	-40.53	-0.55

The table shows values with positive and negative signs; the former for wind action towards building whilst the latter for wind away from building. The wind load for roof is the one that maximises positive moment together with service variable load (all suction values; +58.46N/m², -40.53N/m², -0.55N/m²), while the wind load for gable wall is the maximum value (+94.63N/m²) with a corresponding +34.67N/m² on opposing wall, making wind a secondary load. The hand load was applied in the directions of wind load for gable wall, but was opposed to wind on curved beam as it increases its positive bending moments.

For the roof, since hand loads are applied on surface elements (roofing elements, stud or curtain walls), we redistribute the hand loads between two adjacent joists or girts according to their ratios of simple support between the two elements.

For the parapet loading, we apply an external distributed moment of 4.25kNm on each external curved frame node with rotation outwards (for distributed hand load acting outwards the building). Due to this moment we also apply an outward redistributed shear load of 3.87kN on each curved frame joint directed away from building.

In addition to the former mentioned loads, we have to apply self-weight of non-structural elements (G,2,k) and roof vertical roof service load (Q,1,k).

Eq. 3.3 and Eq. 3.4 using pre-design section geometry yielded an additional intrinsic overweight to be included in the SLS analysis model for SAP2000 (because we run analysis with constant density meanwhile it changes in reality) which is the worst loading situation for the structure. It was applied as joint loads on roof as shown in Table 3.5.

Table 3.5. Additional weight due to shrinkage from real to analytical dimensions

	Shrinkage dimensions (m)		Volume change (m3)	Additional mass (kg)	Overweigh (kN)
	H	b			
Curved beam elt	2.02[a]	0.24	0.2537	161.0	1.578
Joists	0.32	0.08	negligible	0	0
Gable column	0.18	0.06	negligible	0	0
Girts	0.32	0.08	negligible	0	0
superscript 'a' is the modified value for the commercial height of 2.084, while 'b' represents a value function of the length of a particular column					

Counter bows in Table 3.5 will be applied as displacements (curvatures), but applying displacement on curved elements is not possible so we have to convert the displacement into displacement load for SLS analysis (hence the further analysis in 'a' in Table 3.5). The bow of curved elements is analysed first with the chord length subtending the arc element. It has a length of 52.202m (derived from projected length and height of building). We have the point load P causing this displacement in Eq. 3.12.

$$P = \frac{48*9524.308*(10^6)*\left(\frac{(0.24^3)*2.04}{12}\right)*\Delta u}{(52.202^3)} \quad \textbf{(Eq. 3.12)}$$

The bow u caused by the chord length (l,c) is about 16.73m. The Sagitta of an arch of radius of curvature (r) is calculated as;

$$z, chord = r - \sqrt{r^2 - l, c^2} = 174.01 - \sqrt{174.01^2 - 52.202^2} = 8.02m$$

$$\Delta u = u - z, chord = 16.73 - 8.02 = 8.72m$$

This gives P=65.86kN, and was redistributed as radial nodal uplift weight P,dist=3.14kN (on each joist whose positions were discretised on each curved beam).

For columns the discretisation into smaller elements retrained curvature application so we need to apply it as a horizontal load similarly to curved frame elements. This gave P,c in Eq. 3.13 (where l is the column length).

$$P,c = \frac{48*9524.308*(10^6)*\left(\frac{(0.06^3)*0.18}{12}\right)*6.365\text{x}10\text{^}(-3)\text{x}l^2}{(l^3)} = (9427.97/l)N \qquad \textbf{(Eq. 3.13)}$$

The loads on the roof were applied on joists since it was easier to apply in SAP2000 as the joists were already oriented in wind load direction. All other loads were simply added as either vertical or horizontal loads in the global coordinate system. The challenge here lied in the definition of angle of orientation of joists attached to curved elements. The trick used here resided in assigning inclinations to the horizontal, for each joist which was the inclination of the chord subtending the finite arc increment from the previous joist to the next joist positions.

Due to the movement of the curved elements under loading, there was not possibility of defining clearly the offsets by which loads other than wind could be applied so all other loads were applied as vertical and horizontal loads on central joist axes (assumption of minimal induced torsion mechanisms).

3.4.4. Comparative study of structural models

In comparative analysis, the three different models had to be compared based on different criteria such as compression, tension, displacements in the three principal directions and the required volume required for construction. All these criteria were obtainable from SAP2000 from running analysis in ULS except for volume, gotten indirectly from dividing the mass from SAP2000 by the density of 'Movingui'.

Concerning geometry, variation from one model to another is only about the lengths of joists and consequently girts. The first with 5m the second with 8m and the third with 10m joists (the 8m model was design to have a 4m span bordering the building to complete the 100m length. The bracings of the other models were designed similarly as the 5m model. The following Figure 3.5 depicts the different spatial models to be compared.

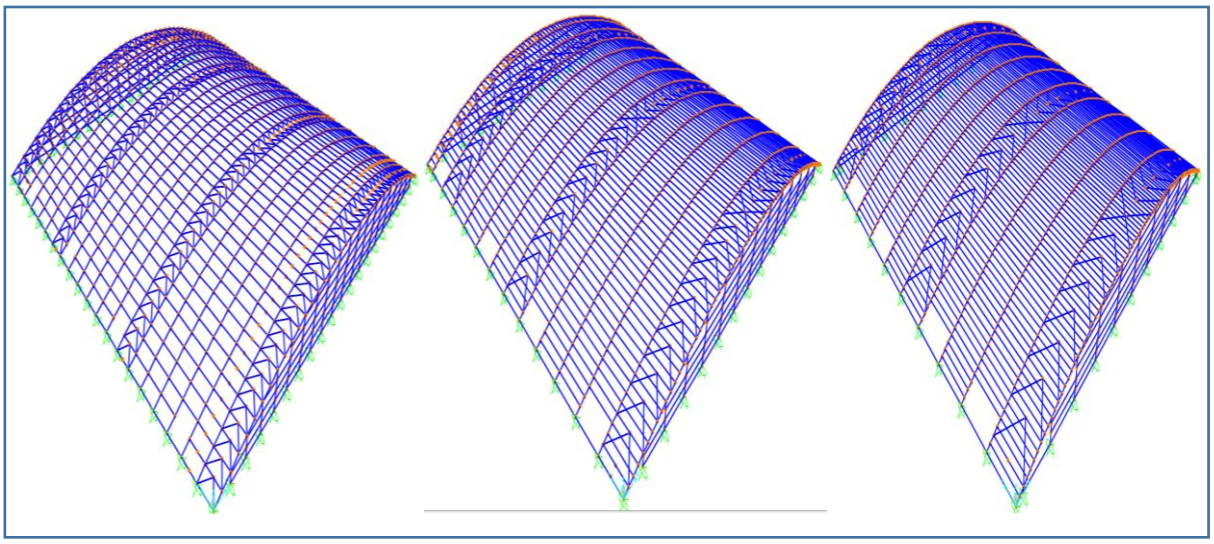

Figure 3.5. Different spatial models from left to right; 5m, 8m and 10m.

Table 3.6 shows the obtained values of the different criteria.

Table 3.6. Different criteria and comparison data for various models

	5m	8m	10m
Compression (kN)	3273	3542	5793
Tension (kN)	3761	4328	6891
min. disp. X (x-1m)	0.6	0.52	0.72
max. disp. X (m)	0.525	0.455	0.63
disp. Y (x10^10m)	1.4	1.7	0.8
min. disp. Z (x-10^1m)	0.099	0.224	0.28
max. disp. Z (x10^1m)	0.066	0.196	0.32
Vol. (m3)	4750.16	4339.01	4968.39

The following star plots (done with EXCEL 2013) shows a visual comparison between the three different models in Figure 3.6.

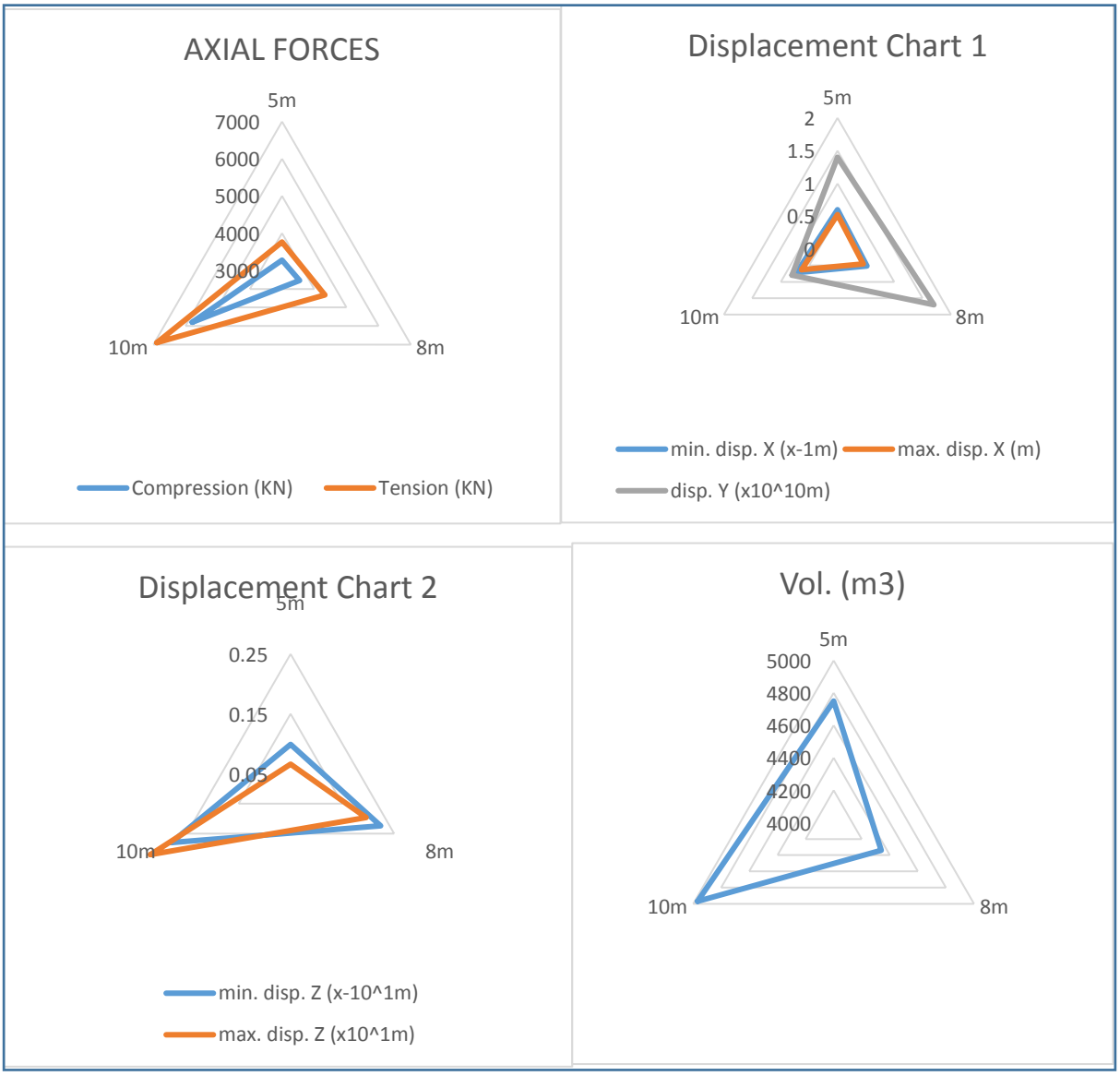

Figure 3.6. Star plot for visual comparison of different spatial models.

From these charts we can observe that the choice of the design model is oriented to the already- The preceding figure confirms the effectiveness of the already chosen pre-design 5m model as it was proven to; be more economical (less volume of wood), have least axially solicited curves, and have least displacements in Z direction. These three criteria were sufficient to claim the 5m model as the best model.

3.4.5. Ultimate limit state verification (ULS)

This consisted in verifying that the pre-designed structure will resist the most adverse loading situations. It was comprised of the following; analysis of braces and bracing systems (this was used in comparison of the different models), analysis of joists and girts analysis of columns, analysis of curved beam and finally slat disposition and splicing.

3.4.5.1. Lateral bracing design and analysis

In the comparative study previously mentioned we used a bracing system for each model adapted to the geometry of the building, got the response from analysis through alternating brace positions from the pre-dimension brace model, all these based on a conventional bracing model found in Glulam Handbook. Recall that the objective of a good bracing system is to reach self-stabilisation primarily within admissible (minimal) displacement boundaries in ULS design.

Adapting the bracing system to building geometry considers respecting effective bracing angles (between 45° and 60°), the simply supported joists, the ability for the brace elements to cross below joists without interfering with their displacements, remaining within allowable span-depth ratios for brace elements and the imperative of using wood. Since the main problematic for design of swimming pools is the fact that iron and steel are easily attacked by chlorides evaporating from treated pool water, we could neither have iron nor steel bracings at positions anywhere above the pool or in the vicinity of the pool hall. This prompted the use of timber for bracing using 'Movingui'. All these considerations brought to the use of 'Model C' in Glulam Handbook Vol.2 (p. 248).

On another hand, alternating brace positions affects analysis results (based in a principal criterion which is the axial load in the principal members; curved frames). The objective here was to have a smooth compression diagram, which prompted through analysis, the removal of longitudinal trusses and the displacement of the outermost transversal trusses to the edge. A smooth compression diagram gives opportunity for using variable inertia section.

Figure 3.7 shows the awaited typical compression diagram with a smooth shape which was most optimal.

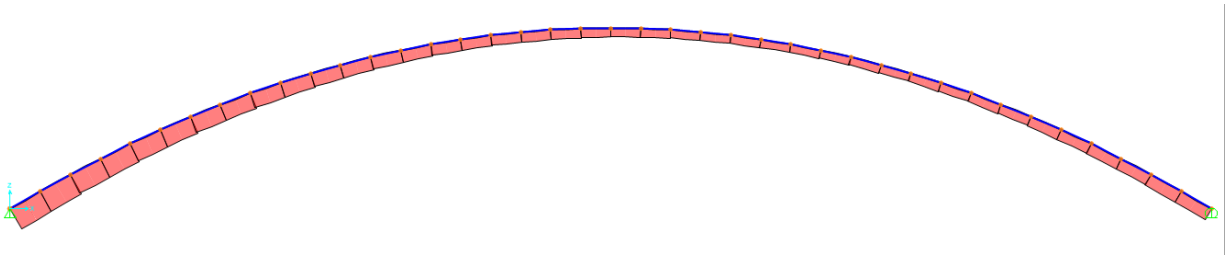

Figure 3.7. Smooth nature of typical compression diagram in all internal curved frames

A view of the optimal bracing models have already been shown in the comparative study

Analysing braces, it was also discovered that increasing section dimensions in the SAP2000 model increased internal failure mechanisms in curved elements (still mainly about axial loads which is the main issue increasing second order effects). This in turn increased the needed

bracing capacity (more braces and greater sections), perpetuating the vicious circle. As a result, we resolved restraining from varying sections further or adding braces on the roof particularly.

The axial loads (both compression and tension) were grouped into two categories; one from 0MN to 0.1MN (internal transversal truss bracers) and from 0.1MN to 1.06MN (external transversal truss bracers). Some braces could not meet axial solicitation requirements for 'Movingui' so we had to introduce a new wood specie 'Eyoum' which was the highest axial resistance tropical specie from available data sheets (CIRAD, TROPIX 6.0 - Fiche n° 235, 2008). It was found for the first group that the lowest axial load resistance 'Movingui' GLT (23.72MPa and 25.54MPa respectively) were resistant to the maximum 4.63MPa solicitation. For the second group, the bracer sections had to be increased (limited to joist section) and it was discovered that medium resistance 'Eyoum' had to be used exceptionally as solid wood (41.53MPa and 44.86MPa) to resist the 40.27MPa and 39.78MPa acting stresses. This will necessitate a more regular inspection of the solid wood bracers to avoid failure. Note that low, medium and high resistances refer to values calculated from mean mechanical resistances and their deviations.

It was also assumed for design that the density difference (hence surcharge for same sections) between 'Movingui' used for running software analysis and the proposed 'Eyoum' will easily be compensated in the curved element analysis as it will have to be designed very conservatively.

All these propositions means particular caution already for selecting 'Eyoum' sections (necessitates non-destructive testing with ultrasound device for example) and well pre-engineered composite sections. Since bracings carry only axial load, the effect of flexure due to its self-weight was neglected same as the effect of shear and torsion in braces is also neglected.

The next figure summarizes the dispositions of different roof constituting elements in a plan view to show FE discretization approximation (Figure 3.8).

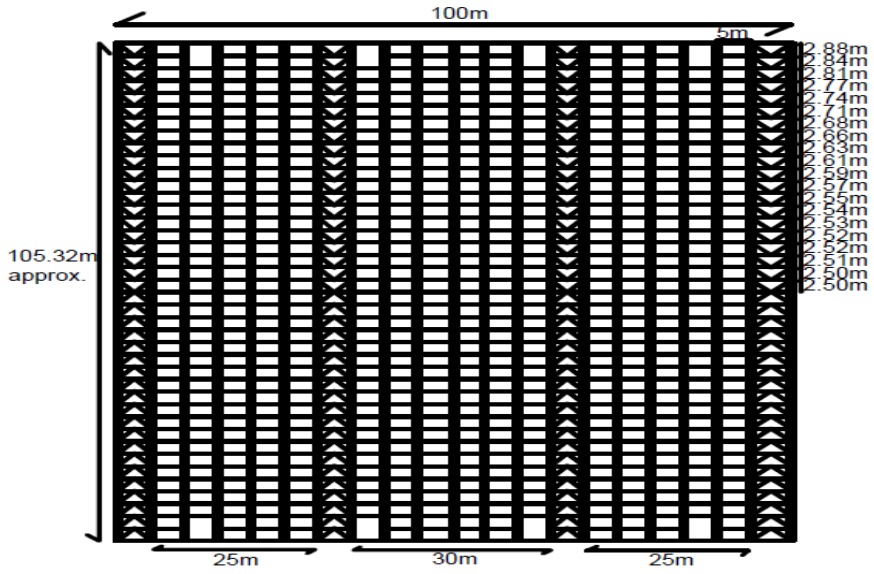

Figure 3.8. Cylindrical Equal area projection roof plan

3.4.5.2. Design of the foundation structure

The first step in designing a foundation structure for this large span curved structure is getting the base reactions from sap 2000. In the global reference system, the maximum reactions were observed. They had values; F,x=-2826.67kN, F,y=0kN, F,z=-1561.11kN and 1342.33kN (for curved frames) and F,x=-2.76kN, F,y=0kN, F,z=420.73kN (for gable frame columns). The negative reaction for vertical curved frame was observed at two extreme pinned abutments (y=0 and y=100). These reactions was used in calculating geotechnical and structural aspects of the foundation, but our interest is finding an adapted foundation type and pre-dimension it and later give a detail foundation plan. From the building floor plan there is limitation in the surface of a possible footing foundation for gable frame columns compared to the curved frame abutments disposing up to 25m inside the building zone but there has to be an equilibrium between structural and economic necessity. Some assumptions were made for pre-designing the foundation structure;

(1). Uniform cohesion less soil type with water table far below (drained soil).
(2). Sandy gravel soil on an average bearing capacity of 0.2MPa at 1.5m below ground surface.
(3). Neglect of support reaction loads' eccentricity and passive soil pressures.

Neglecting self-weight of foundation, static equilibrium at foundation base gives the minimum areas;

$$A, \min(curve) = \frac{1342330N}{0.2Mpa} = 6.712E(6)mm^2\ (2.6m\ side\ square)$$

$$A, \min(column) = \frac{420730N}{0.2Mpa} = 2.11E(6)mm^2\ (1.5m\ side\ square)$$

The external curved frame footing was assumed to have same section as internal one (due to negative reaction). Imposing static equilibrium between inertial drag and horizontal reactions we have the resultant forces ΔF;

$$\Delta F(curve) = 0.3(1.343\text{E}6)N - 2.83E6N = -2.43E6N$$

$$\Delta F(column) = 0.3(4.21E6)N - 2.76\text{E}3N = 1.26E6N$$

The set thickness for isolated footings h was set at 50cm for curve and 25cm for column, giving a maximum column anchorage area of sides b (curve)=65cm and b (column)=31cm from Eq. 3.14 (Chegg, 2020).

$$h \geq \frac{B-b}{4} + 0.05m \qquad \textbf{(Eq. 3.14)}$$

It was observed that friction in the column footing greatly outnumbers the horizontal force, implying the square footing is okay. For the curved frame footing, adjustment in footing dimensions (length parallel to curved frame) was reserved for roller footing pad as it depends on maximum displacement adopted. Also, the friction at base was greatly surpassed by the horizontal force. These prompted the need for a system component to absorb excessive horizontal load. It could be done with an underground grade beam between the two abutments (un-economical), adding counter weight at abutments (also un-economical), using massive footings (un-economical) and finally to cite the best amongst a few is the exploitation of greater depth with short piles (more economical).

The short pile (4m) in question was a driven trapezoidal prism since the pile is analysed as a moment bearing sheet pile wall (bearing moment in horizontal direction parallel to curved frame. Under the assumption of uniform soil up to the depth and closer beyond it, the bearing capacity varies linearly from the pile cap to the base of the pile.

The short pile was chosen to avoid occurrence of a plastic hinge under horizontal loading. The pile well attached and reinforced to the fixed pile cap (footing in this case) and along its length enables the whole vertical foundation to behave as a monolithic structure.

The equilibrium between soil bearing and horizontal reaction gives the pre-dimension of the trapezoidal prismatic section. Through triangle theorem the value of B,cap,5.5m=0.733MPa.

The value of s below means the trapezoidal prism is a sheet pile wall.

$$s = \frac{2*F,h}{(5.5m*B,cap,5.5m-1.5m*B,cap,1.5m)} = \frac{2*2.83\text{E}6N}{1000*(5.5*0.733-1.5*0.2)Mpa} \cong 1517mm$$

Depending on the necessary angle of driving, the height, the thickness at each level of the pile (variable thickness) can only be determined with further geotechnical investigation. The pile is not the vertical load bearer but the square footings, while the shaft of the pile bears horizontal load. Hence for safety reasons, a minimum number of two piles was necessary for each curved frame footing.

For the gable frame foundation, a tie beam was necessary between all column footings and also between all footings below a transversal truss. The span-depth and depth-base ratios ($l/15<h<l/10$) and ($0.3h<b<0.6h$). This gave dimensions for tie sections spanning 5m (15cmx50cm) and (15cmx25cm) respectively for curve and column (the height for the tie below columns is limited by the footing height). These tie beams contribute to the monolithic nature of transversal trusses and gable wall frames.

Since there were traction forces on the foundation, this automatically required traction piles to stabilize the structure. The minimum volume (V,t,p) of pile necessary to counterweigh the traction force on piles is given by the static equilibrium between self-weight (at 350kg/m3 concrete density), traction and bearing force. This means a number of piles on this foundation must have a least that total volume.

$$V,t,p = \frac{720N+1561.11KN}{\frac{350kg}{m3}*9.8m/s^2} = 455.4m^3$$

The length, pile section at cap and the spacing of these grouped piles necessitated further geotechnical investigation and analysis but we ended here. A model of the pre-design foundation plan was given in the ANNEXES.

3.4.5.3. Analysis of Joists and Girts

Figure 3.9 shows the distribution of joists according to their different axial solicitations.

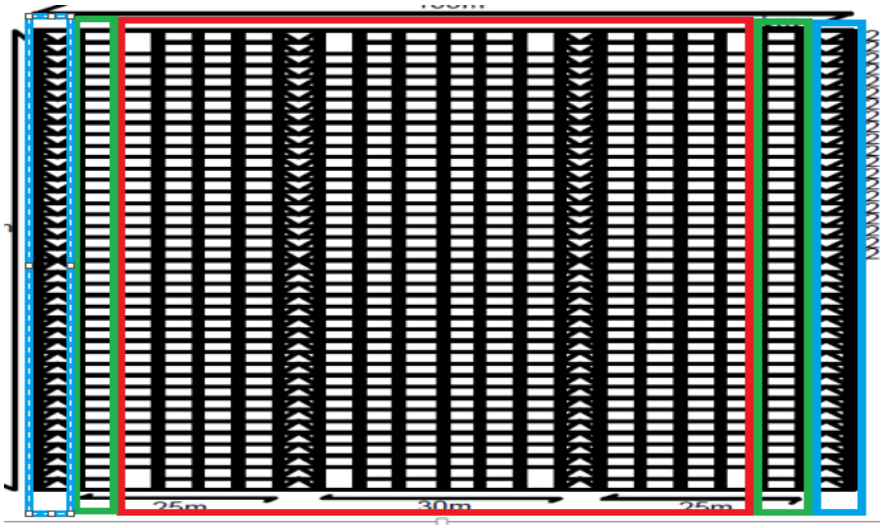

Figure 3.9. Regionalised joists with respect to axial solicitation

From the figure, the red region represents axial loads less than 0.5MN, the green represents axial loads up to -1.1MN and 1.05MN, while the blue zone represents axial loads up to -1.23MN and 1.74MN. For the red region we used medium resistance 'Movingui' GLT (respecticely for compression and tension using negative and no sign for loads) we had stress 18.94MPa resisted by 25.4MPa and 28.24MPa. For the green region there were acting stresses 41.47MPa(C) and 39.44MPa (T) resisted by high resistance solid 'Eyoum' 49.84MPa (C) and 51.50MPa (T). For the blue region the axial solicitations where too high than any available wood specie, so we propose pre-stressed GLT or fibre reinforced GLT which is left out for further research.

Since the axial loads which are the main solicitations defining second order effects were okay, and due to the fact that joists and girts are secondary elements, further detail analysis for other solicitations was left out.

3.4.5.4. Buckling-based design and analysis of columns

The number of columns have been adjusted in the analytical model. Checking was began with axial capacity of the column. It was found maximum compression (-404.8kN). This axial load gave axial stresses of 37.5MPa more than the compressive resistance of high resistance 'Movingui' GLT (25.96MPa). For safety reasons the most adapted material for this stress was high resistance solid 'Eyoum' with a 49.84MPa resistance. This adjustment was possible because the columns rests directly on the floor so do not influence the global structure as material density was varied. It will require intermediate connection systems to span the maximum height but we ended analysis of columns here as it is a straight element (suffers negligible second order effects).

3.4.5.5. Analysis of curved beam

As the curved frames are the main structural elements which suffer heavily and directly from the effects of second order (which is one of the main problematics), detail analysis on the effects of bending and torsional moments has to be carried out.

The maximum axial loads were 3767.5kN and -3025.8kN, giving respectively axial stresses of 7.7MPa and 6.2MPa, they were less than the resistances of low resistance 'Movingui' GLT (23.72MPa and 25.54MPa respectively).

It was observed radial flexures peaking at +31600.11kNm and -990.34kNm. To analyse radial flexure we needed to calculate the following;

$$R, n = {2.04}/{\ln({175.03}/{172.99})} = 174.008m$$

$$y = 175.03 - 174.008 = 1.022m\ (for + ve\ moment)$$

$$y = 174.008 - 172.99 = 1.018m\ (for - ve\ moment)$$

$$e = 174.01 - 174.008 = 2E(-3)m$$

$$\sigma = \frac{31.6}{0.4896 * 2E(-3)} * \frac{1.022}{174.008 - 1.022} = 190.66Mpa(+ve\ moment)$$

$$\sigma = \frac{1}{0.4896 * 2E(-3)} * \frac{1.018}{174.008 - 1.018} = 6.01Mpa(-ve\ moment)$$

The flexural resistance of high resistance 'Movingui' GLT, (36.46MPa) was way smaller than the +ve moment stress. It was discovered through analysis that the applied load combination when varied had little effect on the huge maximum positive moment. The main issue was the self-weight of the curved frames which had high impact on second order moments, so the best solution was using material with lower density. A possible solution would be using a different material with lighter density from CIRAD booklets; 'Ayous' which has around half the density of 'Movingui'. Tangential flexure is limited by bracing so it will left out. Also, the torsional moments were left out pending convergence of a structural model to first, begin with a useful radial flexural capacity. The bending and torsional moments of a typical curved frame are shown in the Figure 3.10.

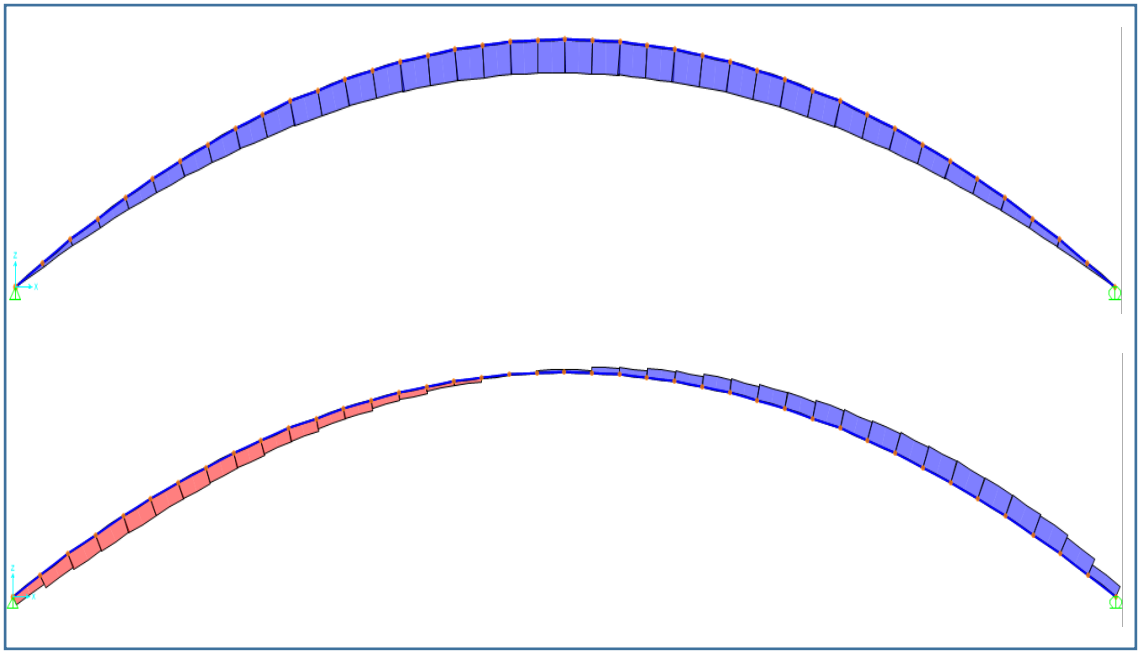

Figure 3.10. Typical curved frame bending moment (top) and torsional moment (bottom).

3.4.5.6. Notched and worn through beam effects

We have to considerate the effect of wearing holes for pins and notching at abutment and ridge, since we have to protect metallic plate elements constituting the pinned connecting systems. Fire resistance entails the use of at least 2mm thick with minimum width of plate of 440mm. We needed the curved beam solicitations at the ground and at the ridge (axial load and shear all acting as shear loads on pins) in order to calculate the necessary number of holes for a given pin type. These where gotten from SAP2000 as the maximum axial load and maximum radial shear amongst each curved frame. Shear in tangential direction is used to calculate the thickness of the splice metal plates.

Based on a previous beta version of the 5m spatial model, a procedure for designing splice base connection systems is shown (for abutment). Table 3.7 shows a shear and axial loads for splice calculations of the beta model.

Table 3.7. Shear and axial loads for splice calculations

	Maximum axial load (kN)	Maximum Radial shear (kN)	Maximum tangential shear (kN)
Abutment	+10778.76	+463.66	+14.62
ridge	+9662.6	-270.67	+74.63

The ridge and abutment splice connecting systems are shown in Figure 3.11.

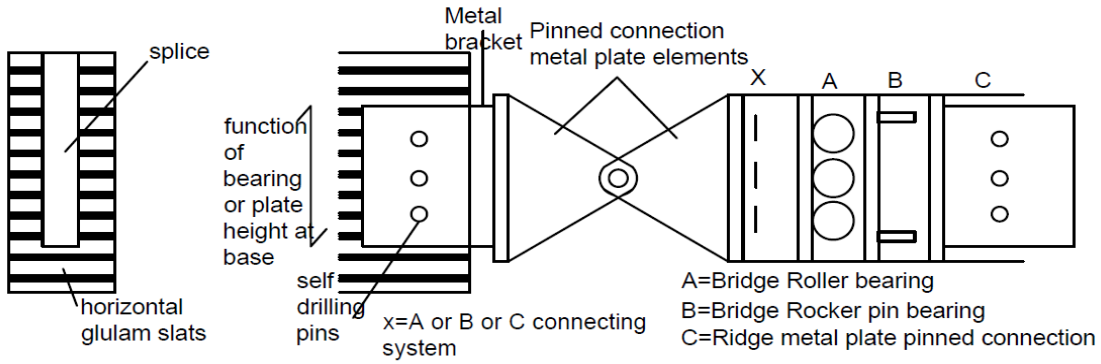

Figure 3.11. Ridge and abutment splice and connecting systems

The metallic brackets was made up of metal plates bored with the necessary number of holes and the GLT elements will require pre-drilling to provide insertion points into hot-rolled S235 (f,y,k=345MPa) steel plates and we will also require galvanized hot–rolled S355 pins about 26cm long and 27mmc thick (Thevenin, 2020). The thickness of the plate (t) is calculated using maximum axial load, considering the residual fire section of curved beams (1.984m).

$$t = {}^{3}/_{2} * \frac{10.779}{({}^{345}/_{1.2}) * 1.948} = 28mm\ (between\ 16\ and\ 40mm)$$

This thickness is sufficient to resist radial and tangential shears.

We calculate shear stress on pins in Eq. 3.15, where V is the resultant of axial stress and radial shear stress from the formula for approximation of shear stress on cylindrical elements;

$$\tau, max \approx \frac{1.38 * V}{n * \pi * \phi^2} \qquad \textbf{(Eq. 3.15)}$$

This gives us the number of pins necessary in each joint for V=10.79MN;

$$number\ of\ pins\ (n) = \frac{1.38 * 10.79}{\left(\frac{345}{1.25}\right) * \pi * 0.027^2} = 24pins$$

Using the rules of spacing for pins and considering residual height of burned section and a load inclination of 177.6° we had the spacing in Figure 3.12 (width of plate greater than 200mm).

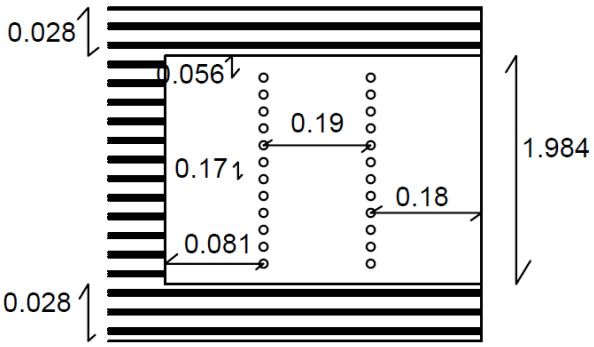

Figure 3.12. Pin spacing

From the diagram and using the previously calculated plate thickness, we have α=0.443, β=1.125. The shear coefficient K,v was;

$$K,v = \frac{6.5*(1+{}^{1.1*0^{1.5}}/_{\sqrt{0.24}})}{\sqrt{0.24}*(\sqrt{(0.443-0.443^2)}+0.8*1.125*\sqrt{({}^{1}/_{0.443}-0.443^2)})} = 4.271 > 1$$

Since K,v is greater than one, the value of K,v to use for calculation is 1

The obtained design shear stress τ,d was;

$$\tau,d = {}^{3*0.07463}/_{2*0.24*0.443*2.04} = 0.516Mpa < 5.885Mpa$$

Now, we have to get the influence of notching to joint curved beam parts. This depends strongly on the position of the notch along the beam, as the difference with the ridge and abutment notch is only β, if the required number of pins have changed. So we first calculate the number of pins with the maximum axial load and radial shear solicitation (12.057MN and 0.4505MN). This gives the number of pins.

$$number\ of\ pins\ (n) = \frac{1.38*12.07}{\left(\frac{345}{1.25}\right)*\pi*0.027^2} = 27pins$$

Given this number was almost the same as before and have used spacing rules almost equal load inclination, we maintained the same connection as before but this time now was done with a plane metal plate with a doubled base length and no more a metal bracket, provided we avoid the region of maximum axial and radial shear loads (we will describe it in the specific recommendations for ULS design). This assumption is of equality in resistance between 24pins and 27 pins is additionally guaranteed by the possibility of metal pins developing plastic resistance in tune compensating the short of 3pins.

3.4.5.7. Dowel joints under flexure

Now concerning the design of circular dowel connectors (for sub-elements of curve frames which are to be assembled on site), the first step is locating them, already done before. That is two 30m chord length and two 22.86m sub-element, each to the former jointed with the latter to form a semi-parabola curved frame element. Using the same beta model, we have the following calculations considering only the effects on wood using pins with d=24mm;

$$r,1 = 0.5(2040mm) - 4(24mm) = 924mm$$

$$r,2 = 924mm - 5(24mm) = 804mm$$

$$n,1\ (max.) = \frac{2*\pi*924}{6*24} = 41$$

$$n,2\ (max.) = \frac{2*\pi*804}{6*24} = 36$$

The value below for total shear force F,v,d considered in-plane maximum moment M,u,d =30795.987kNm and pin shear force V,u,d=1085.897kN.

$$F,v,d = \left(\frac{30795.987KNm}{\pi} * \frac{(41*0.924)+(36*0.804)}{(41*0.924^2)+(36*0.804^2)}\right) - \frac{1085.897KN}{2} = 10698.3KN$$

The total shear stress τ was;

$$\tau = \frac{3*10698.3KN}{2*2.04m*0.24m} = 32.8Mpa$$

Now the acting shears stress was very much larger than shear resistance of 'Movingui' GLT (f,v,d=5.5MPa), predictable due to excessive bending moment. So we end here pending to an optimal model from further research.

3.4.5.8. Slat disposition and splicing

We were previously withheld by the determination of a safe structure. Now done we could recommend element sections. Using 2cm slats and average RFA gluing layer thickness of 0.15mm, we propose then for each elements; 20 slats (0.4x0.1m² joists), 16 slats (0.32x0.08m² joists, girts and gable braces), 99 slats for columns and 101slats for curved beams. Also we have the position of a splice in each curved beam to shorten its assembly length less than 30m. So we will have two pieces for each curved beam one 30m and the other 22.856m so that the maximum moment in curved frame was avoided (the shorter piece is to be placed above the larger piece during execution). Another recommendation is that for joists since they are secondary resisting elements, there is possibility for using lower class (more economical) material such as 'Ayous' to formed combined glulam (GL c), by placing 'Ayous' slats at middle position in-between 'Movingui' or 'Eyoum' joists between section heights where their total stress correspond to the maximum total stress in 'Ayous'. During joist design, since the joint

does not significantly affect joist or curve mechanical properties since we are going to use joist boxes we assume that the chosen dimension of joist boxes will resist all actions. Connections supporting non-structural elements are also assumed this way as they are very smaller than other connection systems. We also have to calculate the resistance of multiple splice finger joists for the elements.

3.4.5.9. Resistance of GLT finger joints

Concerning multiple splice finger joints, the choice of geometry depends on which one suits the best to the assembly plant in terms of reducing cost of gluing, less impacting mechanical resistance and adapting the geometry to available technology for carrying out splicing (the smaller the fingers the more precise equipment need to be). This was done still considering the beta version model. Due to the subjectivity of this geometry design we chose a random geometry (still subject to given geometric ratio) and verified its resistance. We proposed a minimum number of fingers (n) = 3 (at either the giver or receiver end, counting two halve fingers as one). We did this with the diagram for multiple splice finger joint given in the methodology. The Figure 3.13 illustrates the multiple finger slat calculation geometry.

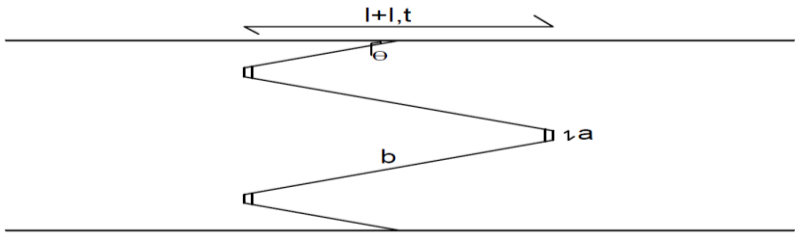

Figure 3.13. Multiple-splice finger joint geometry calculation.

We had as data; n=3, b=15a, 3a+3b=10X (recommended geometric ratio, where X is the base of the element). We obtained a=0.018m, b=0.267m and θ=1.9°. This calculation was carried out on the joist with base 0.08m. Other frame elements will have the same finger geometry by adding number of fingers through out the width of each base. This means the only frame elements we have to verify are the columns and curved beams whose length is greater than 5m. We had a total of 9 fingers at curved elements and 3 fingers at columns with respetctive b,tot of 0.241m and 2.28m.

Having done these, we now calculate the flexural stress acting on each element at the position of the splice joint and find whether it was resisted by the splice joint. (Note that the splice joints are stagered throughout the length of the element and that we have to calculate resistance for indivisual spice joints).

We have the formulas for radial an tangential characteristic flexural stresss (Eq. 3.16 and Eq. 3.17), where b,tot is the total perimeter at base of the multiple-splice and it depends on each elements. The resistance to flexure is 1.3*f,m,g,k.

$$f,m,j,k,rad. = \frac{M*(\frac{0.02}{2})}{b,tot*{}^{(0.01^3)}/_{12}} \quad \textbf{(Eq. 3.16)}$$

$$f,m,j,k,tang. = \frac{M*(\text{base lenght}/2)}{0.02*{}^{(b,tot^3)}/_{12}} \quad \textbf{(Eq. 3.17)}$$

Table 3.8 shows a summary on flexure of multiple-splice finger joints.

Table 3.8. Summary for multiple-splice finger joint resistance in flexure

element	f,m,j,k (MPa)		1.3f,m,g,k (MPa)		State	
	radial	tangential	radial	tangential	radial	tangential
column	44.03	0.078	81.9	133.9	OK	OK
curved beam	316.4	0.434	127.92	210.6	NOT OK	OK

From the table we observe that only the radial flexure in curved beams does not verify. This implies in design, we have to avoid staggering of multiple splice finger joint at the zones near the midle of each curve element (wide about half of the curved beam length) where we have maximum moment even though in reality staggering already helps to mitigate this effect. We do so just in favour of safety.

All necessary calculations concerning the different timber elements to be analysed have beeen made, including notch effect consideration. Some effects which were not considered were the effects of wearing through, and system effects not considered in the design.

3.4.6. Service limit state verification (SLS)

The SLS is a design phase were the structure is made sure to comply with the use it has been intended for in design during its intended life cycle. The different service states was shrinkage and creep. In each state it was analysed and proposed solutions were satisfactory results (displacements) where not met.

3.4.6.1. Shrinkage

The effect of shrinkage was analysed by including the additional loads that were already prepared in the volumetric analysis. It concerned only the main structural elements (curved beams).

Figure 3.14 illustrates shrinkage deflection in global X-direction.

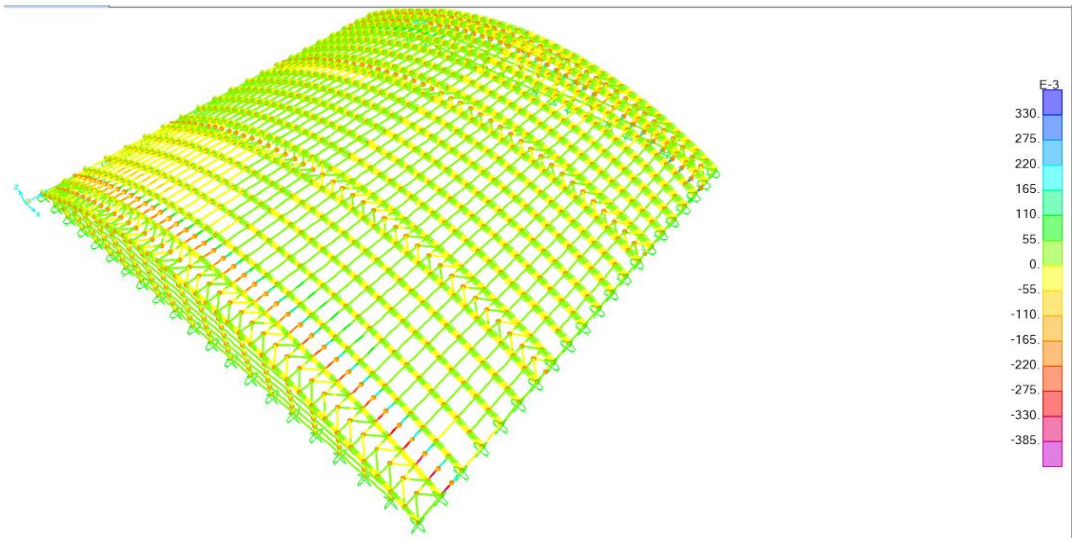

Figure 3.14. Displacements due to shrinkage in X-axis

Figure 3.15 illustrates shrinkage deflection in global Y-direction.

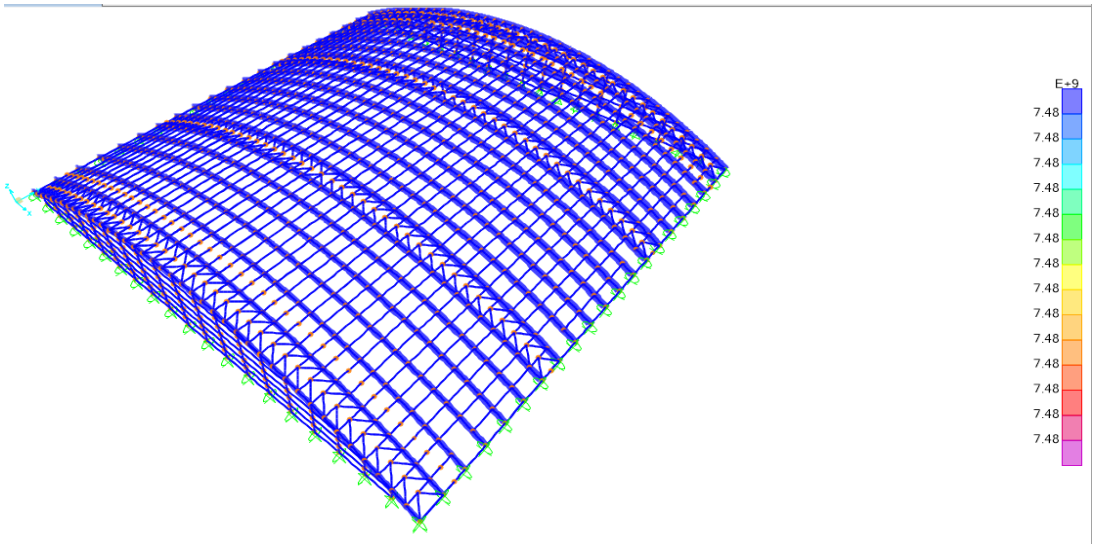

Figure 3.15. Displacements due to shrinkage in Y-axis

Figure 3.16 illustrates shrinkage deflection in global Z-direction.

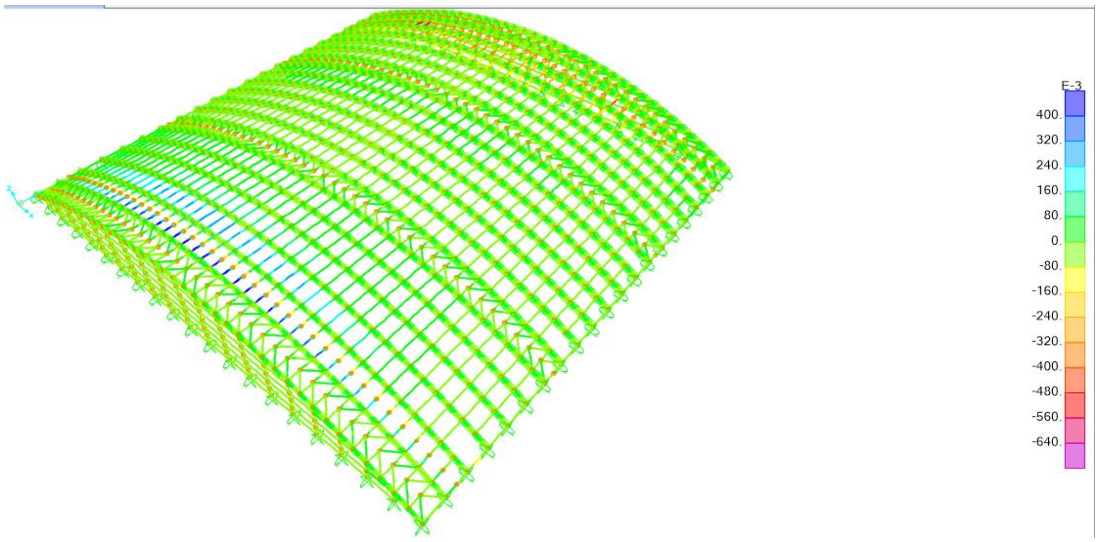

Figure 3.16. Displacements due to shrinkage in Z-axis.

It was noticed that maximum displacements were less than a meter on either side of the roller abutment. This was taken into account to design the roller platform. For deflections in Y-axis, The displacements were almost infinite. This can be explained by the fact that all supports in Y direction were roller supports hence no restrains in that direction and also due to the fact that the structure is too wide for effective transmission of longitudinal loads to the ground no matter the bracing type adopted,. The solution to this in reality rely on inertial drag due to the heavy mass of different structural elements combined which will impede movement in this direction. If not sufficient, damping might be another solution. Finally, it is visible that deflections in Z-axis were minute (less than a meter), but there is already interference with hall geometry. A good solution is lowering the inner pool level by half the curved frame height plus maximum sag (0.72m+1.02=1.74m).

3.4.6.2. Creep

For the effect of creep, it was simply needed to analyse supported straight elements. Given the effects of counter bow were neglected (u,0=0) we have u,inst=u,1 (displacement gotten from running analysis with only G,k loads). It was used the same procedure as for deflection by hand calculation for maximum displacement, where the value of u,2 depends on ridge joists and abutment joists in tangential direction.

$$u, \max = 1.252E(-6)P \ \text{(radial)} \qquad \textbf{(Eq. 3.18)}$$

$$u, \max = 1.485E(-6)P \ \text{(tangential)} \qquad \textbf{(Eq. 3.19)}$$

Table 3.9 shows a summary for deflection effect of creep.

Table 3.9. Summary for the effect of Creep

element	P (rad., kN)	P (tang., kN)	u,max,rad., (m)	u,max,tang., (m)	u,2 rad.(m)	u,2 tang.(m)	$u,2 \leq {}^{l}/_{300}$?
Joists	4.65	2.25	5.822E(-3)	3.341E(-3)	3.49E(-3)	2E(-3)	YES
girts	10.2	0	1.277E(-3)	0	7.66E(-4)	0	YES

Comparison has been done on the global structure with respect to deflection SLS and found safe while critical elements for safety (joists) have been analysed and found safe.

3.4.7. Corrosion safety verification

Corrosion design entails the consideration of a reduction of sections of maximum 4cm thickness into each side of each elements in the analytical model (maximum service time corrosion). We already included it in the analytical model for safety and here we will remove and run analysis of the ULS model under quasi-permanent load combination.

Figure 3.17 illustrates corrosion deflection in global X-direction.

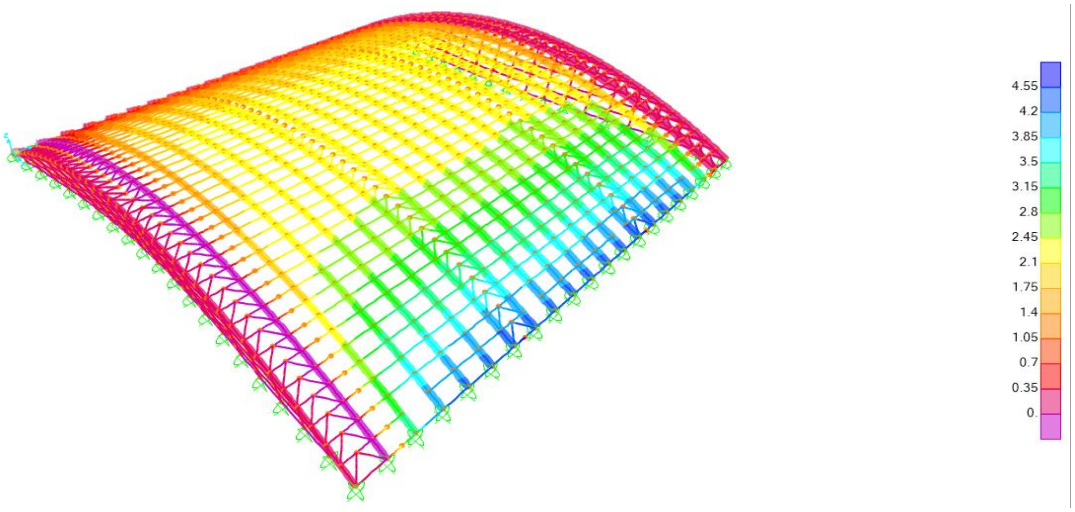

Figure 3.17. Displacements due to corrosion in X-direction

Figure 3.18 illustrates corrosion deflection in global Y-direction.

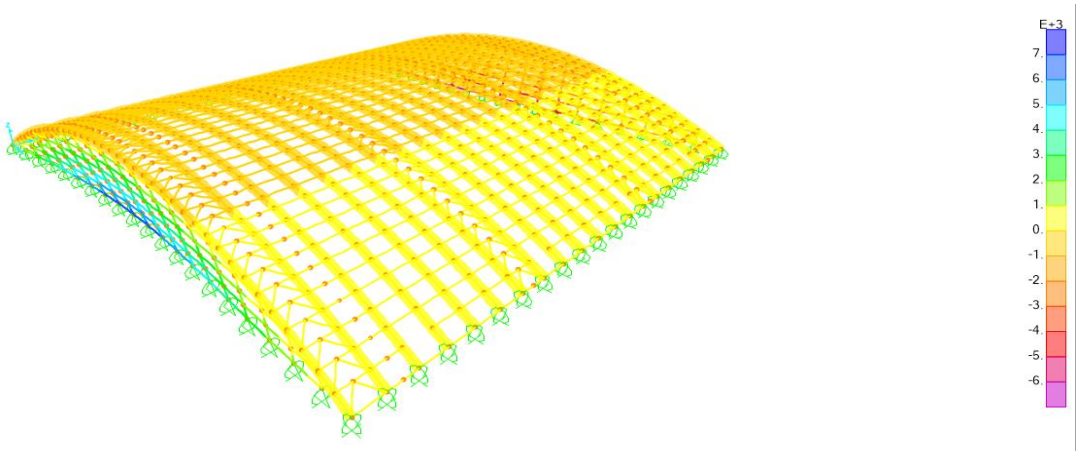

Figure 3.18. Displacements due to corrosion in Y-direction

Figure 3.19 illustrates corrosion deflection in global Z-direction.

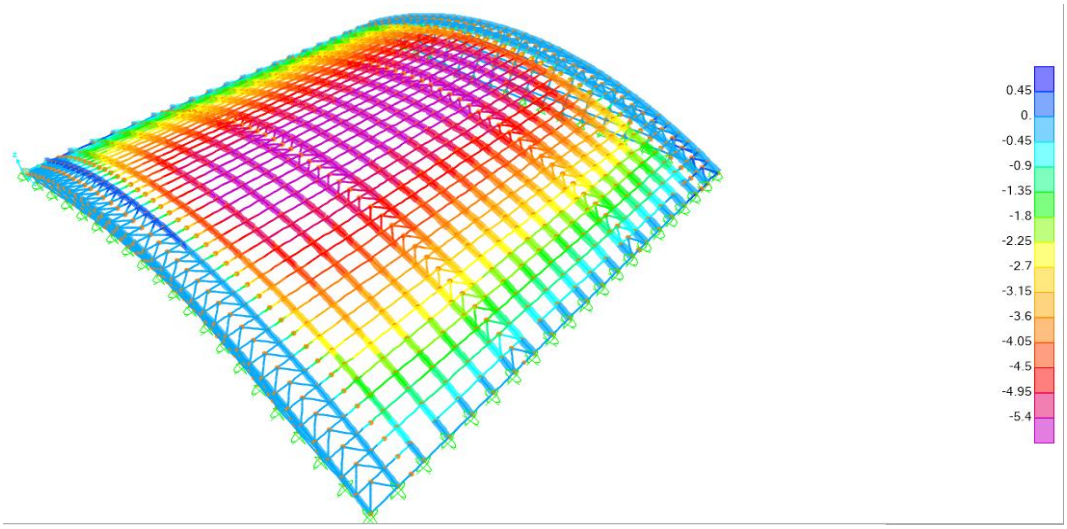

Figure 3.19. Displacements due to corrosion in Z-direction

It was observed in corrosion that the displacement in X direction increased drastically, while that in the Y direction reduced by order of 6 (very drastically but still unrealistic). It was also observed that sagging became exaggerated (more than 5m) and at this point the building is no more even fit for its intended use. All these consider the life span of the building (50years), implying absolute protection from corrosion is necessary during this time. Also if possible replacement of structural elements after a shorter period to avoid that situation. We move on to the next design phase.

3.4.8. Fire safety verification

The main idea in fire safety design is the maintain of structural resistance of primary structural members such as curved beams during the safe exit time for which it is intended to be designed. The design of fire safety was concentrated only on main structural elements

(curved frames) whose integrity must be maintained during evacuation time, and joists above the pool hall since gravitational fall of a ruptured element is dangerous for people under them. The resistance class we chose for the fire design is R30 (greater than R15 due to the large population and the internal architectural design including hall and annex compartments of the building complex, and less than R60 because it is easier to evacuate the larger proportion of population found in the building hall). This gave us t,fi,req=30min.

Derived equations for a design fire resistance parameter, fire young modulus and fire modulus were calculated from Eq. 3.20, Eq. 3.21 and Eq. 3.22 respectively.

$$X, fi, d = K, mod, fi * 1.15 * {}^{X,k}/_{1} \quad \textbf{(Eq. 3.20)}$$

$$E, fi, d = K, mod, fi * {}^{14740Mpa}/_{1} \quad \textbf{(Eq. 3.21)}$$

$$K, mod, fi = 1.0 - \frac{1}{200} * \frac{P}{A,r} \quad \textbf{(Eq. 3.22)}$$

$$d, eff = 21mm + 1 * 7mm = 28mm$$

$$d, char = 0.7mm/min * 30min = 21mm$$

A derived effective area formula is Eq. 3.23.

$$A, eff = (h, max - 2 * 28) * (b - 2 * 28) = (h, max - 56) * (b - 56) \quad \textbf{(Eq. 3.23)}$$

Table 3.10 shows the summary of mechanical properties and resistances.

Table 3.10. Summary of mechanical properties and resistances for A,eff

element	A,eff (m²)	P (m)	K,mod,fi	E,fi,d (MPa)	X,fi,d
joists	6.336*10^(-3)	0.576	0.545	8033.3	0.623*X,k
Curved frame	0.365	4.336	0.941	13870.34	1.082*X,k

In SAP2000, we defined two other similar materials but with the two design fire moduli (E,fi,d) and applied them only to the joists and curves, as they are the only elements we need to analyse under fire combination.

Fire also affects the solicitation parameters on the elements S,f,d. For conservativeness, we have Eq. 3.24

$$S, f, d = 0.6 * S, d \quad \textbf{(Eq. 3.24)}$$

We also have to adjust pin spacing to suit fire resistance for safety as shows Table 3.11.

Table 3.11. Joint hole adjustment due to R >15

	a,1 and a,2 (mm)	a,3 and a,4 (mm)	
		<0.7*(28+15)=30.1	≥0.7*(28+15)=30.1
a,fi (mm)	0.54*(28-15)=7.02	0.54*(28-15)=7.02	0

Since a,3 and a,4 are greater than 30.1mm no adjustment is needed for them. For a,1 and a,2 we need an adjustment of 7mm from its current location, so we have adjustments for a,1=19.7cm and a,2=17.7cm. Adjustment of a.1 is done by impeding on the remaining 8.1cm which is the only adjustable distance in that direction, while a,2 is adjusted by increasing the plate height by 7mm even though it will interfere minimally with the reservation between wood and the plate (2.8cm) considered for burning. Minimum plate thickness (2mm) and plate width (20cm) were both respected with plate width 45.1cm.

After reducing frame sections in SAP2000, and running analysis, we obtained the displacement diagrams for accidental load combination.

Figure 3.20 illustrates fire deflection in global X-direction.

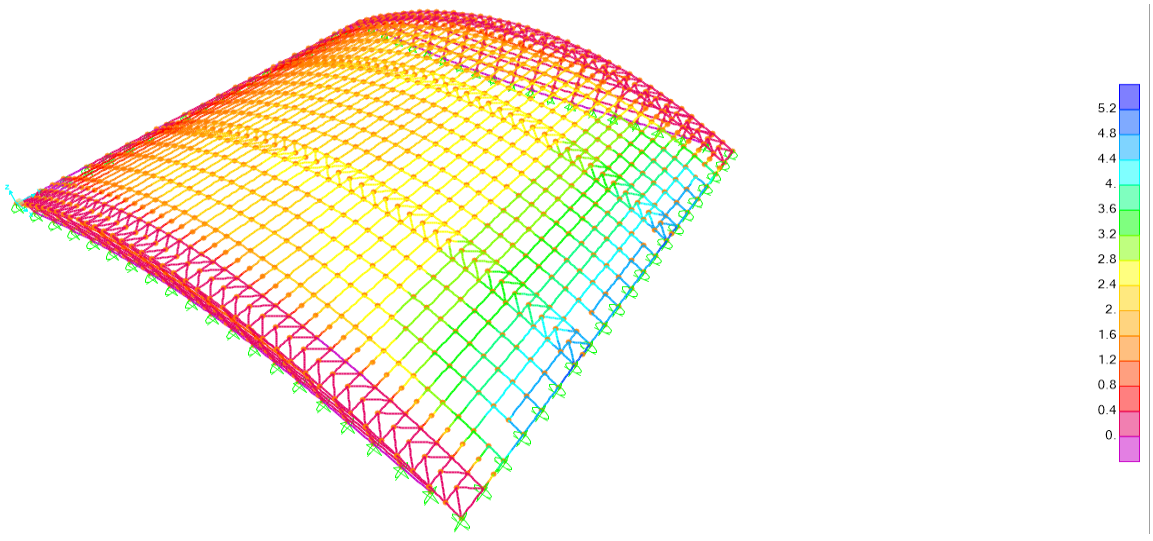

Figure 3.20. Displacements due to fire in X-direction.

Figure 3.21 illustrates fire deflection in global Y-direction.

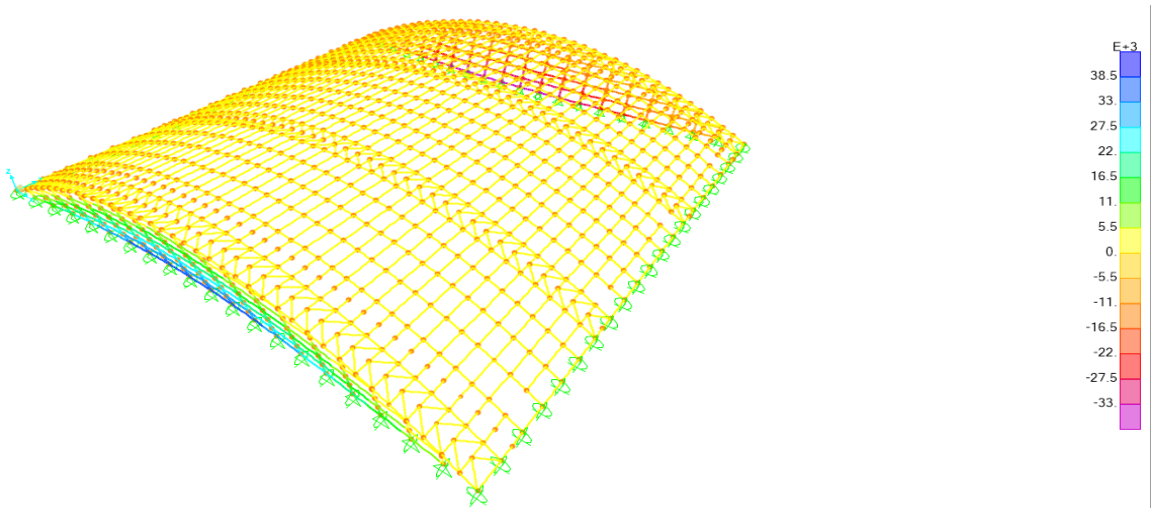

Figure 3.21. Displacements due to fire in Y-direction.

Figure 3.22 illustrates fire deflection in global Z-direction.

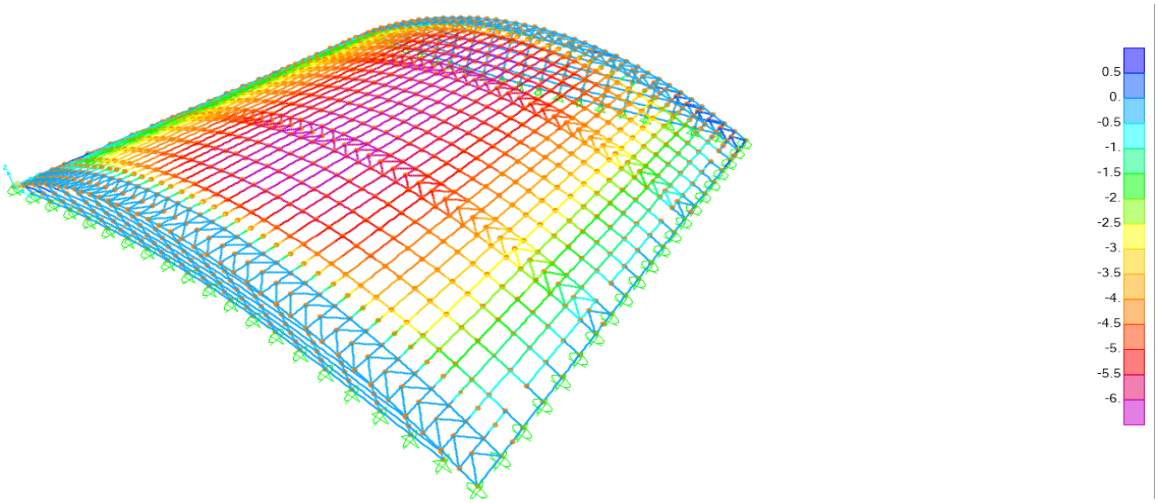

Figure 3.22. Displacements due to fire in Z-direction.

The numerical model in fire design is visibly the worst case scenario for displacement values, as they were lowest in all directions. This appropriately explains why fire is Wood's worst enemy.

There is need to calculate the integrity of the ridge joists against vertical displacements. The load combination for fire design excludes roof service load and hand load so wind is the principal variable load (Q,1,k), and accidental load has already been included in the model for calculation;

$$G,k,1+G,k,2+0.5*Q,1,k=3.834KN$$

For ridge joist in fire combination, we have maximum flexure;

$$\sigma = \frac{M}{0.02*(0.26^3)/12} * \frac{0.26}{2} = 4437.87M\ (radial)$$

The maximum bending moment is 2.4kNm from calculation, giving a fire design bending moment of 1.44kNm. We verify only for radial direction because we assumed the loads above the swimming hall are not inclined enough to receive tangential stress.

The verification is shown in Table 3.12.

Table 3.12. Verification of joists at ridge under fire combination.

σ,rad. (MPa)	f,m,g,d (MPa) rad.	state
6.391	29.08	OK

The maximum axial loads in the curved frames were 1718kN and -1470kN, providing axial stresses of 4.5MPa and 3.87MPa respectively for accidental load combination. By far less stress than resistances (low resistance 'Movingui' for the case with 23.72MPa and 25.54MPa respectively). This was enough to rely-on and say the structure is safe to evacuate completely in 30min.

It was discovered with numerical analysis that generally for safety verifications, the building safety was sound in the limit states of SLS, under corrosion and fire all with few adapted solutions proposed. As for ULS, it prompted solutions proposed which necessitated further research. Verification were carried on the most solicited structural members and adopted for the others.

Conclusion

From the results and interpretations, it was noted the fact that precision is an important element of spatial timber reticular structure design (architecture, geometry, actions on the structure etc.). It was also noted that there is an optimal structural model design from the comparative study, which is having the least joist length (provided no joist span constraint and the existence of material strength constraints). We proposed varied solutions promptly to identified design issues. It was obtained that the building necessitates further research to guarantee ULS safety, hence total building safety.

GENERAL CONCLUSION

The topic of the thesis was 'numerical analysis of spatial timber reticular structures'. A timber arc frame building was designed and analysed using 'SAP2000v21'. The numerical analysis took into consideration the second order effects which would pose problem in computation of the very large structure if calculated handily. It was also taken into consideration the problem of corrosion by designing with Glued-Laminated Timber (GLT). We designed a spatial structure and analysed numerically, using Eurocode 0, 1, 3, 5 and 8. During design was encountered several challenges. First of all learning timber construction technology and related concepts which prompted a pay visit on-site fabrication plant and construction site. Another challenge was to architecturally define the building, learning new concepts such as 'HVAC' and 'CFM'. Using 'FE' theory to design joist location on main beams also posed a though challenge. Designing secondary elements too was a tedious task to obtain solicitation parameters, as the software recognised the roof as spatial structure, so impossibility of assigning distributed loads on roof elements. Also, there was a challenge in defining a suitable material (solid wood) for axially highly solicited members as the basic timber 'Movingui' was being exceeded at some locations. These challenges were all overcome with different techniques which were proposed, except for the last challenge cited (concerning material adapted for high axial solicitation). To this challenge, a proposition was made (pre-stressing and reinforcement) which will necessitate further research. Further perspectives consist in further investigation in flexural and torsional moments in curved members, detail verification of each other elements and detail joint calculations. A visual depiction of the building design was given in the ANNEXES. The predefined objectives were not all met since some important criteria where pushed forward for further detail analysis due to non-convergence of different solutions implemented. Some important aspects of global design where met and treated, and under assumptions of the used design model, the specific objectives of SLS, corrosion and fire were met and one of the main problematic as per usage of chloride corrosion resistant material (GLT) was met. From this, it was concluded that the designed GLT Olympic swimming pool was **NOT** safe, but emphasis is laid here on the contribution made for building in general and timber construction in particular with the proposed solutions for general building safety.

ANNEXES

GLT MANUFACTURE

Annex 1: Slat curving machinery

TABLE FROM SAP2000

TABLE: Material Properties 02 - Basic Mechanical Properties

Material	UnitWeight	UnitMass	E1	E2	E3	G12	G13	G23	U12	U13	U23	A1	A2	A3
Text	KN/m3	KN-s2/m4	KN/m2	KN/m2	KN/m2	KN/m2	KN/m2	KN/m2	Unitless	Unitless	Unitless	1/C	1/C	1/C
MOVINGUI	60.946	6.219	9524308	1552462	685750	819090	737182	81909	0.369	0.428	0.618	0.0000065	0.0000065	0.0000065

Annex 2: Table of material properties from SAP2000

3D RENDERING WITH REVIT 2016

Annex 3: Panoramic View of Building

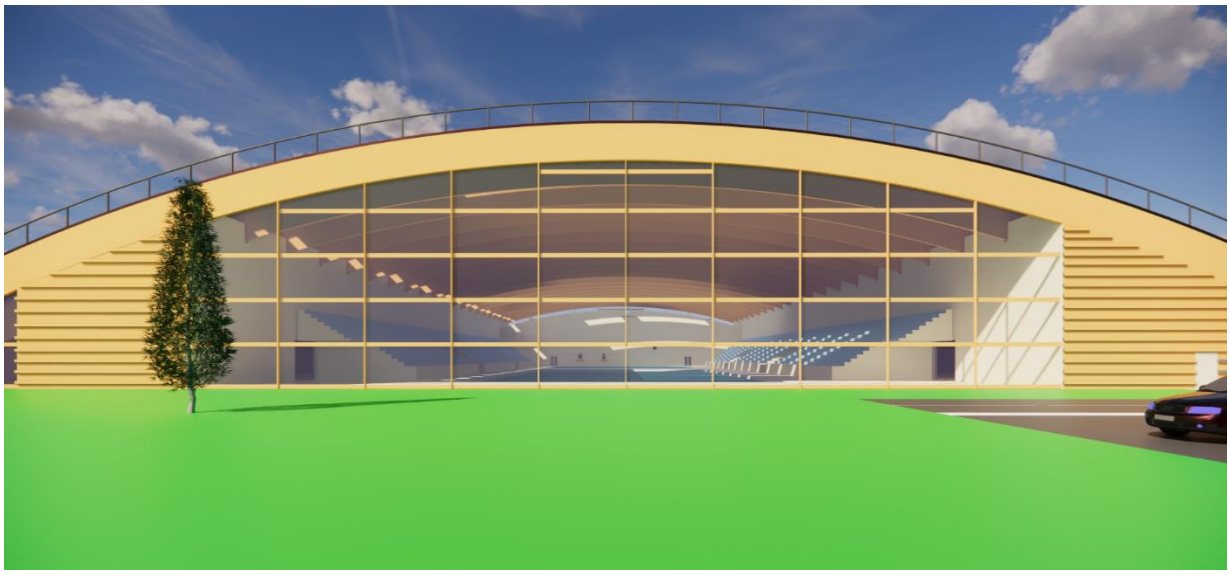

Annex 4: Building East View

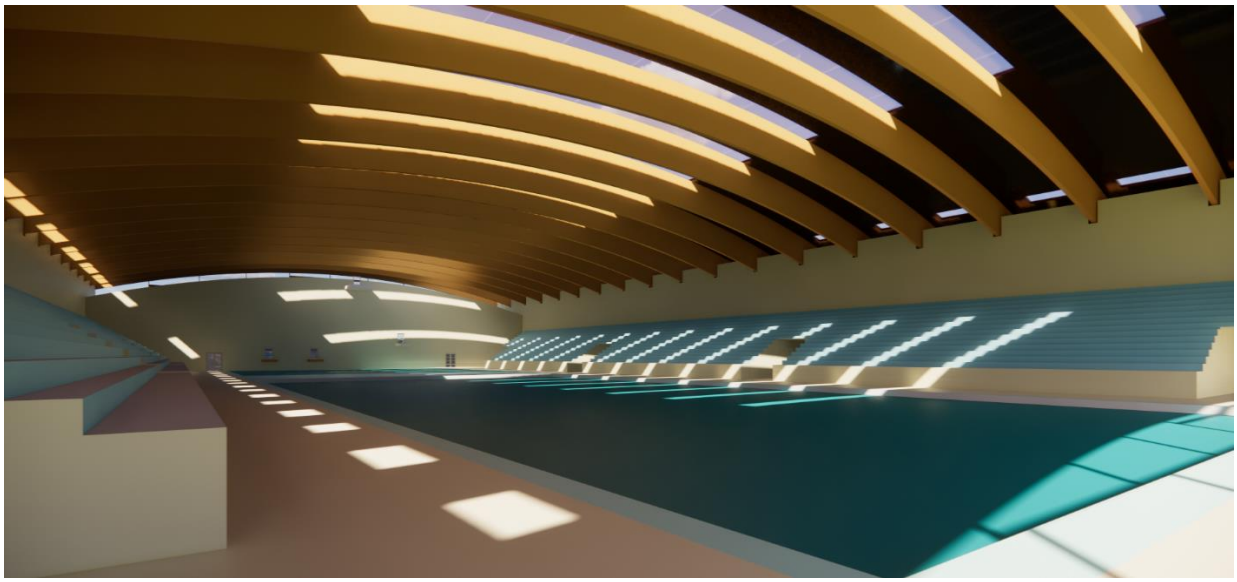

Annex 5: Internal building conical perspective 1

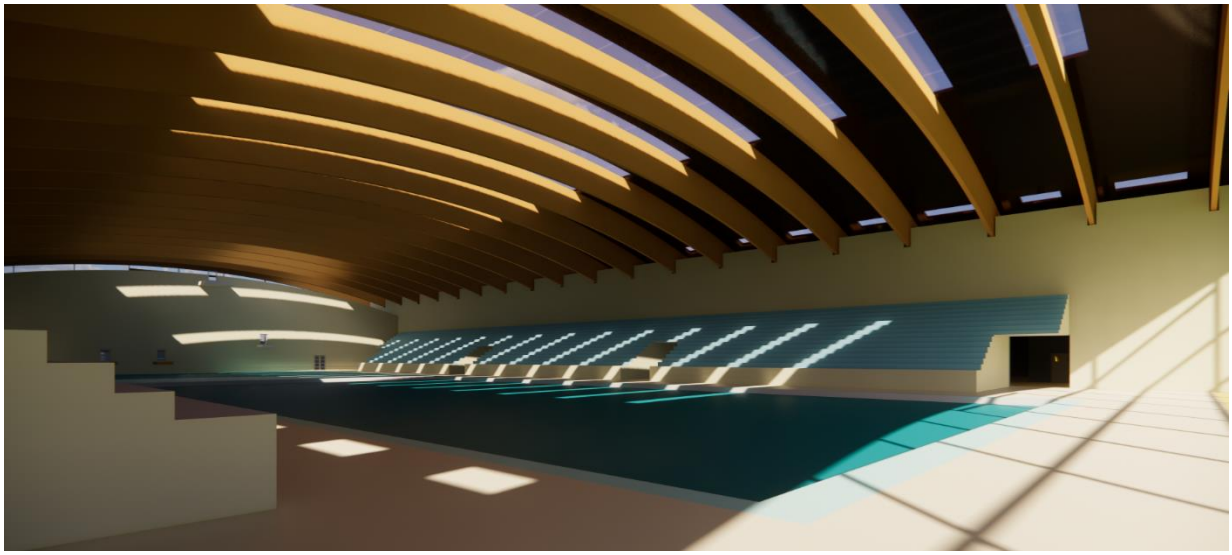

Annex 6: Internal building conical perspective 2

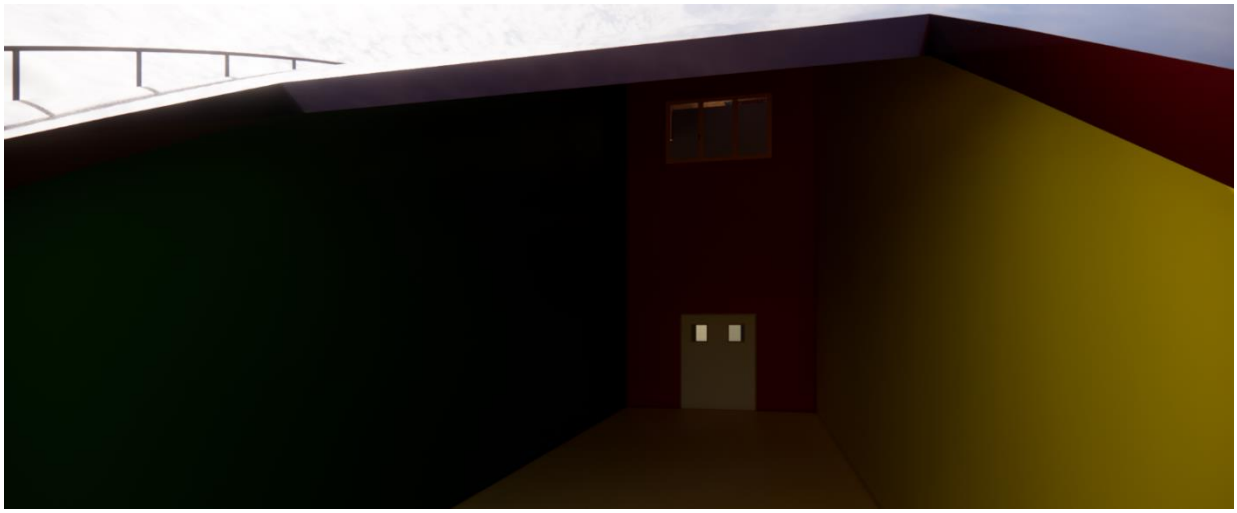

Annex 7: Supporter/Viewer entry in conical perspective

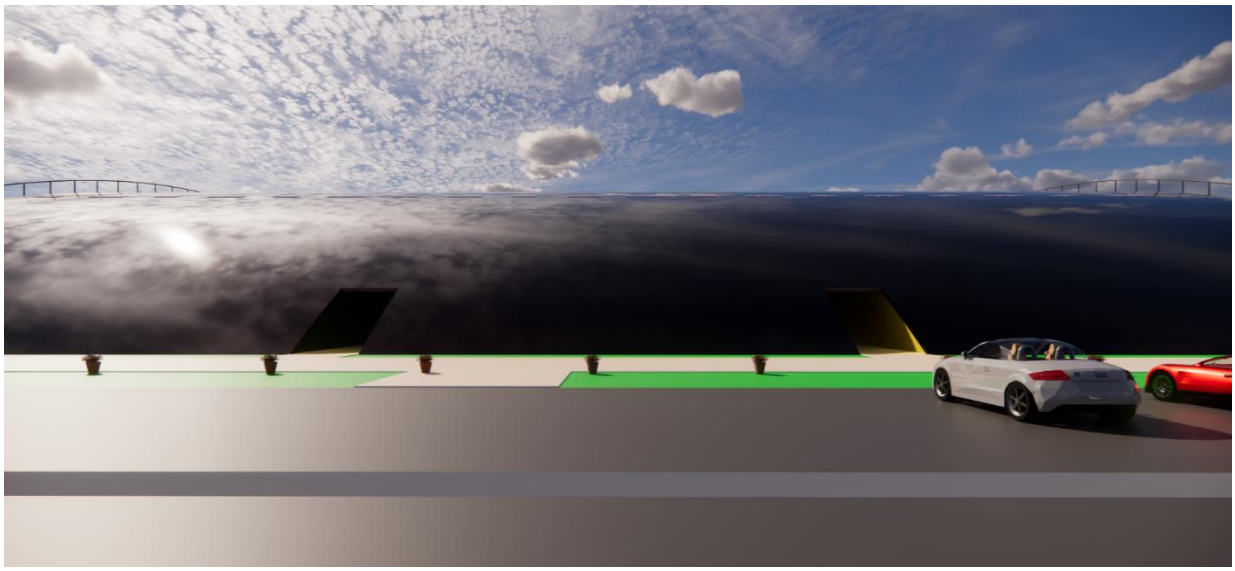

Annex 8: South View of building

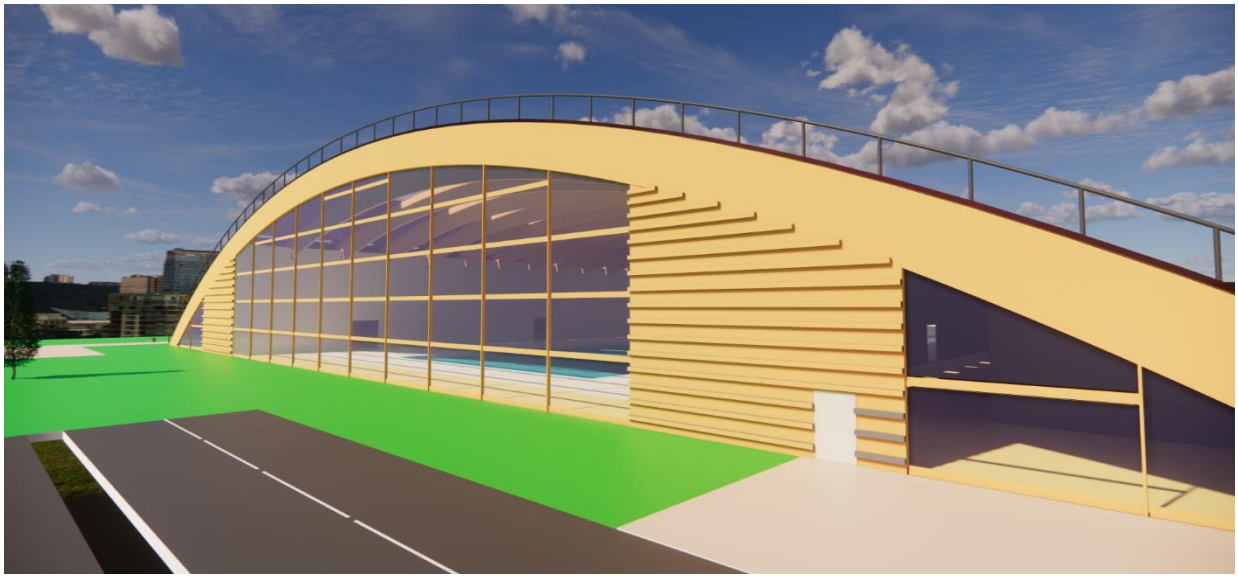

Annex 9: Tilted East view showing personnel door and parking

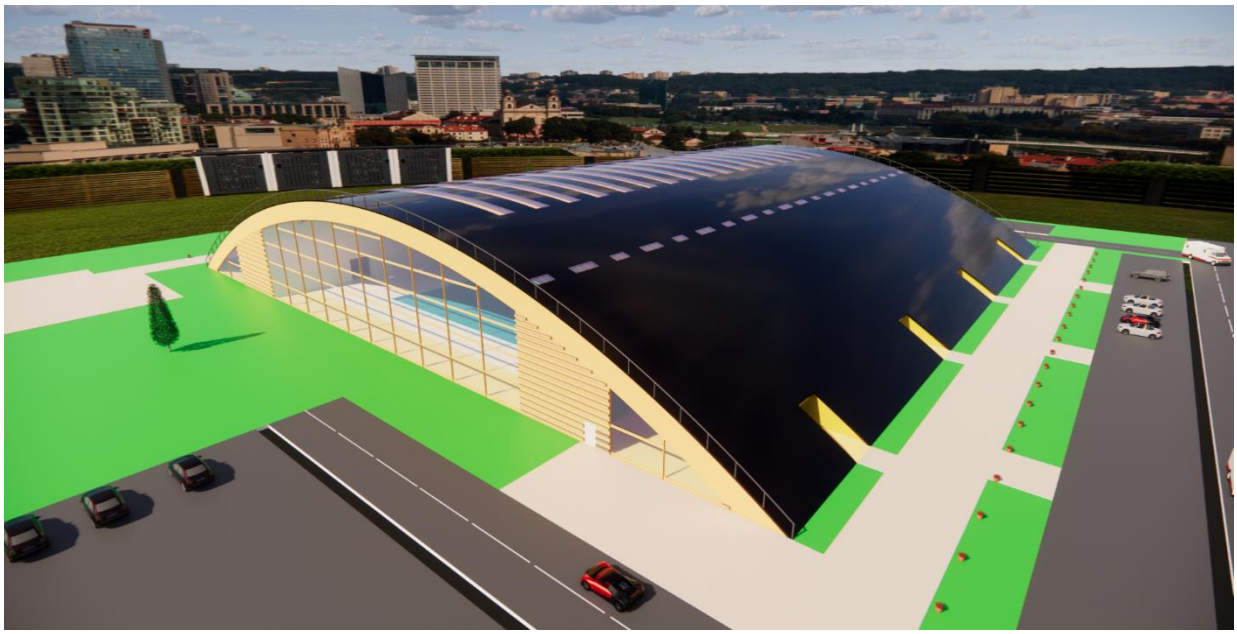

Annex 10: Aerial 3D view of building

FOUNDATION PLANS

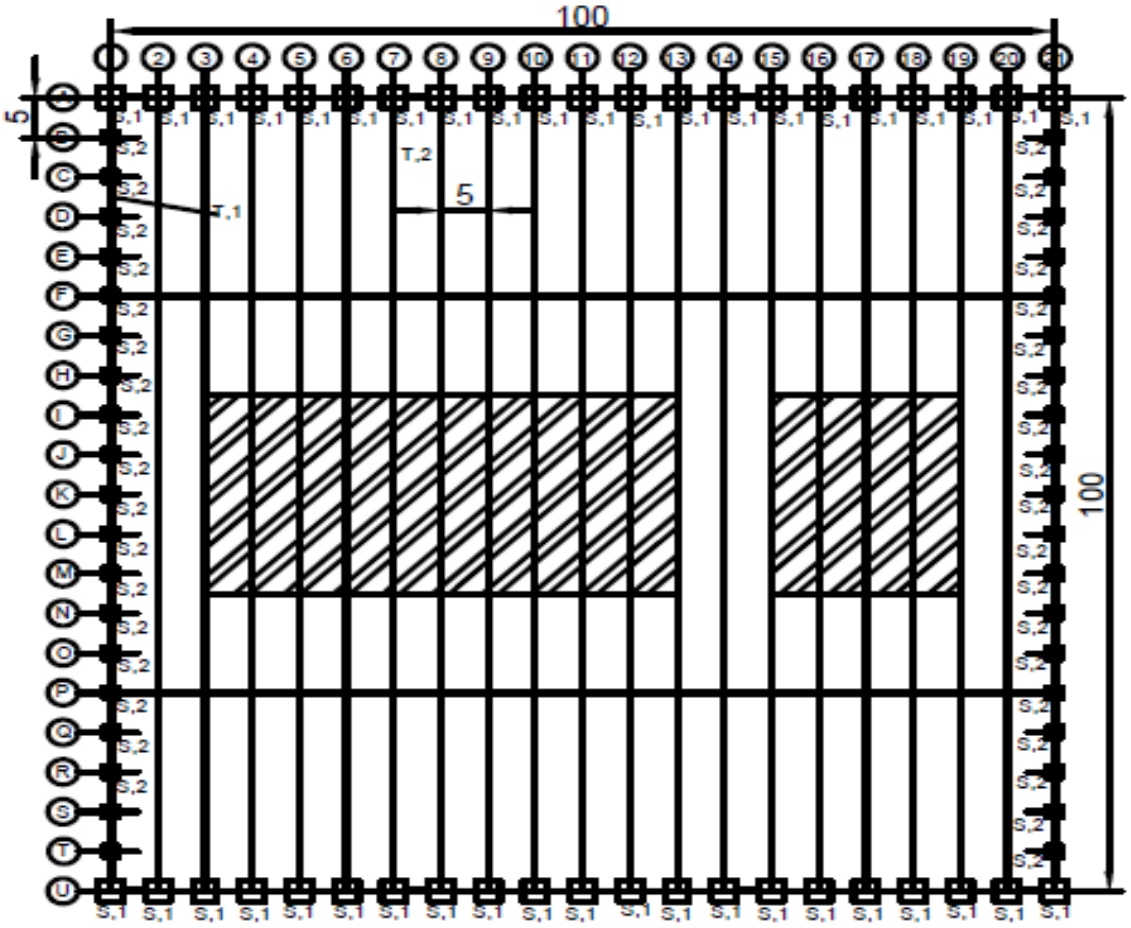

Annex 11: Gross foundation plan

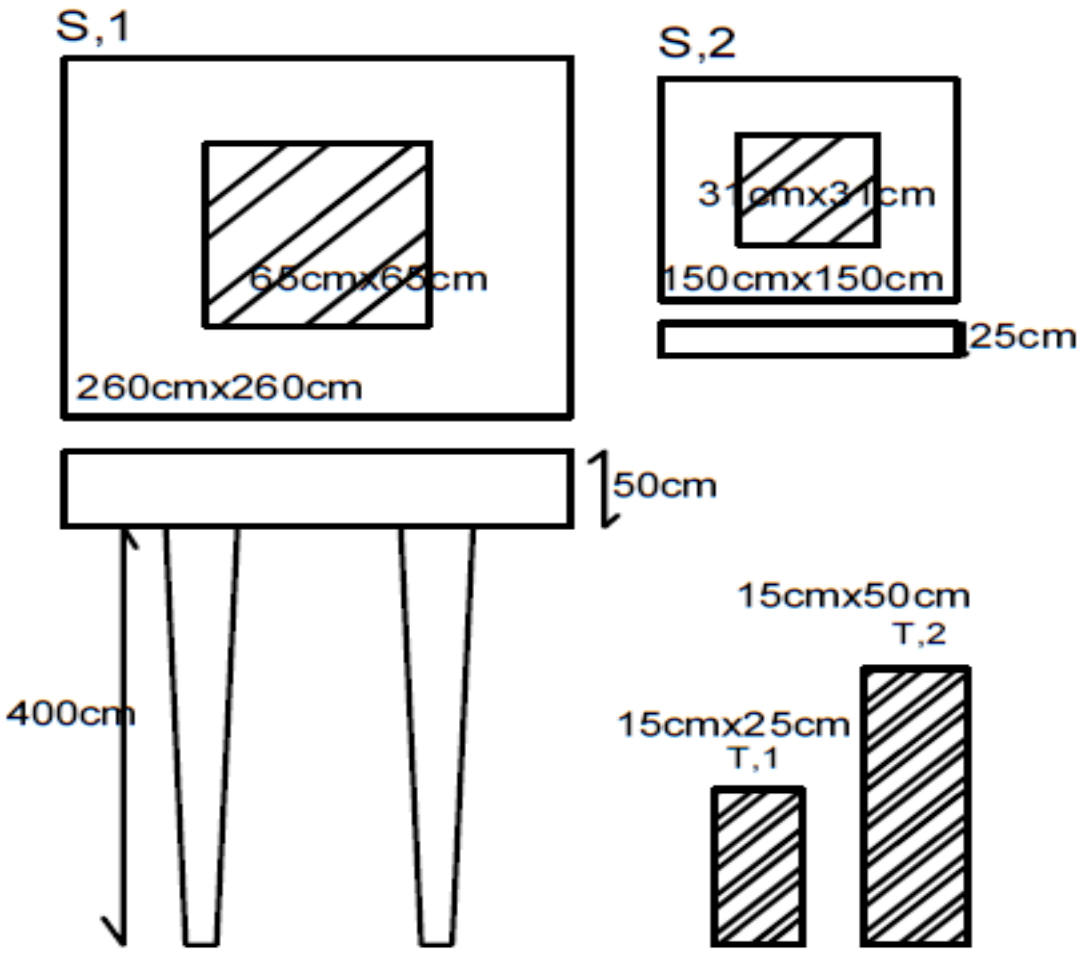

Annex 12: Detail foundation plan

TIMBER MECHANICAL PROPERTIES

Annex 13: Table of solid timber properties

Solid-timber characteristic property (f,i,k=f,i,l,k)	Source	Formula	Value
f,m,k	Tropix 5.0	(-)	103MPa
f,t,0,k	EN 338	0.6 f,m,k	61.8MPa
f,t,90,k,	EN 384	min (0.6;0.0015ρ,l,k)	0.6MPa
f,c,0,k	Tropix 5.0	(-)	53MPa (64MPa average[a])
f,c,90,k	EN 384	0.015ρ,l,k	10.02MPa
f,v,k	Brencollc	(-)	12.75MPa
E,o,mean	Tropix 5.0	(-)	14740MPa
E,0.05	EC5	0.84 E,o,mean	12381.6MPa

Annex 14: Table of glulam properties

GLT characteristic property	Source	Formula	Value
f,m,g,k	prEN 1194	1.2+ f,t,0,k	63MPa
f,t,0,g,k	prEN 1194	9+0.75 f,t,0,k	55.35MPa
f,t,90,g,k,	prEN 1194	1.15 f,t,90,k	0.69MPa
f,c,0,g,k	prEN 1194	(1.5-0.01f,c,0,k) f,c,0,k	51.41MPa (55.04MPa avrge.)
f,c,90,g,k	STEP1[a]	(-)	10.02MPa
f,v,g,k	European Journal of Wood...	$f,v,k/\eta_{,0.05}$	11.92MPa[b]
E,o,mean,g	STEP1[a]	(-)	14740MPa
E,0.05,g	EC5	(-)	12381.6MPa
$E_{,R}$	Wood handbook	0.163E,0.05,g	2018.201MPa [c]
$E_{,T}$	Wood handbook	0.072E,0.05,g	891.475MPa [c]
$G_{,LR}$	Wood handbook	0.086E,0.05,g	1064.818MPa [c]
$G_{,LT}$	R.H. Sangree	$0.9G_{,LR}$	958.336MPa
$G_{,RT}$	R.H. Sangree	$0.1G_{,LR}$	106.4818MPa
$\nu_{,LR}$	Wood handbook	(-)	0.369[c]
$\nu_{,LT}$	Wood handbook	(-)	0.428[c]
$\nu_{,RT}$	Wood handbook	(-)	0.618[c]
‘a’ represents deduction from invariance of property from solid to glulam for highest resistance glulam classes of softwood, ‘b’ represents radial shear stress as tangential shear stress is assumed that of solid wood given we use good quality RFA for gluing , ‘c’ represents properties assumed similar to that of white oak wood			

Annex 15: Saint Vincent Palotti parish Nlongkak (top), Institut Siantou Superieur main building (bottom-left) and St Peter and Paul Anglophone Parish Simbock (bottom-right).

Annex 16: Some GLT manufacturing machines from top-left to bottom-right; splinting machine, four-side moulder, vacuum wood drying machine, circular saw table machine and hydraulic press.

BIBLIOGRAPHY

(ASC), A. S. (2020, July 16). *ASC Inc (Advanced Structural Connectors)*. Récupéré sur advancedstructuralconnectors.com: http://advancedstructuralconnectors.com/product/mscpt-multiple-truss-hangers/

A. Ghali, A. M. (2017). Chapter 1 Structural Analysis Modelling. Dans A. M. A. Ghali, *Structural Analysis: A unified classical and matrix approach 7th edition* (pp. 16, 17). Boca Raton: Taylor & Francis Group, LLC.

A. Ghali, A. M. (2017). Chapter 3 Introduction to the analysis of statically indeterminate structures. Dans A. M. A. Ghali, *Structural Analysis: A unified classical and matrix approach 7th edition* (p. 85). Boca Raton: Taylor & Francis Group, LLC.

Abdullahi Abubakar Mas'ud, A. V.-R.-S. (2020, May 12). *ResearchGate.* Récupéré sur www.researchgate.net: https://www.researchgate.net/figure/Map-of-Cameroon-showing-the-mean-monthly-wind-speed-10-m-above-height-42_fig5_315657918

Aicher, S. A. (2018). Bondline shear strength and wood failure of European and tropical hardwood glulams. *European Journal of Wood and Wood Products*, 1205–1222.

Apolinarska, A. A. (2018). *Complex Timber Structures from Simple Elements.* Poznan: Poznan University of Technology.

Applied, E. (2020, March 7). *EurocodeApplied.com*. Récupéré sur eurocodeapplied.com: https://eurocodeapplied.com/design/en1991/wind-pressure-flat-roof

Bauder. (2020, March 7). *Bauder.* Récupéré sur www.bauder.co.uk: https://www.bauder.co.uk/technical-centre/downloads/design-guides/flat-roof-design-guide.pdf

Bhatia, A. (2020, March 8). *CED engineering.com PHD FOR THE PROFESSIONAL.* Récupéré sur www.cedengineering.com: https://www.cedengineering.com/userfiles/HVAC%20-%20Natural%20Ventilation%20Principles%20.pdf

Bois, R. (2020, May 21). *Twiza.* Récupéré sur fr.twiza.org: https://fr.twiza.org/article/86/info-bois-n-1-les-abaques

Brenco, L. (2020, July 7). *Brenco Exotic Woods*. Récupéré sur brencollc.com: http://brencollc.com/movingue

BSI. (1999). *Schedule of Weights of building materials (BS 648:1964).* London: BSI.

BSI. (2002). *BRITISH STANDARD Loading for buildings - Part 2: Code of practice for wind loads.* London: BSI.

CEN. (2005). *Eurocode 8: Design of structures for earthquake resistance-Part 5: Foundations, retaining structures and geotechnical aspects.* London: BSI.

CIRAD, D. F. (2003). *TROPIX 5.0 - Fiche n° 153.* Paris: CIRAD.

CIRAD, D. F. (2008). *TROPIX 6.0 - Fiche n° 235.* Paris: CIRAD.

CIRAD, D. F. (2012). *TOPIX 7.* Paris: CIRAD.

Construction, A. I. (2012). CHAPTER 2 WOOD PROPERTIES. Dans A. I. Construction, *TIMBER CONSTRUCTION MANUAL Sixth Edition* (pp. 54, 55). Hoboken: John Wiley & Sons, Inc.

Constructor, T. (2020, June 12). *The Constructor Civil Engineering Home*. Récupéré sur theconstructor.org: https://theconstructor.org/structures/bridge-bearings-types-details/18062/

Council, M. (2020, May 8). *merton* . Récupéré sur www.merton.gov.uk: https://www.merton.gov.uk/assets/Documents/www2/corporate_guidance_on_the_basic_calculation_for_hall_or_room_safe_occupancy_figures_june_2013.pdf

Crocetti, R. (2016). Large-Span Timber Structures. *Proceedings of the World Congress on Civil, Structural, and Environmental Engineering (CSEE'16)* (pp. 1, 3). Prague: Proceedings of the World Congress on Civil, Structural, and Environmental Engineering (CSEE'16).

DOUBLET. (2020, May 2). *DOUBLET*. Récupéré sur fr.doublet.com: https://fr.doublet.com/tribune

Dúbravská, K. (2018). TIMBER FRAME CONSTRUCTION FIRE RESISTANCE EVALUTION. *ACTA FACULTATIS XYLOLOGIAE ZVOLEN*, 159−173.

Economy, T. M. (2015). DIMENSIONS STANDARDS. Dans T. M. Economy, *Guide de la construction en bois au Cameroun Prise en compte des normes 2015* (p. 24). Yaounde: MINEPAT, République du Cameroun.

ENGLAND, S. (2011). Pool surround requirement. Dans S. ENGLAND, *Swimming Pools Updated Guidance for 2011* (p. 27). London: Sport England.

Ephraim, I. (2008, April 23). THE PRIME MINISTER, HEAD OF GOVERNMENT. *DECRET N°2008/0737/PM DU 23 AVR 2008 fixant les règles de sécurité, d'hygiène et d'assainissement en matière de construction.* Yaounde, Center, Republic of Cameroon: PRIME MINISTER'S OFFICE.

Eva Frühwald, T. T. (2007). *Design of safe timber structures How can we learn from structural failures in concrete, steel and timber?* Lund: Division of Structural Engineering, Lund University.

Falke, R. '. (2016, March 24). *Contracting Business*. Récupéré sur www.contractingbusiness.com: https://www.contractingbusiness.com/service/article/20868246/use-the-air-changes-calculation-to-determine-room-cfm

FRANCE, G. H. (2020, Febuary 20). *Portail du BOIS LAMELLE.* Récupéré sur www.glulam.org: http://www.glulam.org/wp-content/uploads/GlulamHandbook_Volume2_Corr02.pdf

FRANCE, G. H. (2020, March 21). *Portail du BOIS LAMELLE.* Récupéré sur http://www.glulam.org: http://www.glulam.org/wp-content/uploads/GlulamHandbook_Volume3_Corr02.pdf

Freemeteo, 2.-2. (2020, May 12). *freemeteo.es*. Récupéré sur freemeteo.es: https://freemeteo.es/weather/yaounde/longterm/monthly/?gid=2220957&mn=4&language=english&country=cameroon

Gerard, B. C. (2020, Febuary 12). *WEST FORESTRY COMPANY Societe d'Expliotation Forestiere au Cameroun.* Récupéré sur etswfc.e-monsite: http://etswfc.e-monsite.com

GEROLD, M. (s.d.). Challenges in Timber Innovations in composite construction connecting techniques outlook . *Timber Constructions of deflying nature*.

Hamakareem, M. I. (2020, April 4). *The Constructor Civil Engineering Home*. Récupéré sur theconstructor.org: https://theconstructor.org/structural-engg/types-frame-structures/35850/

Hessong, A. (2020, March 7). *hunker*. Récupéré sur www.hunker.com: https://www.hunker.com/12615529/typical-glass-curtain-wall-weight

https://www.woodproducts.fi/content/glued-laminated-timber. (2020, Febuary 11). Glued laminated timber. Helsinki , Uusimaa, Finland.

Inc., C. (2020, April 11). *Chegg Study*. Récupéré sur www.chegg.com: https://www.chegg.com/homework-help/definitions/frame-5

ISO, 2. (2020, May 20). *ISO Online Browsing Platform (OBP)*. Récupéré sur www.iso.org: https://www.iso.org/obp/ui/#iso:std:iso:14122:-3:ed-2:v1:en

Jack Porteous, A. K. (2007). Chapter 6 Design of Glued Laminated Members. Dans A. K. Jack Porteous, *STRUCTURAL TIMBER DESIGN to Eurocode 5* (pp. 205,207). Oxford, Malden, Carlton: Blackwell Publishing Ltd.

Jack Porteous, A. K. (2007). Chapter 9 Design of Stability Bracing, Floor and Wall Diaphragms. Dans A. K. Jack Porteous, *STRUCTURAL TIMBER DESIGN to Eurocode 5* (p. 340). Oxford, Malden, Carlton: Blackwell Publishing Ltd.

KASSOUL, P. A. (2020, November 12). *HASSIBA BENBOUALI UNIVERSITY OF CHLEF*. Récupéré sur www.univ-chlef.dz: https://www.univ-chlef.dz/fgca/CHAPITRE-2-FONDATIONS.pdf

Katarína Dúbravská, Ľ. T. (2018). TIMBER FRAME CONSTRUCTION FIRE RESISTANCE EVALUTION. *ACTA FACULTATIS XYLOLOGIAE ZVOLEN*, 159−173.

Knut Einar Larsen, N. M. (2016). Like seasoned timber, never gives: the durability of wood as a building material. Dans N. M. Knut Einar Larsen, *Conservation of Historic Timber Structures An ecological approach* (pp. 85 -87). Oslo: Butterworth-Heinemann.

Knut Einar Larsen, N. M. (2016). Something nasty in the woodshed: alternatives to toxic chemicals. Dans N. M. Knut Einar Larsen, *Conservation of Historic Timber Structures An ecological approach* (p. 93). Oslo: Butterworth-Heinemann.

Koutromanos, I. (2018). Finite Element Software. Dans I. Koutromanos, *Fundamentals of Finite Element Analysis Linear Finite Element Analysis* (p. 8). Hoboken, West Sussex: John Wiley & Sons.

Koutromanos, I. (2018). Strong and Weak Form for One-Dimensional Problems. Dans I. Koutromanos, *Fundamentals of Finite Element Analysis Linear Finite Element Analysis* (p. 17). Hoboken, West Sussex: John Wiley & Sons.

Logan, D. L. (2017). Introduction, CHAPTER 1. Dans D. L. Logan, *A First Course in the Finite Element Method SIXTH EDITION* (pp. 7- 8). Platteville: Cengage Learning.

Logan, D. L. (2017). Introduction, CHAPTER 1. Dans D. L. Logan, *A First Course in the Finite Element Method SIXTH EDITION* (pp. 15 - 16). Platteville: Cengage Learning.

Ltd, E. I. (2020, March 10). *ExpertsMind.com*. Récupéré sur www.expertsmind.com: http://www.expertsmind.com/questions/cross-section-of-exogenous-tree-30118331.aspx

MAGNUS, L. (2008). *HISTORIC TIMBER ROOF STRUCTURES (Master thesis, Catholic University of Leuven, Leuven, Belgium).* Leuven: Retrieved from https://bwk.kuleuven.be/mat/publications/masterthesis/2008-magnus-msc.pdf .

MANAGEMENT, A. O. (2020, March 7). *AIRM.* Récupéré sur http://www.airm.ie/: http://www.airm.ie/system/download_images/53/original/GFF%20-%20flat%20Roof.pdf?1393261490

Mayo, J. (2015). Foreword: timber for the 21st century. Dans J. Mayo, *SOLID WOOD Case Studies in Mass Timber Architecture, Technology and Design* (p. vii). Abingdon, New York: Routledge.

Mayo, J. (2015). Part 1 Building with Wood. Dans J. Mayo, *SOLID WOOD Case Studies in Mass Timber Architecture, Technology and Design* (pp. 3-4). Abingdon, New York: Routledge.

Mayo, J. (2015). Part 1 Building with Wood. Dans J. Mayo, *SOLID WOOD Case Studies in Mass Timber Architecture, Technology and Design* (p. 3). Abingdon, New York: Routledge.

Mayo, J. (2015). Preface. Dans J. Mayo, *SOLID WOOD Case Studies in Mass Timber Architecture, Technology and Design* (p. viii). Abingdon, New York: Routledge.

MINISTRY OF ENVIRONMENT, P. O. (2017). *Cameroon's Forest Investment Plan.* Yaounde: MINISTRY OF ENVIRONMENT, PROTECTION OF NATURE AND SUSTAINABLE DEVELOPMENT.

NAFFA International, I. (2020, March 7). *NAFFA INTERNATIONAL.* Récupéré sur www.naffainc.com: http://www.naffainc.com/x/IRC2000/TABLES/WeightofMaterials.htm

NATATION, F. I. (2017). *PART IX FINA FACILITIES RULES 2017-2021.* Lausanne: FEDERATION INTERNATIONALE DE NATATION.

Nitin S. Gokhale, S. S. (2008). 1.Introduction to Finite Element Analysis. Dans S. S. Nitin S. Gokhale, *Practical Finite Element Analysis First Edition* (p. 1). Pune: Finite to Infinite.

OXFORD UNIVERSITY PRESS, A. D. (2020, January 18). *ENCYCLOpedia.com.* Récupéré sur www.encyclopedia.com: https://www.encyclopedia.com/computing/dictionaries-thesauruses-pictures-and-press-releases/numerical-methods

Psalti, E. M. (2017). *Numerical Analysis of historical timber frame structures.* Cataluña: Universidad Politécnica de Cataluña.

R.H. Sangree, B. S. (2009). Experimental and numerical analysis of a halved and tabledtraditional timber scarf joint. *Construction and Building Materials 23*, 615–624.

Royer, T. R. (2015, August). POST-FRAME BUILDINGS and the International Building Code. *Frame Building News*, 1.

Ryan E. Smith, D. A. (2015). *SOLID TIMBER CONSTRUCTION PROCESS PRACTICE PERFORMANCE.* Logan: University of Utah, Integrated Technology in Architecture Center, College of Architecture and Planning.

Samuel V. Glass, S. L. (2014). Investigation of historic equilibrium moisture content data from the Forest Products Laboratory. General Technical Report FPL–GTR–229. Dans S. L. Samuel V. Glass, *Table 9—EMC table reprinted from the 1999 Wood Handbook (FPL 1999b)* (p. 25). Madison: U.S. Department of Agriculture, Forest Service, Forest Products Laboratory.

SAS, V. L. (2020, May 21). *WEISROCK lamellix.* Récupéré sur www.vosgeslam.fr: https://www.vosgeslam.fr/upload/tinymce/pdf/poutres-droites-lamelle-colle.pdf

Schwedler, M. (2016). *Integrated structural analysis.* Berlin: Fakultät Bauingenieurwesen der Bauhaus-Universität Weimar.

SEDIBOIS, U. (1996). Bois lamellé collé - Fabrication et Classes de résistance. Dans U. SEDIBOIS, *STRUCTURE EN BOIS AUX ETATS LIMITES INTRODUCTION A L'EUROCODE 5 STEP 1 Materiaux et Bases de calcul* (pp. III-4-5, III-4-6). Paris: UNFCMP.

SEDIBOIS, U. (1996). Chapitre III-1 Le bois, materiau de construction. Dans U. SEDIBOIS, *STRUCTURE EN BOIS AUX ETATS LIMITES INTRODUCTION A L'EUROCODE 5 STEP 1 Materiaux et Bases de calcul* (pp. III-1-1). Paris: UNFCMP.

SEDIBOIS, U. (1996). Preambule. Dans U. SEDIBOIS, *STRUCTURES EN BOIS AUX ETATS LIMITES INTRODUCTION A L'EUROCODE 5 STEP 1 Materiaux et Bases de calcul.* Paris: UNFCMP.

SEDIBOIS, U. (1996). *STRUCTURES EN BOIS AUX ETATS LIMITES INTRODUCTION A L'EUROCODE 5 STEP 1 Materiaux et Bases de calcul.* Paris: UNFCMP.

Service, U. S. (2010). *Wood Handbook Wood as an Engineering Material.* Wisconsin: Forest Products Laboratory.

SIS. (2017). *Sawn timber - Assessment of drying quality (SS-EN 14298).* Stockholm: SIS.

SRL, R. B. (2020, July 25). *rothoblaas*. Récupéré sur www.rothoblaas.com: https://www.rothoblaas.com/index.php/products/fastening/brackets-and-plates/concealed-connections/alumini

SWEDISHWOOD. (2020, June 7). *SWEDISHWOOD*. Récupéré sur www.swedishwood.com: https://www.swedishwood.com/building-with-wood/construction/wood-and-wood-based-products/structural-elements/

Tereňová, Ľ. (2018). TIMBER FRAME CONSTRUCTION FIRE RESISTANCE EVALUTION. *ACTA FACULTATIS XYLOLOGIAE ZVOLEN*, 159−173.

The Ministry of Economy, P. a. (2015). DIMENSIONS STANDARDS. Dans P. a. The Ministry of Economy, *Guide de la construction en bois au Cameroun Prise en compte des normes 2015* (p. 21). Yaounde: MINEPAT, République du Cameroun.

The Ministry of Economy, P. a. (2015). ELEMENTS TECHNIQUES DE CONSTRUCTION - ETC. Dans P. a. The Ministry of Economy, *Guide de la construction en bois au Cameroun Prise en compte des normes 2015* (p. 39). Yaounde: MINEPAT, République du Cameroun.

The Ministry of Economy, P. a. (2015). ELEMENTS TECHNIQUES DE CONSTRUCTION - ETC. Dans P. a. The Ministry of Economy, *Guide de la construction en bois au Cameroun Prise en compte des normes 2015* (pp. 39-58). Yaounde: MINEPAT, République du Cameroun.

The Ministry of Economy, P. a. (2015). ORIGINE DES BOIS-LEGALITES. Dans P. a. The Ministry of Economy, *Guide de la construction en bois au Cameroun Prise en compte des normes 2015* (p. 11). Yaounde: MINEPAT, République du Cameroun.

Thevenin. (2020, July 26). *Ets Thévenin et Cie*. Récupéré sur www.thevenin-cie.com: https://www.thevenin-cie.com/catalogue/broches-galvanisees-chaud/broche-acier-galvanise-27-x-220-cl-68

topographic-map.com. (2020, March 9). *topographic-map.com*. Récupéré sur topographic-map.com: https://en-gb.topographic-map.com/maps/lpdv/Yaounde/

TRADA, T. I. (2007). Connections. Dans T. I. TRADA, *Manual for the design of timber building structures to Eurocode 5* (p. 146). London: The Institution of Structural Engineers,.

Weather-Atlas. (2020, Febuary 16). *Weather-Atlas*. Récupéré sur www.weather-atlas.com: https://www.weather-atlas.com/en/cameroon/yaounde-climate

Webster, M. (2020, Febuary 12). *Merriam Webster*. Récupéré sur www.merriam-webster.com: https://www.merriam-webster.com/dictionary/numerical%20analysis

Winter, S. (2012). *Timber roofs multi-functional structures from design to fire safety.* Guimarães: Universidade do Minho.

www.glued-laminated-timber.com. (2020, November 14). *Bs Holz Brettschichtholz*. Récupéré sur www.glued-laminated-timber.com: https://www.glued-laminated-timber.com/publish/binarydata/brettschichtholz/bild0962.jpg

Xingwu Zhang, R. X. (2016, August 10). Analysis of Laminated Plates and Shells Using B-Spline Wavelet on Interval Finite Element. *International Journal of Structural Stability and Dynamics*, p. 3.

Yu-Qiu Long, S. C.-F. (2009). Preface. Dans S. C.-F. Yu-Qiu Long, *Advanced Finite Element Method in Structural Engineering* (pp. iii - iv). Beijing, New York: Tsinghua University Press, Beijing and Springer-Verlag GmbH Berlin Heidelberg.